Copy 6
RM L51K14

NACA

RESEARCH MEMORANDUM

CALIBRATION OF THE SLOTTED TEST SECTION OF THE LANGLEY 8-FOOT TRANSONIC TUNNEL AND PRELIMINARY EXPERIMENTAL INVESTIGATION OF BOUNDARY-REFLECTED DISTURBANCES

By Virgil S. Ritchie and Albin O. Pearson

Langley Aeronautical Laboratory
Langley Field, Va.

NATIONAL ADVISORY COMMITTEE
FOR AERONAUTICS

WASHINGTON
July 7, 1952

NACA RM L51K14

NATIONAL ADVISORY COMMITTEE FOR AERONAUTICS

RESEARCH MEMORANDUM

CALIBRATION OF THE SLOTTED TEST SECTION OF THE LANGLEY 8-FOOT TRANSONIC TUNNEL AND PRELIMINARY EXPERIMENTAL INVESTIGATION OF BOUNDARY-REFLECTED DISTURBANCES

By Virgil S. Ritchie and Albin O. Pearson

SUMMARY

The transonic flow in the $\frac{1}{9}$-open slotted test section of the Langley 8-foot transonic tunnel was surveyed extensively and calibrated at Mach numbers up to about 1.14. The uniformity and angularity characteristics of the flow were entirely satisfactory for testing purposes.

The reliability of pressure-distribution measurements for a fineness-ratio-12 nonlifting body of revolution in the slotted test section was established by comparisons with body pressure distributions obtained from theory, from free-fall tests, and from other wind-tunnel tests. The effects of boundary interference on the body pressure distributions measured in the slotted test section were shown to be negligible at subsonic Mach numbers and at the higher supersonic Mach numbers obtained. At low supersonic Mach numbers, however, portions of the body pressure distributions were influenced by boundary-reflected disturbances which increased in intensity and moved downstream with increase in Mach number. The effect of the disturbances on body pressures was ascertained and their effect on body drag was shown to be small, particularly when the body was located off the test-section center line to reduce focusing of the reflected disturbance waves.

Experimental locations of detached shock waves ahead of axially symmetric bodies at low supersonic speeds in the slotted test section agreed satisfactorily with predictions obtained by use of existing approximate methods.

INTRODUCTION

The need of additional testing facilities for investigating aerodynamic problems at transonic speeds has in recent years prompted a number

of modifications of the Langley 8-foot high-speed tunnel. For several years prior to 1950 the tunnel was operated with an axisymmetrical fixed nozzle which produced subsonic Mach numbers up to 0.99 and a supersonic Mach number of 1.2 (see reference 1), but the value of the tunnel for testing purposes was limited because of the "blind spot" between Mach numbers of 0.99 and 1.2 in which uniform flows suitable for testing were unattainable. With the advent of the slotted test section (reference 2), however, the means were at hand for changing the test section Mach number continuously from 0 to some low supersonic value and at the same time reducing the solid blockage effects at subsonic speeds. Consequently, early in 1950, the Langley 8-foot high-speed tunnel was converted to slotted-tunnel operation and henceforth will be designated as the Langley 8-foot transonic tunnel. A preliminary investigation of the converted tunnel resulted in the design of a suitable slotted section for producing uniform flow but did not include detailed surveys of the test-section flow (see reference 3).

The purpose of the present investigation was twofold: (1) to survey and calibrate the flow in the slotted test section and (2) to ascertain the reliability of pressure-distribution measurements for a typical non-lifting transonic model in the slotted test section. The second part of the investigation included extensive pressure measurements and schlieren observations needed to evaluate the nature and approximate magnitude of test-section boundary effects on the model pressures.

SYMBOLS

Flow quantities and model coefficients:

ρ	mass density of air
V	airspeed
a	speed of sound in air
p_l	local static pressure
p_o	stream static pressure
q_o	stream dynamic pressure $\left(\frac{1}{2}\rho V^2\right)$
P	pressure coefficient $\left(\frac{p_l - p_o}{q_o}\right)$

P_{sonic} pressure coefficient corresponding to the speed of sound

$(\Delta p/q_o)_{max}$ maximum change in pressure coefficient at model surface due to effect of boundary-reflected disturbances at supersonic speeds

C_D body drag coefficient based on body frontal area

M Mach number (V/a)

M_{TC} Mach number corresponding to ratio of stream total pressure to pressure in test chamber surrounding the slotted section

M_o average Mach number in test section; stream Mach number; Mach number ahead of shock

M_1 Mach number behind shock

θ_v mean flow inclination (measured in vertical plane) to the horizontal, deg, positive for upflow

Shock locations:

L_S axial distance required for model nose shock to traverse the supersonic flow to test-section boundary and reflect back to surface of model near test-section center line

L_M axial distance required for free-stream Mach line, starting at model nose, to traverse the supersonic flow to test-section boundary and reflect back to surface of model near test-section center line

x_{SB} axial distance from sonic point on body to location of detached shock ahead of body nose

y_{SB} radial distance from body center line to sonic point on body surface

β acute angle between weak shock wave and the flow direction

Geometry of tunnel and model:

x axial distance downstream of slot origin; distance downstream of model nose

y	radial distance from tunnel center line
l	basic length of body-of-revolution model
α	angle of attack of model

APPARATUS AND METHODS

The Slotted Test Section of the Langley 8-Foot Transonic Tunnel

The Langley 8-foot transonic tunnel is a single-return type of tunnel which operates at a stagnation pressure approximately equal to atmospheric pressure. Although the tunnel was originally of circular cross section throughout, with an 8-foot throat diameter, it has recently been fitted with a throat liner which is of dodecagonal cross section and which is slotted in the axial direction downstream of the effective minimum section of the tunnel (fig. 1, section BB). The slots (slot shape 11, reference 3) are located at the vertices of the twelve wall panels comprising the closed portion of the throat boundary (fig. 1, section CC). Each slot tapers gradually from zero width at the effective minimum section to a full-open width 96 inches downstream, where the combined widths of all slots comprise approximately one-ninth of the inside periphery of the tunnel. Downstream of the 96-inch station the width of the panels between slots remains constant. The slots are terminated at the 169-inch station. The divergence angle of the wall panels in the slotted test section is 5 minutes. More complete details concerning the liner, and, in particular, the design of the slot shape and ordinates of the diffuser-entrance noses at the downstream end of the slotted section, are given in reference 3.

The geometric cross-sectional area of the liner at the minimum section (fig. 1, section BB) is approximately 42.64 square feet. At a typical model test location 85 inches downstream of the minimum section the cross-sectional area is about 42.87 square feet.

Flow-Survey Instrumentation and Methods

The characteristics of the flow in the slotted test section were investigated by means of pressure measurements and schlieren observations near the center line and by means of pressure measurements at the wall.

Pressure and temperature measurements.- Static-pressure measurements were obtained from 0.031-inch-diameter orifices located in the surfaces along the center lines of diametrically opposed wall panels 5 and 11, and in the surface of a 2-inch-diameter cylindrical survey tube (fig. 1).

The wall orifices were located approximately 2 inches apart axially in the slotted section and as far as 60 inches upstream of the slot origin. The cylindrical-tube orifices were arranged in four axial rows spaced 90° apart. A single row contained orifices located 6 inches apart in a 60-inch-long region immediately upstream of the slot origin, 2 inches apart in a 24-inch-long region just downstream of the slot origin, 6 inches apart in the 24- to 60-inch downstream region, and 2 inches apart in the region extending from 60 to 160 inches downstream of the slot origin. The three other rows contained orifices spaced 2 inches apart in the region from about 72 to 112 inches downstream of the slot origin; in this region the orifice locations in the four rows were staggered so that static-pressure measurements could be obtained at $\frac{1}{2}$-inch intervals. The surface of the cylindrical tube was kept free of irregularities in the vicinity of pressure orifices.

The cylindrical survey tube was alined approximately parallel to the geometric center line of the slotted test section. The nose of the tube was located about 9 feet upstream of the slot origin and was held in position by means of three 0.060-inch-diameter stay wires spaced 120° apart angularly; the downstream end was located in the tunnel diffuser and was supported by means of the model-support system shown in figure 1. A small amount of sag existed along the unsupported length of the tube but this did not affect the pressure measurements. The tube was capable of axial movement to permit measurements at intervals as close as desired. Interchangeable off-set adapters were used to locate the tube 6 inches and 15 inches off the center line at any desired angular position.

Local static-pressure measurements obtained by means of the orifices in the wall panel and in the cylindrical tube surfaces were assumed to be equal to those outside the boundary layer except in the vicinity of shock where the pressure changes would occur over an axial distance greater at the surface than outside the boundary layer.

Stream total-pressure measurements were obtained in the subsonic flow region upstream of the slot origin by means of several total-pressure tubes, one located in the ellipsoidal nose of the cylindrical survey tube (fig. 1), and others in the low-speed section upstream of the contraction cone. Measurements also were obtained near the center line of the slotted test section by using a total-pressure rake consisting of eight 0.050-inch-diameter tubes, 3 inches long and mounted ahead of a 1° included-angle wedge.

Pressures were measured by use of multiple-tube manometers containing tetrabromoethane and by use of U-tubes containing kerosene. All manometer tubes were photographed simultaneously.

[redacted]

The temperature of the flow mixture in the tunnel was controlled in order to reduce possible humidity effects on the flow in the test section. Temperature measurements were obtained at a number of stations between the tunnel center line and wall in the low-speed section upstream of the contraction cone by use of thermocouples in conjunction with a recording potentiometer.

Schlieren optical system.- Schlieren observations were obtained to supplement pressure measurements of flow phenomena by use of the temporary single-pass system shown in figure 2. This system utilized 1-foot-diameter parabolic mirrors and was mounted on large movable support structures which permitted observations at any desired test-section windows in the horizontal plane or in a plane 30° from the horizontal. A spark source was used for photographic recording. The entire system was located within the test chamber and was operated by remote control.

Determination of Mach number.- The flow Mach number, the parameter used for presenting most of the results of the present surveys, was obtained by relating simultaneously measured values of the stream total pressure and local static pressures. Indications of the flow Mach number were also obtained from measured values of the angularity of weak shocks. A schlieren picture of weak intersecting shock waves, produced by small two-dimensional surface irregularities on opposite wall panels, is given in reference 3. Conical shock waves produced by a 10° included-angle cone of 1-inch maximum diameter were used not only for indicating the value of the stream Mach number but also for indicating the degree of flow uniformity in the slotted test section.

Flow angularity measurements.- The mean angularity of the flow with respect to a horizontal plane near the center line of the slotted test section was measured by use of the null-pressure-type instrument shown in figure 3. This instrument, a 3° included-angle cone, contained 0.010-inch-diameter static-pressure orifices located symmetrically in opposite surfaces. The sensitivity of this instrument to angle-of-attack changes, expressed in terms of the pressure differential between orifices in opposite surfaces and in the plane of angle change, was of the order of 0.6 percent of the stream dynamic pressure per degree change of angle in the transonic speed range. This sensitivity was not great but was within the possible error in instrument-attitude measurements. Such measurements, obtained by careful use of a cathetometer during actual testing, were estimated to include possible inaccuracies not exceeding 0.1°. The procedure for measuring the flow inclination consisted of, first, orientating the instrument so that pressure orifices in opposite surfaces were situated in the vertical plane of measurement, and secondly, varying the instrument attitude by means of a remotely controlled angle-changing mechanism in the support system until the pressures at the opposite surfaces were equal. The instrument attitude was determined carefully by means of cathetometer readings for this indicated null-pressure

[redacted]

condition, and the procedure was repeated with the instrument inverted. The arithmetical average of instrument-attitude measurements with the instrument erect and inverted was assumed to compensate for possible asymmetry of the instrument and to indicate the mean direction of the flow.

Rapid variations of the flow angularity with time were indicated by means of pressure-fluctuation measurements in the slotted test section. For these measurements a 3° included-angle cone was equipped with a small electrical pressure cell (mounted inside the cone) which connected directly to static-pressure orifices located 180° apart in the cone surface. Periodic differences in pressure between the orifices in opposite surfaces of the cone were measured by means of a recording oscillograph. The indicated pressure differences were expressed in terms of flow-angularity changes by use of a steady-state calibration of the pressure differential between orifices in opposite surfaces of the cone with respect to cone-attitude changes in the plane of the orifices. This pressure differential in the transonic range was of the order of 5 pounds per square foot per degree change in cone attitude with respect to the flow, whereas the sensitivity of the pressure cell was approximately 0.25 pound per square foot. The accuracy of the pressure cell was maintained over a frequency range from 0 to 300 cycles per second.

Jet-boundary interference effects.- In order to ascertain the value of the slotted test section for testing purposes a high-fineness-ratio body of revolution was tested at zero angle of attack through the Mach number range from about 0.60 to 1.14 and the measured body-surface pressure distributions were compared with essentially interference-free distributions from other sources. The particular body shape used in this investigation, a fineness-ratio-12 body for which coordinates are given in reference 4, was selected because of the availability of theoretical and experimental pressure distributions. The wind-tunnel model consisted of the forward 83.7 percent (33.5 in.) of a 40-inch-long basic body; a 3.25° semiangle support sting joined the body at the 83.7-inch body-length station (see fig. 4). This model contained static-pressure orifices (0.020 in. in diameter) spaced 2 inches apart axially along the length of the body and arranged in rows at various angular locations (reference 5) but only the pressure measurements at the upper and lower surfaces were used for the comparisons shown in this paper. Small surface discontinuities existed at model-component junctures, at an imbedded mirror in the upper surface, and at faired surfaces over filled bolt holes.

The reflection of disturbances from the slotted-test-section boundary and the effect of such reflections on model pressure distributions were examined by testing both the body of revolution (fig. 4) and a wing-body combination (fig. 5) at supersonic speeds and correlating measured pressures at model and wall surfaces with schlieren pictures of the flow

field near the model surface. The wing-body combination consisted of the previously described body of revolution (fig. 4(c)) fitted with a 45° sweptback airfoil of NACA 65A006 section, 12-inch semispan, and 1-square-foot plan-form area. Static-pressure orifices (0.020 in. in diameter) were located in upper and lower surfaces of the airfoil at five semispan stations (see reference 5) but for the present surveys pressures were measured mainly at the 60-percent and some at the 80-percent semispan stations where the airfoil chord was about 5.70 and 5.05 inches, respectively. Pressure orifices at these wing stations were located at chordwise intervals no greater than 10 percent of the chord. Static-pressure orifices (0.018 in. in diameter) also were located at axial intervals of about 0.75 inch along the length of the model-support sting in order to measure pressures in the compression region at the base of the model and to aid in locating wall-reflected disturbances. Transition was fixed at 10-percent-chord and 12-percent-body-length stations for the wing and body of revolution, respectively.

The control of model attitude during tests in the slotted test section was effected by means of cathetometer observations and a remotely controlled angle-changing mechanism in the model-support system.

PRECISION OF DATA

The maximum random error in the indicated Mach number, as obtained from pressure measurements throughout the transonic range covered by these surveys, was estimated to be no greater than 0.003 in shock-free flow. For measurements behind shocks an additional error in the indicated Mach number was possible because of failure to correct for changes of the stream total pressure through the shocks; this error, however, was negligible at the lower supersonic Mach numbers and did not exceed 0.002 for normal shocks at a Mach number of 1.14.

Probable errors in Mach numbers indicated by angularity measurements of weak shocks in supersonic flow were of the order of 0.002. This error corresponds to an estimated inaccuracy of 0.2° in the measurement of the angularity of two-dimensional shocks from the test-section walls. The angularity of sharply defined conical shocks could be measured with an inaccuracy of only about 0.1°.

The differences between Mach numbers determined from pressure measurements and those from shock-angularity measurements at supersonic speeds corresponded closely to the estimated possible errors in determining the Mach number (see fig. 6).

Estimated possible errors in the model-surface pressure coefficients obtained from tests in the slotted test section were generally of the order of magnitude of 0.005 and did not exceed about 0.010.

The sensitivity of the schlieren optical system, when properly adjusted, was sufficient to permit the detection of a conical shock whose strength corresponded to a Mach number change of about 0.003.

The possible error in measuring the flow angularity was estimated to be about 0.1°. A like error in measuring the model angularity introduced the likelihood of errors as great as 0.2° in model alinement with respect to the flow direction.

RESULTS AND DISCUSSION

Test-Section Calibration

Flow uniformity.- The results of pressure surveys in the slotted test section are presented in figures 7 to 9 in terms of the local Mach number. The stream total pressure used, in conjunction with local static pressures, to determine the Mach number distributions of figures 7 to 9 was found to be essentially constant throughout the survey region near the test-section center line and was in close agreement with values measured in low-speed regions upstream of the slotted section. The Mach number distributions shown in figures 7 and 8 are associated with the flow characteristics soon after the slotted-throat installation and with a diffuser-entrance nose located 142.5 inches downstream of the slot origin (nose A, reference 3). Figure 9 presents wall and center-line Mach number distributions obtained from surveys conducted at a later date and with a longer diffuser-entrance nose (nose B, reference 3) located 114.6 inches downstream of the slot origin. This nose, designed to reduce the power requirements for the tunnel and thereby raise the maximum attainable Mach number, utilized different nose arrangements for subsonic and supersonic operation (see reference 3).

The Mach number distributions in the slotted test section with diffuser-entrance nose A (figs. 7 and 8) indicated that (1) the flow in the slotted test section was essentially free of gradients (except in the Mach number range from about 0.90 to 1.08 where a slight positive Mach number gradient existed) and was sufficiently uniform for testing purposes (disturbances in the flow generally increased with Mach number but in no instances did deviations from the average stream Mach number exceed 0.006 in a 36-inch-long test region at Mach numbers up to 1.13), (2) the length of the uniform-flow region available for model testing purposes decreased with Mach number but was approximately 60 inches long at a Mach number of 1.13, and (3) the Mach numbers measured near the center line of the uniform-flow region agreed reasonably well with those at the wall.

The results of surveys in the slotted test section following a long period of model testing and with diffuser-entrance nose B (fig. 9) indicate that the Mach number attainable at maximum tunnel power was increased slightly but the test section was shortened at its downstream end by use of the new diffuser-entrance-nose arrangement. The Mach number distributions of figure 9 also indicate a decrease in the uniformity of the test-section flow since the time of the initial surveys; over a 36-inch-long region the maximum deviations from the average stream Mach numbers indicated in figure 9 were as much as 0.010 as compared to deviations of as much as 0.006 in figure 8. This deterioration of the flow was assumed to be due to the effect of discontinuities appearing in the wall-panel surfaces, probably near window edges, during prolonged periods of tunnel operation when insufficient attention was given to maintenance of wall-panel smoothness.

The degree of test-section flow uniformity indicated by Mach number distributions was checked over a portion of the test region at supersonic speeds by examining schlieren pictures for the presence of stream disturbances equal to or stronger than a shock of known strength introduced in the flow. The results of the flow-uniformity check are illustrated in figure 10. A 10° included-angle cone was alined approximately parallel to the flow direction near the test-section center line, and schlieren pictures were made of the flow field about and ahead of the cone at stream Mach numbers of 1.035 and 1.075. The schlieren pictures were obtained for only the horizontal plane (light path through windows in panels 3 and 9) since the largest wall-surface discontinuities were known to exist on wall panel 12 and disturbances from this panel were most readily detected from horizontal schlieren surveys. The attached conical shocks were the only disturbances visible in the schlieren pictures (fig. 10) and, since these shocks were three dimensional and therefore more difficult to detect than two-dimensional disturbances, it was concluded that no abrupt disturbances of greater strength than that of the conical shock existed in the flow. (Because the conical shocks shown in figure 10 were weak, they are not very distinct in the schlieren pictures; dots have therefore been superimposed on the shock lines to emphasize their location.) The strength of the attached conical shock, expressed in terms of the Mach number decrement through the shock, is no greater than 0.004 and 0.003 at stream Mach numbers of 1.035 and 1.075, respectively (fig. 10). Mach number decrements calculated from conical-flow theory (reference 6) are in close agreement with the two experimental points. In determining these experimental points the Mach number decrements across the cone shocks were obtained by use of oblique shock theory (reference 7) with shock angles measured directly from the schlieren pictures. For the stream Mach numbers and the test-section region concerned, the experimental schlieren-survey data of figure 10 appear to be consistent with the pressure-survey data in indicating the presence of no abrupt steady flow disturbances of significant strength.

The measured angularity of conical shocks (fig. 10) offered indications of the value of the supersonic stream Mach number which were

consistent with those indicated by pressure measurements (figs. 8 and 9) and by the angularity of weak two-dimensional disturbances from wall panels (fig. 6).

Flow calibration.- The stream flow in the slotted test section was calibrated with respect to the pressure in the chamber surrounding the slotted section, a procedure employed for smaller slotted tunnels reported in references 2 and 8.

A typical model-removed calibration curve showing the variation with test-chamber Mach number of the average Mach number over a region 30 inches in diameter and 36 inches long near the test-section center line is presented in figure 11. The data for this calibration were taken from the distributions of figure 8. An average value of the stream Mach number over the 30-inch-diameter region was obtained by fairing through the test points from the ten different positions of the survey tube. This faired value for the average stream Mach number varied almost linearly with, but was always smaller than, the indicated test-chamber Mach number. The Mach numbers measured at the ten survey locations did not differ from the average stream Mach number by more than 0.004 and 0.006 up to Mach numbers of 1.00 and 1.13, respectively.

In figure 12 a comparison is made of model-removed flow calibrations over a 36-inch-long region (from 68 to 104 in. downstream of the slot origin) at the test-section center line for data from figure 8 (early surveys with diffuser-entrance nose A) and from figure 9 (later surveys with diffuser-entrance nose B). The agreement between the two surveys is shown to be very good for the particular flow region calibrated.

The effect of a model on the Mach number of the incoming flow upstream of the model test region was examined. The use of pressure measurements at the wall to check the trend of the stream flow ahead of the model was considered applicable, particularly at supersonic speeds where disturbances are propagated approximately along Mach lines. This supposition was checked experimentally by comparing Mach number distributions along the slotted-section wall upstream of a wing-fuselage model (fig. 5) with wall distributions for the model-removed case. The results of this comparison for small lifting attitudes of the model (fig. 13) indicated close agreement between model-in and model-removed Mach number distributions upstream of the model location. The only discrepancy in the data of figure 13 appears immediately upstream of the model nose at a test-chamber Mach number of 1.025 where the bow wave ahead of the nose influences the model-in Mach number slightly. The evidence of figure 13 was supported by additional measurements with the same model at higher angles of attack (fig. 14). The latter data are presented to show the variation with test-chamber Mach number of the model-in and model-removed Mach numbers at the test-section wall approximately 10 inches upstream of the model-nose location. The data shown in figure 14 were obtained over a long period of time and included measurements with the wing-fuselage model at angles of attack as great as 20° and with diffuser-entrance noses A and B; the data from the many separate runs were in relatively close agreement. The combined data of figures 13 and 14

reveal generally that, for the model-to-tunnel size of this comparison, the pressures on the test-section wall ahead of the model were not greatly influenced (and therefore the validity of the model-removed calibration was not much affected) by the presence of a model at different lifting attitudes.

Although no quantitative comparisons are presented, it is believed from past experience in the calibration of high-speed wind tunnels that the over-all precision of calibration for a slotted test section, using the test-chamber pressure as a calibration reference, is superior to that for a conventional closed test section with subsonic speeds. In particular, the use of the pressure in the chamber surrounding the slots as a reference pressure in calibrating the stream flow is believed to avoid inconsistencies which may arise from the use of the static pressure indicated by a wall orifice located upstream of the minimum section.

Flow angularity.- The mean angularity of the flow in the slotted test section was measured at a center-line station 85 inches downstream of the slot origin. The measurements were limited to the vertical plane and employed the null-pressure-type instrument of figure 3 and the methods outlined earlier. A 2° included-angle wedge was first used for the flow-inclination measurements but it proved inadequate because of excessive bending near the leading edge and damage to the leading edge due to the impact of foreign particles in the air stream. The 3° included-angle cone was less sensitive than the wedge but was superior in its relative freedom from tip bending and damage. The flow-inclination results (fig. 15), obtained from average measurements with the cone erect and inverted, indicated a mean upflow angle of approximately 0.1° which did not appear to change appreciably with Mach number. The scatter in measurements ranged up to about ±0.1° from the mean indicated angularity. Careful measurements of the vertical angularity of wall panels 6 and 12 revealed that the geometric center line between these two panels was different from the horizontal by approximately 0.05° in the direction of the indicated upflow.

Fluctuations of the stream flow angularity with time were measured by means of an electrical pressure pickup in the 3° included-angle cone. The results of these measurements indicated rapid variations of about 0.4° from the mean flow angle shown in figure 15. The fluctuations were greatest at frequencies from approximately 10 to 85 cycles per second throughout the transonic speed range.

Model Testing and Boundary Interference

A preliminary investigation of boundary interference effects on pressure-distribution and drag measurements for a nonlifting body of revolution (fig. 4) in the slotted test section was conducted in order

to ascertain the reliability of typical model test data obtained from the slotted test section of the Langley 8-foot transonic tunnel. This investigation involved the comparison of experimental body data from the slotted test section with essentially interference-free data from other sources and the examination of the slotted-test-section data for the presence of solid blockage and boundary-reflection effects. Experimental data from the investigation were also used in examining several flow phenomena of concern with regard to transonic testing in the slotted test section. The stream Mach numbers at which body data were obtained in the slotted test section ranged from about 0.6 to 1.136. The test Reynolds number, based on model length, ranged from approximately 9.5×10^6 to 11.0×10^6.

Flow phenomena, including shock reflections, with nonlifting body of revolution and wing-body combination at center line of slotted test section.- Some flow phenomena of interest in connection with the transonic testing of models in the slotted test section are illustrated in figures 16 and 17. These data were obtained from tests of the nonlifting body of revolution (fig. 4(c)) and the wing-body combination (fig. 5) at the center line of the slotted test section.

At very high subsonic speeds (figs. 16(a) to 16(c)) the supersonic-flow expansions around the maximum-thickness region of the body of revolution (and the local shock formations associated with model-surface discontinuities and with the compression region near the base of the body) did not extend to the test-section boundary. The failure of the model-field expansions to affect significantly the Mach number distributions at the test-section wall at a stream Mach number of 0.990 (fig. 16(c)) offered evidence as to the essential absence of boundary interference for the model size used and also indicated an alleviation of choking in the slotted test section (tests of the body in a closed test section of the same size would have resulted in choking at a stream Mach number of about 0.985).

At supersonic speeds (figs. 16(d) to 16(l) and 17(a) to 17(d)) the model field shocks and expansions are shown to impinge upon the test-section boundary at axial locations which permit the reflection of disturbances back to the surface of the model in the low-supersonic range. The model nose shock (bow wave) and the expansions over the upstream portion of the model are the disturbances of concern with regard to the production of boundary interference on model measurements. The shock-wave reflections are illustrated (figs. 16(d) to 17(f)) by means of both schlieren pictures and model-surface and wall Mach number distributions. In these figures the lines drawn to connect the schlieren-field shocks with shock locations (maximum compression regions) at the wall were not necessarily accurate representations of the actual shock curvature in either the stream or the boundary layer.

Effect of boundary interference on pressure-distribution and drag measurements for nonlifting body of revolution at center line of slotted test section.- The comparisons of figures 18 to 20 were employed to ascertain the reliability of body pressure-distribution measurements in the slotted test section and in particular to obtain approximate effects of boundary interference on the body pressures at supersonic speeds. The interference-free model-surface pressure distributions given in figure 18 included those obtained from theory for the basic shape of the body (fig. 4(a)), from free-fall tests for a 120-inch-long model (fig. 4(b)), and from tests of the wind-tunnel model (fig. 4(c)) in the 92-inch-diameter axisymmetrical closed test section of reference 1. The closed-test-section data at high subsonic speeds were corrected for blockage effects by use of relations described in reference 9. The free-fall and theoretical distributions shown in figure 18 were obtained from reference 4, which utilized linearized theory and Prandtl-Glauert adjustments for the theoretical distributions at subsonic stream Mach numbers up to 0.95 and methods of reference 10 for the distributions at Mach numbers of and larger than about 1.05. The essentially interference-free pressure distributions shown in figures 19 and 20 were obtained from tests of the wind-tunnel model in the slotted test section of the Langley 16-foot transonic tunnel. The wind-tunnel pressure coefficients used in figures 18 to 20 were averaged from coefficients for upper and lower surfaces in order to reduce possible deviations due to model alinement errors and surface irregularities; coefficients from the Langley 8-foot transonic tunnel were also average values from a number of different runs which repeated the model pressure measurements closely.

At subcritical speeds ($M_o \leq 0.95$) no significant effects of boundary interference on body pressures were expected since reference 2 reported essentially zero interference for a nonlifting body in a slotted test section with a ratio of body cross-sectional area to tunnel cross-sectional area of 0.123 as compared to the ratio of about 0.0014 for the body and test section used for the present investigation. The close agreement expected of the pressure distributions from the slotted test section of the Langley 8-foot transonic tunnel and the various interference-free distributions was realized (figs. 18(a), 19(a), 19(b), and 20), except for discrepancies in the comparisons with free-fall data in the maximum-thickness region of the body (fig. 18(a)); these discrepancies cannot be readily explained unless the free-fall body, which was three times the size of the wind-tunnel model, differed slightly in shape from the wind-tunnel model and the basic shape in this region. Apparent discrepancies in the comparison with free-fall and theoretical pressure distributions near the base of the body (fig. 18(a)) are to be expected since the shapes of both the basic body and the free-fall body differed from that of the wind-tunnel model in this region.

At supercritical stream Mach numbers from about 0.95 to 1.00 the agreement of the pressure-distribution measurements from the slotted

test section of the Langley 8-foot transonic tunnel with those from the Langley 16-foot transonic tunnel (fig. 19(b)) and from free-fall tests (fig. 18(a)) was consistent with that at lower speeds; this agreement attested the essential absence of boundary-interference effects on pressure measurements for the model (cross-sectional area of model only 0.14 percent of tunnel cross-sectional area) in the $\frac{1}{9}$- open slotted test section at stream Mach numbers up to 1.00.

At very low supersonic Mach numbers ($M_o \leq 1.025$) no appreciable effects of boundary-reflected compression waves on model-surface pressures could be detected (figs. 16(e), 18(b), 19(c), and 20) but significant effects of reflected overexpansions were indicated (figs. 19(c), 20(b), and 20(c)). Pressure distributions from the Langley 16-foot transonic tunnel, used as a basis for reference in figures 19 and 20, were not available at close enough Mach number intervals to define completely the variation of the interference-free pressure distribution with Mach number, nor did the data appear to be entirely free of interference effects at a Mach number of 1.019 where overexpansions (apparently due to reflected boundary disturbances similar to those described for the Langley 8-foot transonic tunnel) were indicated (figs. 19(c) and 20(f)). The data were sufficient, however, to provide approximate indications of boundary effects on pressure-distribution measurements for the body in the slotted test section of the Langley 8-foot transonic tunnel.

At supersonic Mach numbers slightly greater than 1.025, the effects of reflected compression shocks on model-surface pressures became significant and increased with Mach number. At Mach numbers of and greater than about 1.040, the reflected shocks were visible in schlieren pictures (figs. 16(g) to 16(n)) and influenced the model-surface pressures strongly (figs. 18(b), 19(c), and 20(b) to 20(f)). The model-surface pressures downstream of the region affected by the reflected compression wave were influenced by overexpansions and those upstream of the compression region were free of boundary interference. At $M \geq 1.120$ the reflected compression was downstream of the model base (fig. 16(n)) and no boundary interference was apparent (fig. 18(b)). The agreement at Mach number 1.2 of interference-free pressure distributions from tests of the model in the 92-inch-diameter axisymmetrical closed test section of reference 1 with theoretical and free-fall distributions from reference 4 is consistent with that of the interference-free slotted-test-section data at lower supersonic Mach numbers (fig. 18(b)). The close agreement of interference-free body-surface distributions from the slotted and closed test sections of the Langley 8-foot transonic tunnel with theoretical distributions (fig. 18(b)) constitutes an experimental verification of the methods of reference 10 for computing pressure distributions on a slender body of revolution at supersonic speeds.

The maximum effects of boundary-reflected disturbances on surface pressures for the fineness-ratio-12 body of revolution in the Langley 8-foot transonic tunnel at supersonic speeds (fig. 21) were determined from maximum differences between experimental pressure coefficients from the Langley 8-foot and 16-foot transonic tunnels as shown in figure 20. The expansion components of boundary-reflected disturbances for the body tested in the $\frac{1}{9}$- open slotted test section of the Langley 8-foot transonic tunnel were shown to affect body-surface pressures more strongly than did the compression component at stream Mach numbers less than 1.035 whereas the reverse was indicated at Mach numbers greater than 1.035. The indications of figure 21 are only approximate, however, because of the limited amount of data available from the Langley 16-foot transonic tunnel.

The effects of boundary-reflected disturbances on pressure distributions for the nonlifting body of revolution at the center line of the Langley 8-foot transonic tunnel slotted test section (figs. 18 to 21) were interpreted in terms of effects on body drag coefficients. In ascertaining these effects, comparisons were made (fig. 22) of body drag coefficients obtained from pressure-distribution and force tests in the slotted test section of the Langley 8-foot transonic tunnel with essentially interference-free data from free-fall tests (reference 4) and from pressure-distribution tests in the Langley 16-foot transonic tunnel (slight interference effects present in the latter data measured at $M_o = 1.019$ were removed, approximately, before determining the pressure drag). The drag coefficients from pressure-distribution tests were obtained by integrating measured model-surface pressures and included skin-friction drag estimates from reference 11. The force-test body drag coefficients shown in figure 22 were obtained from unpublished experimental data for the model described in reference 12 and were corrected for sting-support tares. Estimated maximum inaccuracies of the body drag coefficients (based on body frontal area) shown in figure 22 were approximately ±0.016 for the data obtained from force tests in the Langley 8-foot transonic tunnel and within ±0.010 for those obtained from free-fall tests.

Approximate boundary-interference effects on body drag measurements for the nonlifting body of revolution at the center line of the Langley 8-foot transonic tunnel slotted test section were taken as the differences between these drag measurements and the interference-free measurements (fig. 22). Correlation of these drag differences (fig. 22) with corresponding body-surface pressure distributions (figs. 18 to 20) revealed the close interrelation of the pressure-distribution and drag measurements and the dependence of the drag-coefficient changes on the effects of boundary-reflected disturbances. The indicated body drag decrements (fig. 22) at Mach numbers from 1.00 to 1.02 were apparently

due to the effect of reflected overexpansions slightly upstream of the maximum-thickness region of the body, whereas drag increments at Mach numbers from 1.02 to 1.07 and drag decrements at Mach numbers from 1.07 to about 1.12 were due to the passage over the rear portion of the body of reflected overexpansions and compressions, respectively. At Mach numbers greater than about 1.12 the slight discrepancy between the free-fall data and those from force and pressure-distribution tests in the Langley 8-foot transonic tunnel could be attributed to differences in body shape or to possible inadequacies in sting-support tare corrections but the magnitude of the indicated discrepancy is within estimated possible inaccuracies in the experimental data. The maximum effects of boundary reflections on body drag coefficients with the body at the slotted-test-section center line did not exceed about 0.04 when coefficients were based on body frontal area. Although these maximum boundary-reflection effects were not much greater than the accuracy of measurement normally attainable by means of the internal balance system used for measuring model forces, they were considered sufficient to justify a brief experimental investigation of a possible means of reducing the effects.

Reduction of interference effects at supersonic speeds by testing model off center line of slotted test section.- An attempt to reduce the intensity of boundary-reflected disturbances at the model was made by testing the nonlifting body of revolution (fig. 4(c)) at a distance of about 10.3 inches off the geometric center line of the slotted test section. Body drag coefficients obtained from pressure-distribution measurements with the body located off the test-section center line were affected less by boundary interference than were those obtained from tests of the body at the center line (see fig. 22). This reduction in interference effects on body drag can be attributed to a slight reduction in intensity (and distribution over a greater axial distance) of boundary-reflected disturbances at the body surface, as shown by the comparison (fig. 23) of center-line and off-center body-surface Mach number distributions at a stream Mach number of 1.050 (this Mach number was used for the comparisons in order that effects of both compression and expansion components of boundary-reflected disturbances might be illustrated). The slight reduction in intensity of the reflected compression from the portion of the boundary nearest to the off-center model (fig. 23) can be attributed to the avoidance of concentrated focusing from all wall panels. The significant reduction in intensity of compressions from wall panels farthest from the off-center model (fig. 23) is believed due not only to the reduced focusing effect and to the greater distance from the boundary but also to their interaction with overexpansions from wall panels nearest to the model.

The off-center location of the model therefore appears advantageous with regard to the reduction in intensity of boundary-reflected disturbances, especially the expansion components of such disturbances, and the attendant reduction in interference effects on model drag and pressure-distribution measurements. A disadvantage of the off-center location,

[redacted]

however, lies in the significant reduction in length of the region available for strictly interference-free supersonic testing.

Model lengths for interference-free supersonic testing at center line of slotted test section.- It has been shown that at supersonic Mach numbers the model-surface pressures upstream of the region affected by the boundary-reflected compression are free of boundary-interference effects (figs. 18 to 20) and that for a given Mach number the length of the interference-free region is greatest when the model is located at the center line of the test section (fig. 23). The axial distance L_S required for the bow wave ahead of the model to reflect from the test-section boundary and strike the surface of the model at the test-section center line is shown in figure 24. This distance, obtained from schlieren pictures and pressure measurements at stream Mach numbers from 1.04 to 1.126 and from pressure measurements at Mach numbers as low as 1.025 is expressed in terms of the distance L_M required for the reflection of Mach lines from the tunnel wall. The ratio L_S/L_M increased from a value of about 0.35 at a stream Mach number of 1.025 to about 0.81 at a Mach number of about 1.10 after which the ratio remained approximately constant except near a Mach number of 1.109 where it tended to increase slightly and then decrease as the reflected shock approached and moved downstream of the base of the model. This influence of the model tail shock on the progress of the reflected shock past the base of the model is illustrated in figures 16(l) and 16(m). An L_S/L_M value of 0.815 obtained from tests of a somewhat similar body at a stream Mach number of 1.2 in the closed nozzle of reference 1 was consistent with those shown in figure 24 for Mach numbers greater than about 1.10. At the low supersonic Mach numbers of this investigation, the L_S/L_M ratio was approximately the same for both the axisymmetrical fuselage and the swept-back wing attached to the fuselage.

The distance ratios given in figure 24 neglect the effect of the model boundary layer, which permits the compression due to the incident shock to be transmitted several inches upstream of the shock location, and are therefore not strictly representative of axial distances available for interference-free supersonic testing. If the compression region is assumed to extend about 3 inches upstream of the shock location, the axial distances available for interference-free supersonic testing with the model at the center line of the slotted test section would range from about 4 inches at a Mach number of 1.025 to approximately 36 inches at a Mach number of 1.14 (fig. 25) and would not exceed 75 percent of the axial distance required for the reflection of Mach lines. At the very low supersonic Mach numbers the length of the interference-free test region is influenced to some extent by the location of the detached shock wave ahead of the model.

Location of detached shocks ahead of axisymmetrical nonlifting bodies.- Schlieren and pressure data for the body of revolution (see fig. 16) and schlieren pictures of shocks ahead of blunt-nose (90° angle) total-pressure tubes (fig. 26) tested in the slotted section of the Langley 8-foot transonic tunnel provided experimental information concerning the location of detached shock waves ahead of axisymmetrical bodies at low-supersonic speeds. The experimental data from the Langley 8-foot transonic tunnel are compared with experimental data from other sources (references 4 and 13 to 15) and with approximate theory (reference 13) in figure 27. The data used in these comparisons are expressed in terms of the ratio of shock distance ahead of body sonic point to the body radius at the sonic point, x_{SB}/y_{SB}, a parameter used in reference 13. The sonic point for the body of revolution tested in the Langley 8-foot transonic tunnel was obtained from body-surface pressure measurements (average values from a large number of runs) at each test Mach number; that for the 90° body (total-pressure tube) tested in the Langley 8-foot transonic tunnel was assumed to occur at the shoulder of the body for all Mach numbers.

The experimental locations of the bow waves ahead of the body of revolution in the slotted test section of the Langley 8-foot transonic tunnel agreed closely with experimental data from references 4 and 13 to 15; those for the 90° body in the Langley 8-foot transonic tunnel agreed closely except at stream Mach numbers of 1.015 and 1.036 (fig. 27). The apparent discrepancies offered by these two experimental points are not due to errors in measurement; they are believed to be due to the two-dimensional nature of the bow wave ahead of the row of total-pressure tubes. (Reference 13 shows the ratio x_{SB}/y_{SB} to be much larger for the two-dimensional case than for the axisymmetrical case.) The single bow wave existing ahead of the row of eight total-pressure tubes at the low-supersonic Mach numbers of 1.015 and 1.036 changes to individual bow waves ahead of each tube at higher Mach numbers (fig. 26).

The general agreement of the experimental data with theoretical approximations (geometric and continuity methods) from reference 13 is considered satisfactory. The experimental data appear to agree more closely with the geometric-method approximations at very low supersonic Mach numbers and with the continuity-method approximations at stream Mach numbers greater than approximately 1.10.

Applicability of boundary-reflection information from present investigation to tests of other models in slotted test section.- Although each wind-tunnel test model offers a different problem with regard to the effects of boundary-reflected disturbances, the results of the body-of-revolution tests reported earlier in this paper should prove useful in predicting probable disturbance phenomena and evaluating experimental data for other models.

For strictly interference-free supersonic testing the model length is dependent on the axial distance required for model disturbances to reflect from the test-section boundary back to the model surface; this distance varies with Mach number and is greatest when the model is located at the test-section center line. The shock-reflection distances shown in figure 24 and the interference-free model lengths given in figure 25 are applicable only for center-line testing of models of approximately the size and shape of the body of revolution used in this investigation; larger models of this shape or bluff bodies of the same maximum diameter will produce bow waves located farther upstream and thereby reduce the reflection distances and model lengths shown in figures 24 and 25, respectively. The approximate interference-free model length for a given axially symmetric shape can be estimated by use of figures 24 and 27, together with knowledge of the sonic-point location and the model radius at the sonic point. At very low supersonic Mach numbers the use of figure 27 to ascertain detached-shock locations ahead of axially symmetric bodies is limited to single bodies; several adjacent axially symmetric bodies located in the same plane of measurement may produce detached shocks located considerably upstream of that for a single body (see figs. 26 and 27).

For supersonic testing of models whose lengths permit the impingement of boundary-reflected disturbances, the effects of boundary interference on the free-air characteristics of the models are dependent on the model configurations and the model locations with respect to the test-section center line (interference effects less for model off center line than for one on center line). The effects of boundary reflections on pressure and drag measurements for the fineness-ratio-12 body of revolution used in the present investigation are applicable only for models of approximately the same size and shape, but the described flow phenomena with the body of revolution in the slotted test section should be useful in interpreting the direction of boundary-reflection effects on test data for other models. The influence of model-attitude changes on indicated boundary-reflection effects for the body of revolution was not included in the present investigation, but probable approximate influences may be inferred from experimental results given in reference 16. Reference 16 also indicates that flow disturbances capable of introducing drag-coefficient changes of the order of 0.002 (drag coefficient based on wing plan-form area) may not greatly affect the lift and pitching-moment characteristics of a complete airplane model. Additional studies are needed to verify and supplement these preliminary indications of boundary-reflection effects on models at lifting attitudes in the slotted test section.

CONCLUDING REMARKS

The characteristics of the transonic flow in the slotted test section of the Langley 8-foot transonic tunnel were investigated. The results of flow surveys, with and without a typical model in the slotted test section, warranted the following conclusions:

1. The uniformity of the transonic flow near the center line of the slotted test section was entirely satisfactory for testing purposes. Deviations from the average stream Mach number in a model test region 36 inches long and 30 inches in diameter generally increased with Mach number but did not exceed approximately 0.006 at stream Mach numbers up to 1.13 provided the tunnel wall surfaces were kept sufficiently smooth.

2. The ratio of the test-chamber pressure to stream total pressure provided a reliable index of the test-section Mach number independent of model configuration or attitude.

3. The direction of the air stream agreed within the limits of experimental error (0.1°) with the geometric center line of the test section.

4. The use of slots to reduce choking limitations at stream Mach numbers near 1.0, reported earlier for small tunnels, was substantiated by tests of a 3.33-inch-diameter body of revolution in the approximately 88-inch-diameter slotted test section.

5. Interference effects due to boundary-reflected disturbances were present in pressure-distribution and drag measurements for a 33.5-inch-long fineness-ratio-12 body of revolution (nonlifting) in the slotted test section at low supersonic speeds; the effects were reduced by testing the body off the test-section center line in order to avoid focusing of the reflected disturbance waves. No boundary interference was present at the higher supersonic speeds attained.

6. The model length for interference-free supersonic testing increased with Mach number but did not exceed about 75 percent of the axial distance required for reflection of Mach lines.

7. Experimental locations of bow waves ahead of axially symmetric bodies were in satisfactory agreement with theoretical locations predicted from the approximate methods of NACA TN 1921.

8. An experimental verification of the method of NACA TN 1768 for predicting pressure distributions over slender bodies of revolution at

supersonic speeds is afforded by the close agreement of theoretical pressure distributions for a fineness-ratio-12 body of revolution with interference-free distributions measured in the Langley 8-foot transonic tunnel.

Langley Aeronautical Laboratory
National Advisory Committee for Aeronautics
Langley Field, Va.

REFERENCES

1. Ritchie, Virgil S., Wright, Ray H., and Tulin, Marshall P.: An 8-Foot Axisymmetrical Fixed Nozzle for Subsonic Mach Numbers up to 0.99 and for a Supersonic Mach Number of 1.2. NACA RM L50A03a, 1950.

2. Wright, Ray H., and Ward, Vernon G.: NACA Transonic Wind-Tunnel Test Sections. NACA RM L8J06, 1948.

3. Wright, Ray H., and Ritchie, Virgil S.: Characteristics of a Transonic Test Section with Various Slot Shapes in the Langley 8-Foot High-Speed Tunnel. NACA RM L51H10, 1951.

4. Thompson, Jim Rogers: Measurements of the Drag and Pressure Distribution on a Body of Revolution throughout Transition from Subsonic to Supersonic Speeds. NACA RM L9J27, 1950.

5. Loving, Donald L., and Estabrooks, Bruce B.: Transonic-Wing Investigation in the Langley 8-Foot High-Speed Tunnel at High Subsonic Mach Numbers and at a Mach Number of 1.2. Analysis of Pressure Distribution of Wing-Fuselage Configuration Having a Wing of 45° Sweepback, Aspect Ratio 4, Taper Ratio 0.6, and NACA 65A006 Airfoil Section. NACA RM L51F07, 1951.

6. Staff of the Computing Section, Center of Analysis (Under Direction of Zdeněk Kopal): Tables of Supersonic Flow around Cones. Tech. Rep. No. 1, M.I.T., 1947.

7. Neice, Mary M.: Tables and Charts of Flow Parameters across Oblique Shocks. NACA TN 1673, 1948.

8. Ward, Vernon G., Whitcomb, Charles F., and Pearson, Merwin D.: An NACA Transonic Test Section with Tapered Slots Tested at Mach Numbers to 1.26. NACA RM L50B14, 1950.

9. Herriot, John G.: Blockage Corrections for Three-Dimensional-Flow Closed-Throat Wind Tunnels, with Consideration of the Effect of Compressibility. NACA Rep. 995, 1950. (Formerly NACA RM A7B28.)

10. Thompson, Jim Rogers: A Rapid Graphical Method for Computing the Pressure Distribution at Supersonic Speeds on a Slender Arbitrary Body of Revolution. NACA TN 1768, 1949.

11. Young, A. D.: The Calculation of the Total and Skin Friction Drags of Bodies of Revolution at Zero Incidence. R. & M. No. 1874, British A.R.C., 1939.

12. Osborne, Robert S.: A Transonic-Wing Investigation in the Langley 8-Foot High-Speed Tunnel at High Subsonic Mach Numbers and at a Mach Number of 1.2. Wing-Fuselage Configuration Having a Wing of 45° Sweepback, Aspect Ratio 4, Taper Ratio 0.6, and NACA 65A006 Airfoil Section. NACA RM L50H08, 1950.

13. Moeckel, W. E.: Approximate Method for Predicting Form and Location of Detached Shock Waves ahead of Plane or Axially Symmetric Bodies. NACA TN 1921, 1949.

14. Heberle, Juergen W., Wood, George P., and Gooderum, Paul B.: Data on Shape and Location of Detached Shock Waves on Cones and Spheres. NACA TN 2000, 1950.

15. Laitone, Edmund V., and Pardee, Otway O'M.: Location of Detached Shock Wave in Front of a Body Moving at Supersonic Speeds. NACA RM A7B10, 1947.

16. Ritchie, Virgil S.: Effects of Certain Flow Nonuniformities on Lift, Drag, and Pitching Moment for a Transonic-Airplane Model Investigated at a Mach Number of 1.2 in a Nozzle of Circular Cross Section. NACA RM L9E20a, 1949.

[redacted]

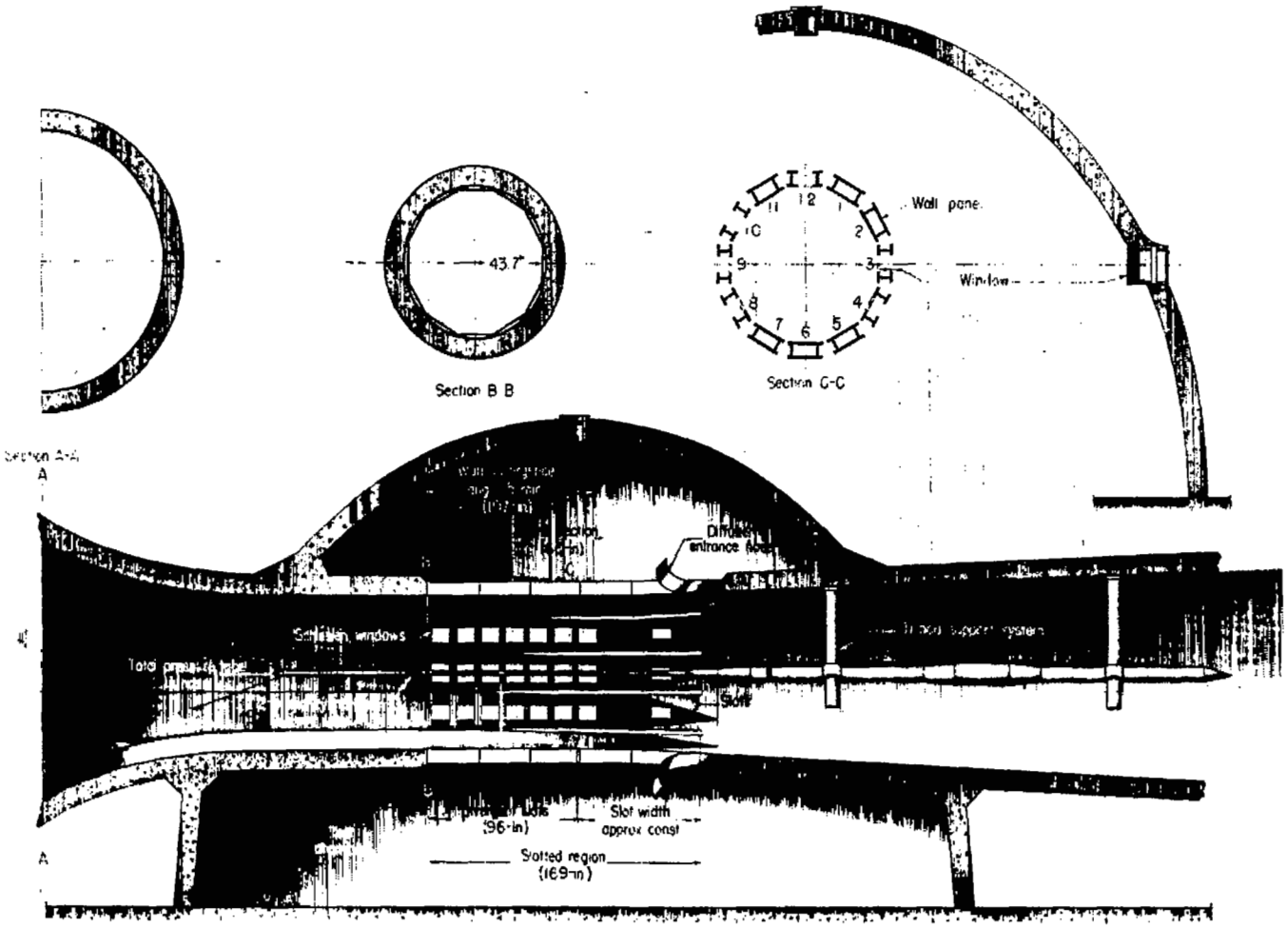

Figure 1.- Views of throat region of Langley 8-foot transonic tunnel showing slotted test section, cylindrical survey tube, and support system.

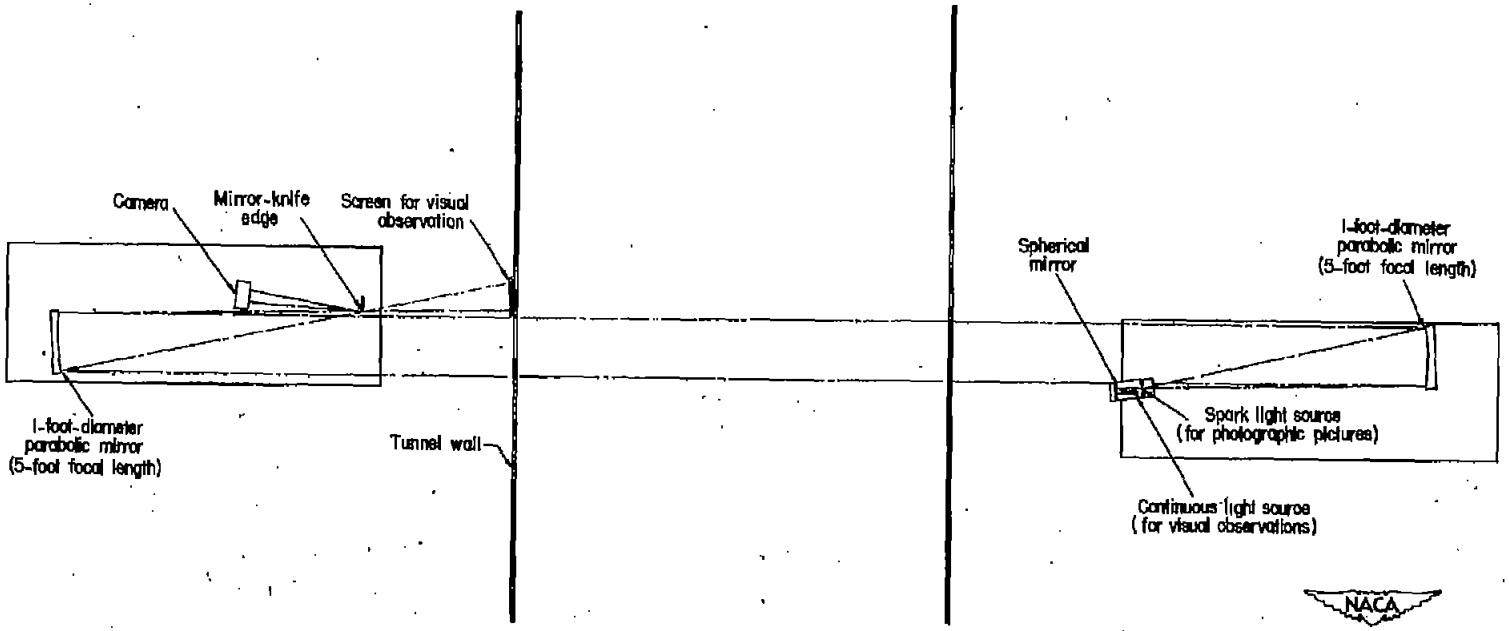

Figure 2.- Temporary schlieren system used in connection with slotted-test-section flow surveys.

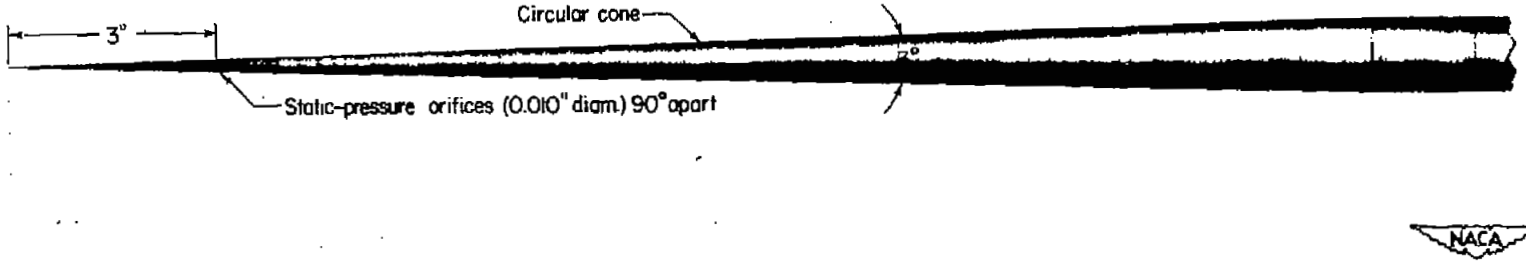

Figure 3.- Null-pressure-type instrument (3° cone) used for measuring angularity of flow in slotted test section.

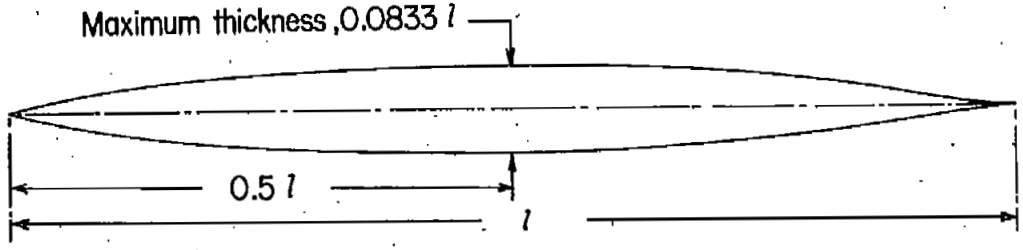

(a) Basic body shape.

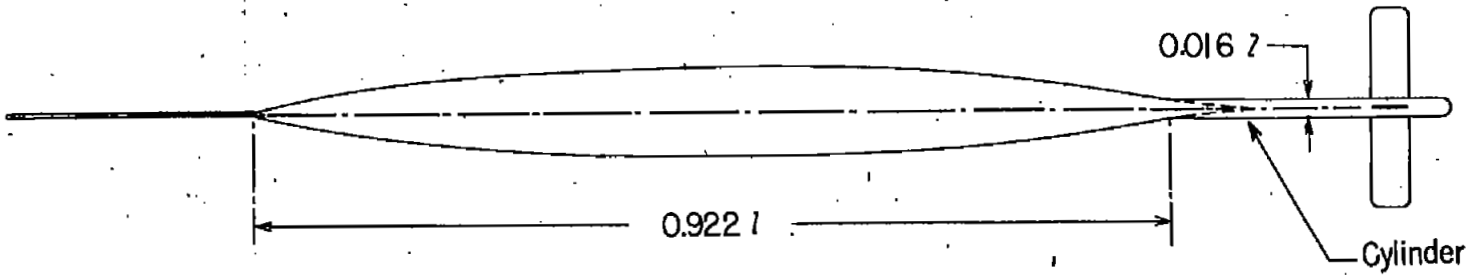

(b) Free-fall body.

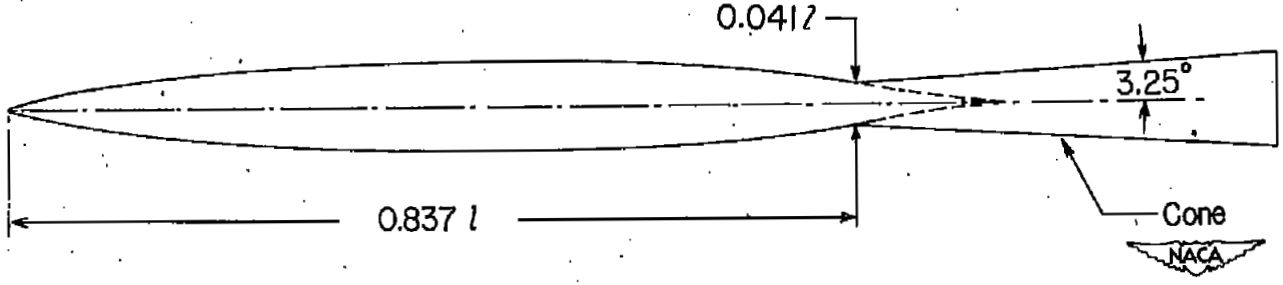

(c) Wind-tunnel model.

Figure 4.- Body of revolution used for comparison of body-surface pressure distributions obtained from wind-tunnel tests with those from free-fall tests and theory.

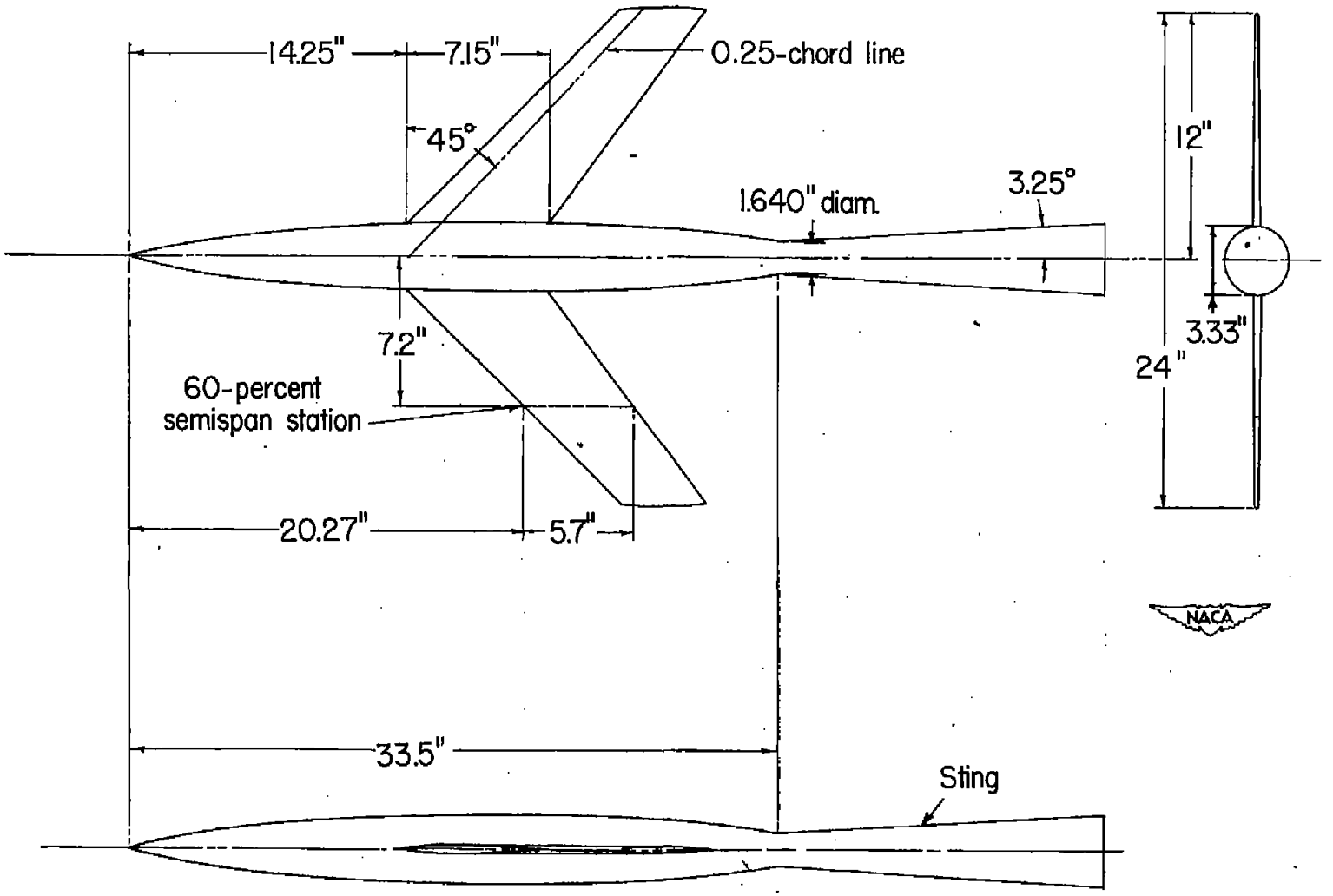

Figure 5.- Transonic-airplane model investigated in connection with flow surveys in slotted test section.

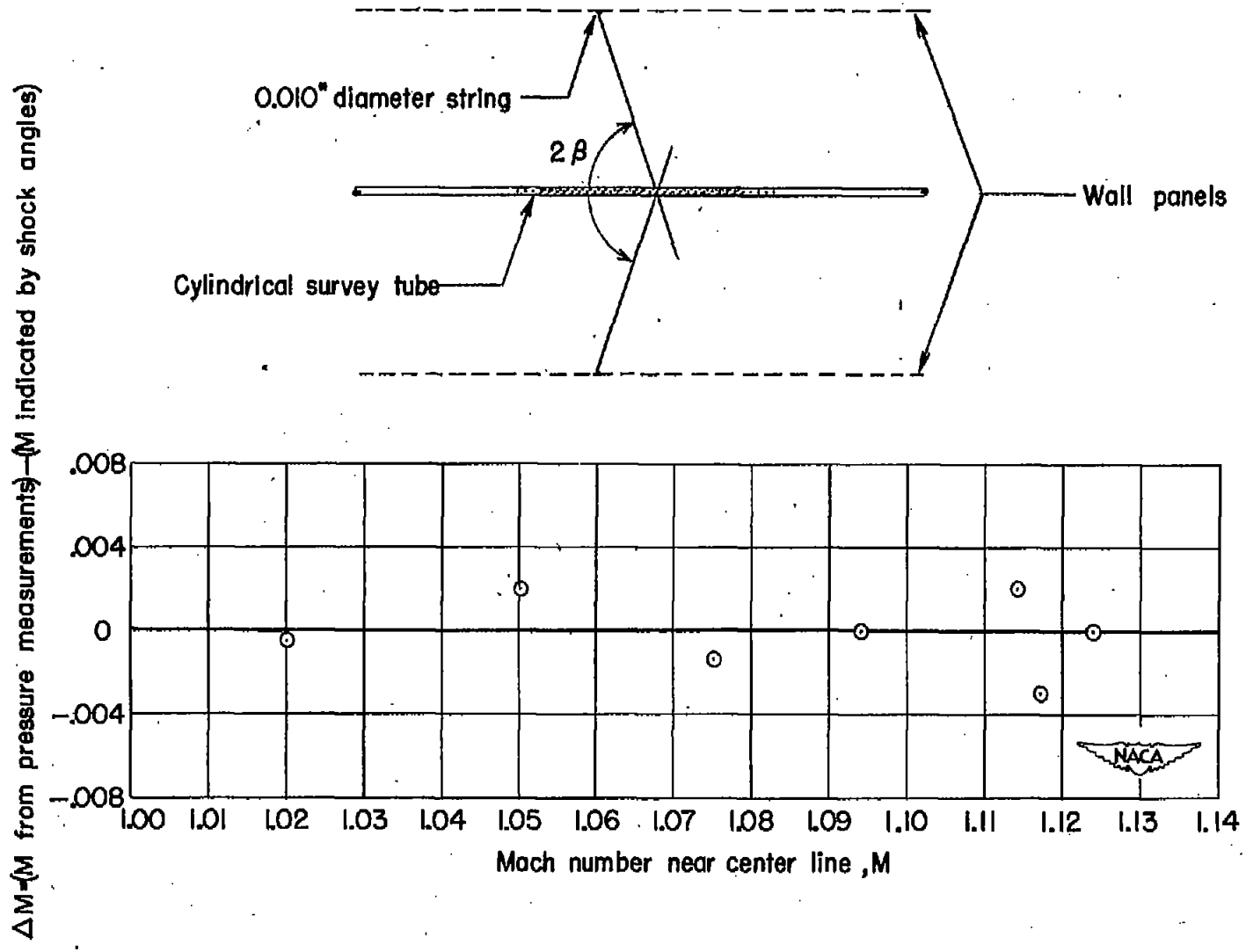

Figure 6.- Agreement of flow Mach numbers obtained from pressure measurements at test-section center line with those indicated by measured angularity of weak shocks produced by 0.010-inch-diameter strings fastened to wall panels.

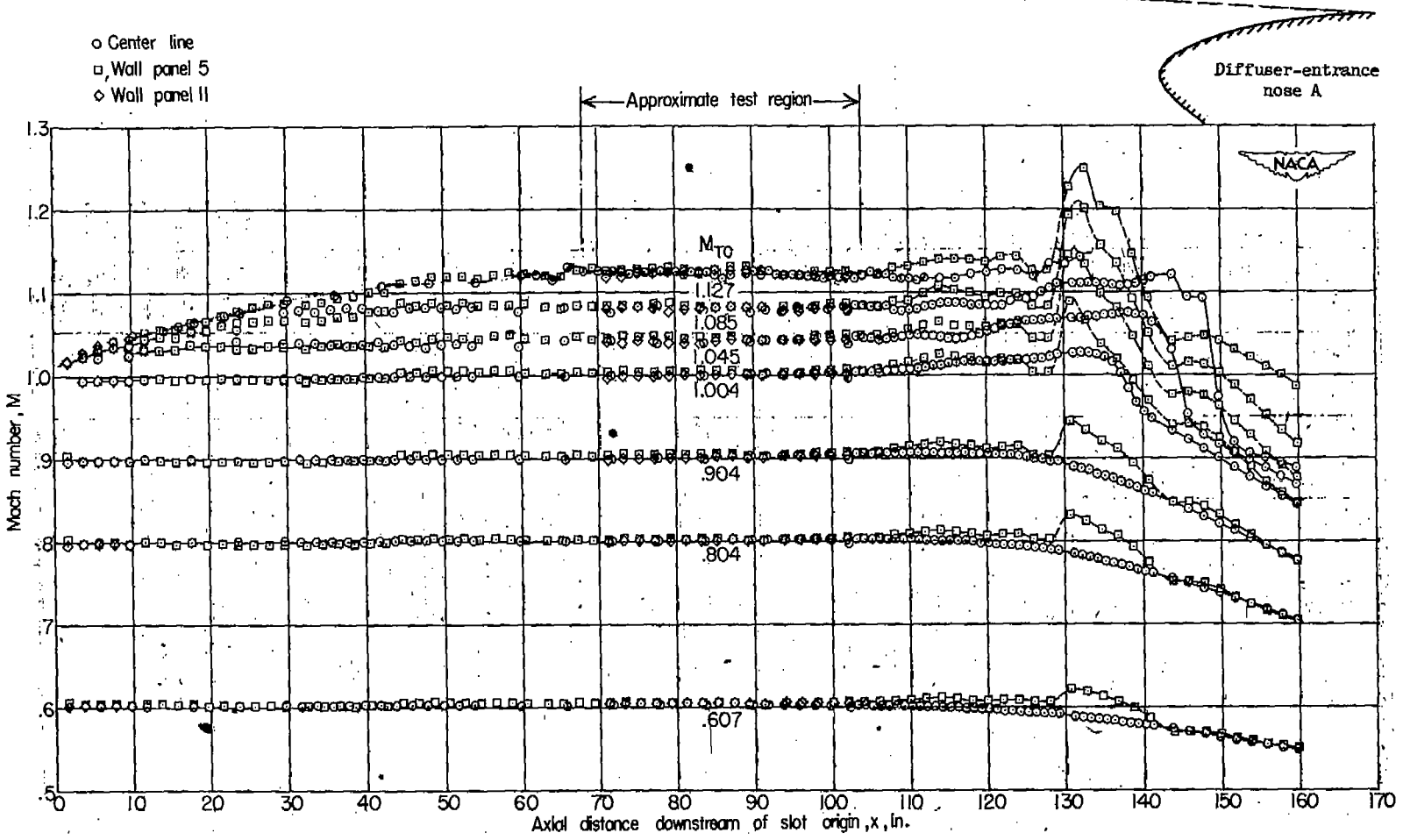

Figure 7.- Mach number distributions measured axially along center line and wall of entire throat region of tunnel with model removed from slotted test section. Diffuser-entrance nose A.

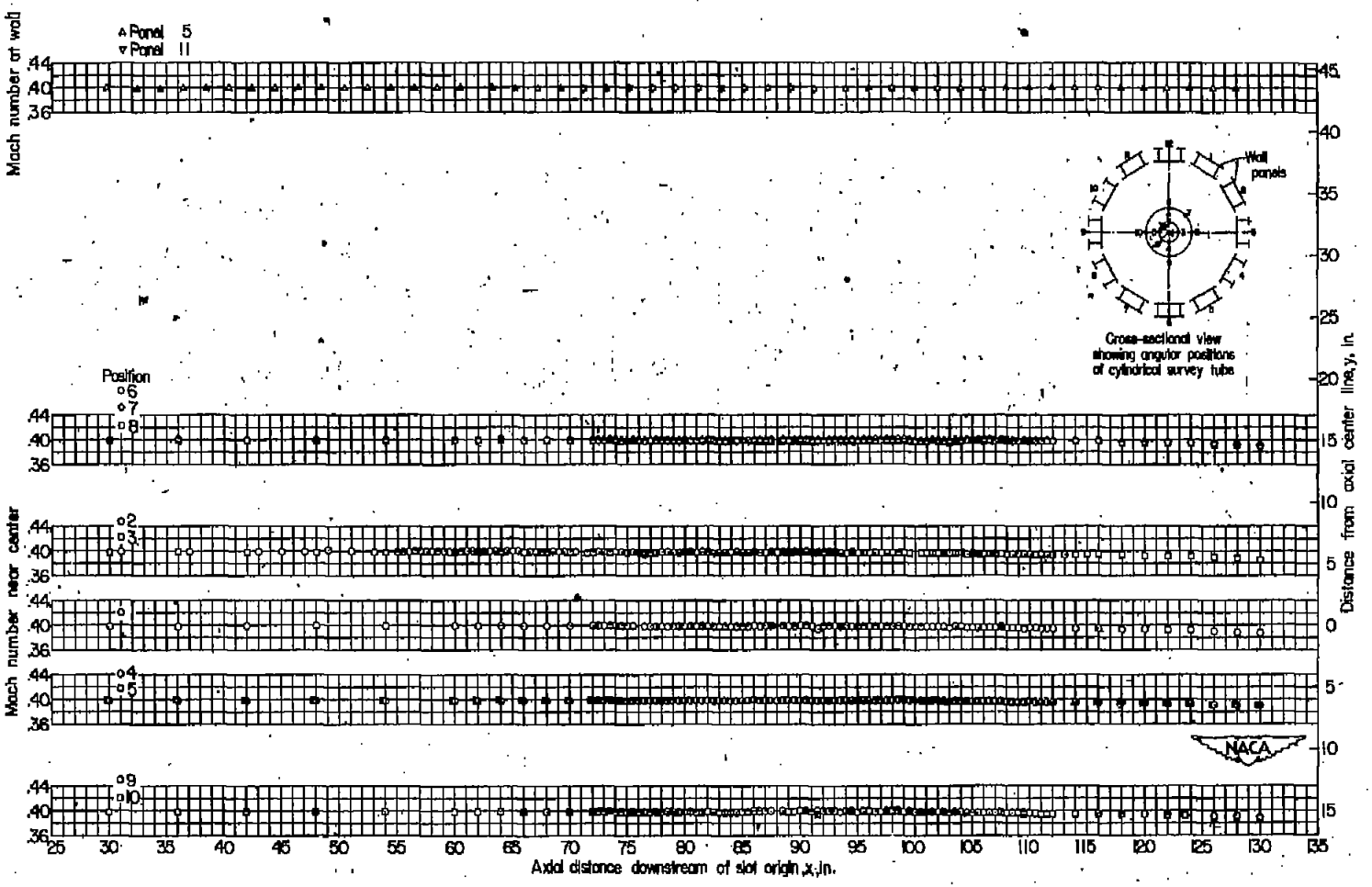

(a) $M_{TC} = 0.40$.

Figure 8.- Basic flow-survey charts showing Mach number distributions axially along wall and near center line of slotted test section with model removed. Diffuser-entrance nose A.

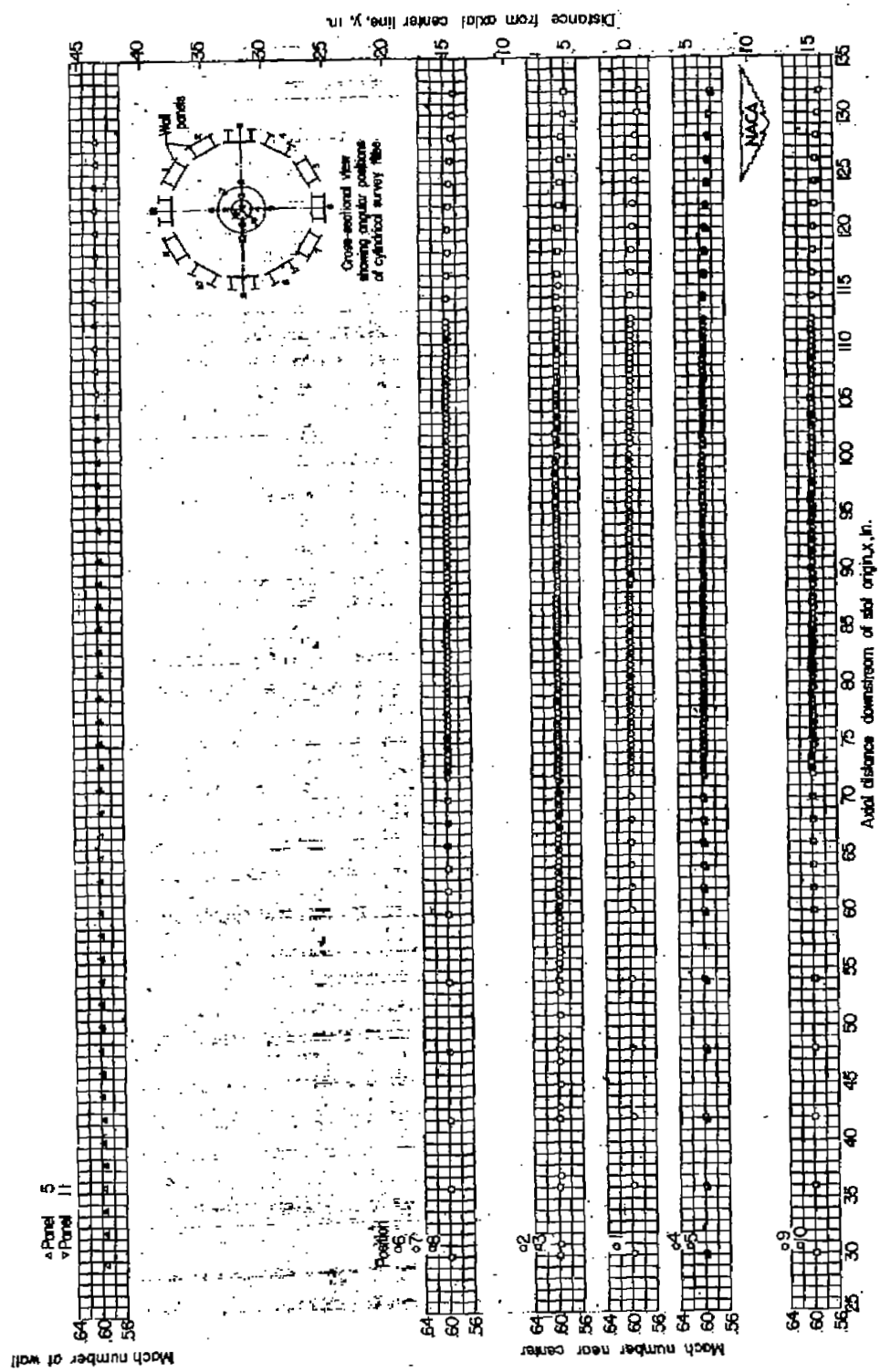

(b) $M_{TC} = 0.60$.

Figure 8.- Continued.

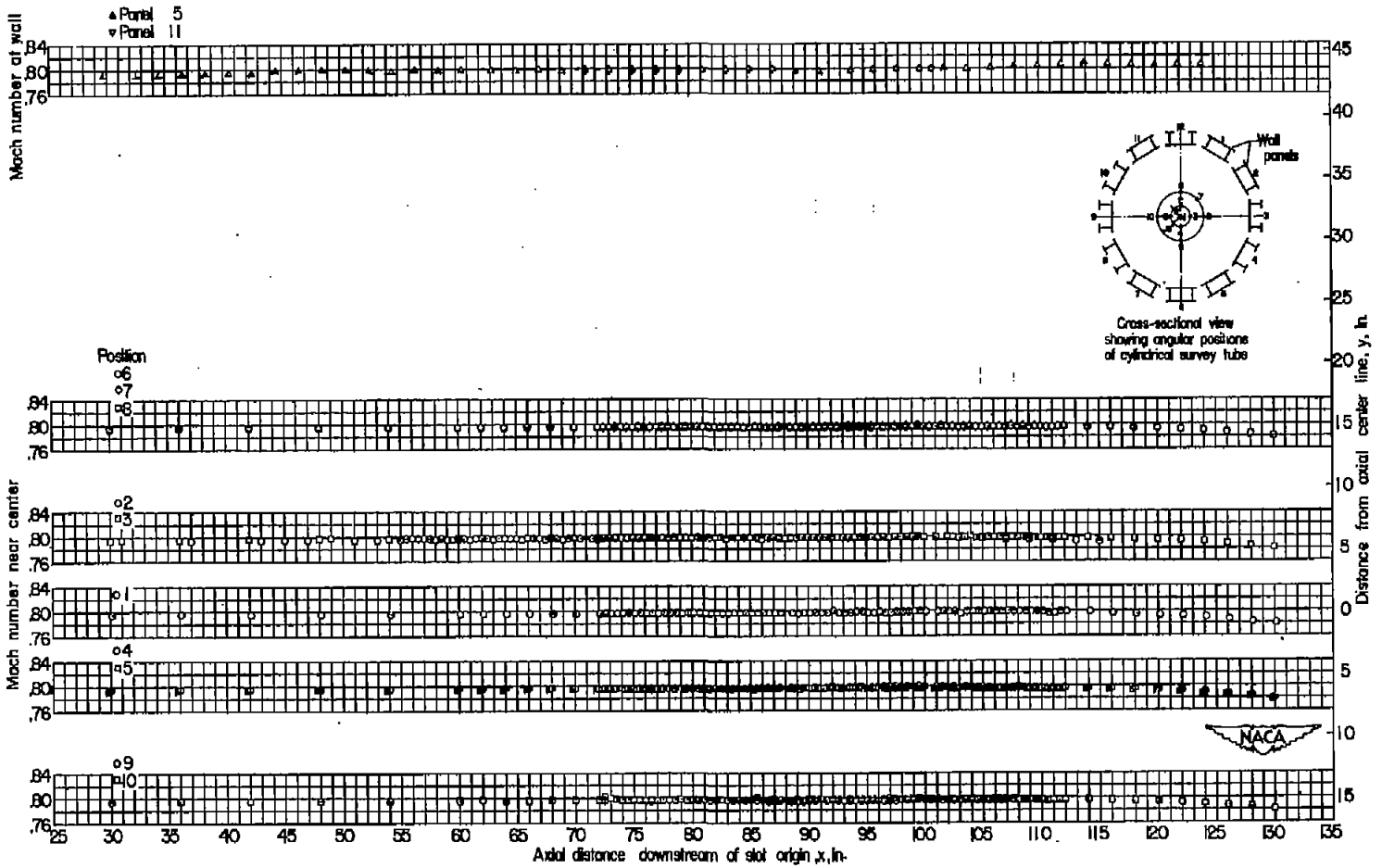

(c) $M_{TC} = 0.80$.

Figure 8.- Continued.

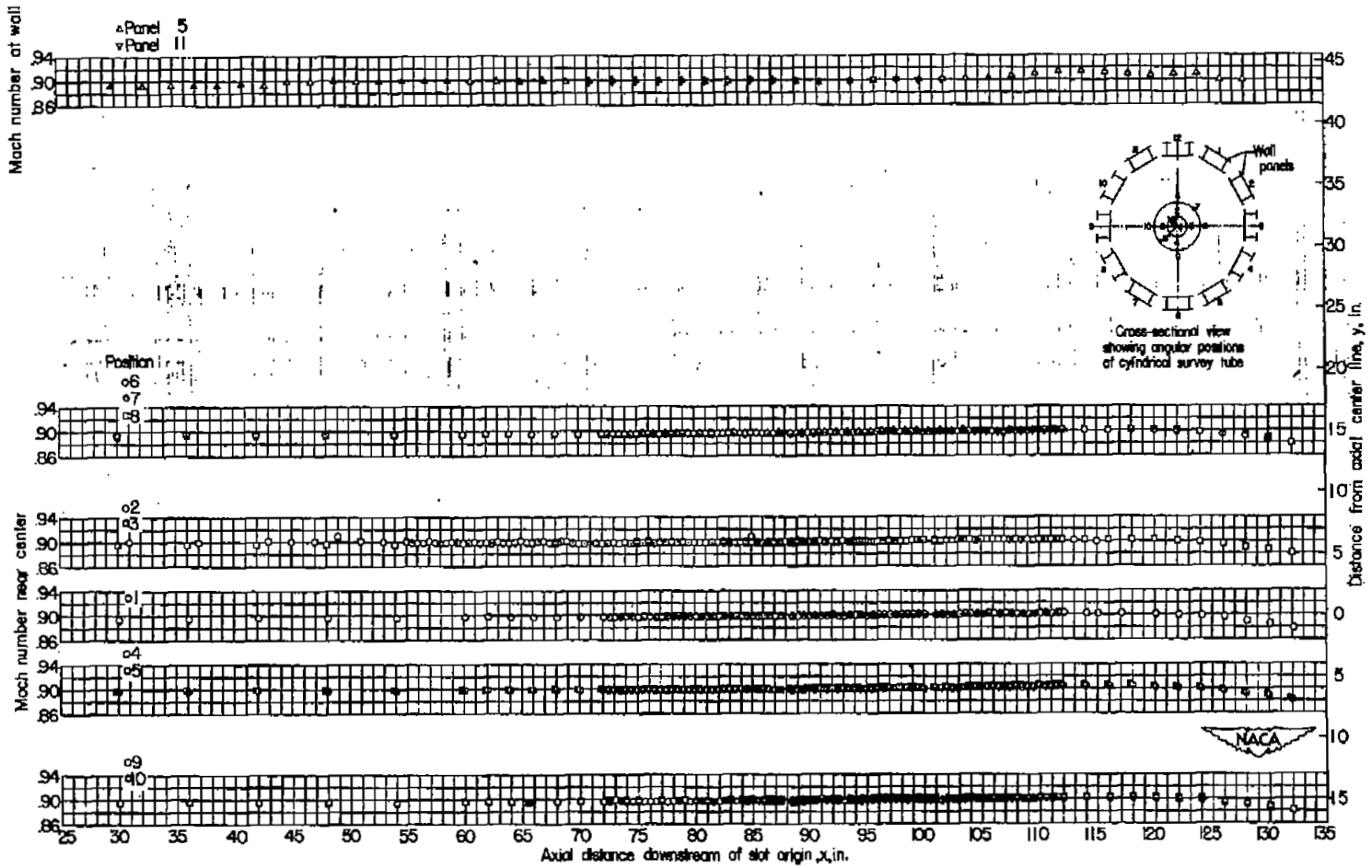

(d) $M_{TC} = 0.90$.

Figure 8.- Continued.

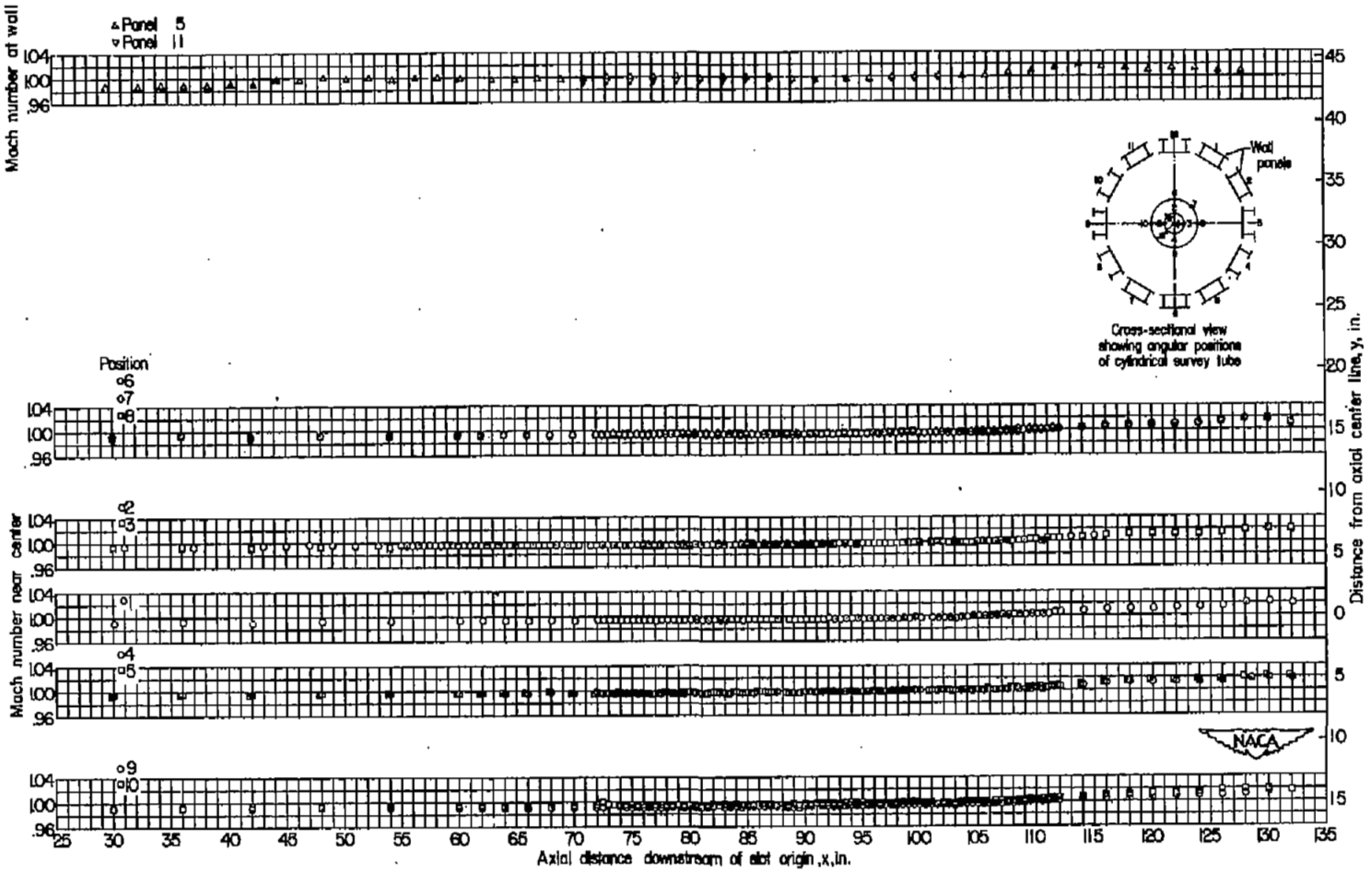

(e) $M_{TC} = 1.00$.

Figure 8.- Continued.

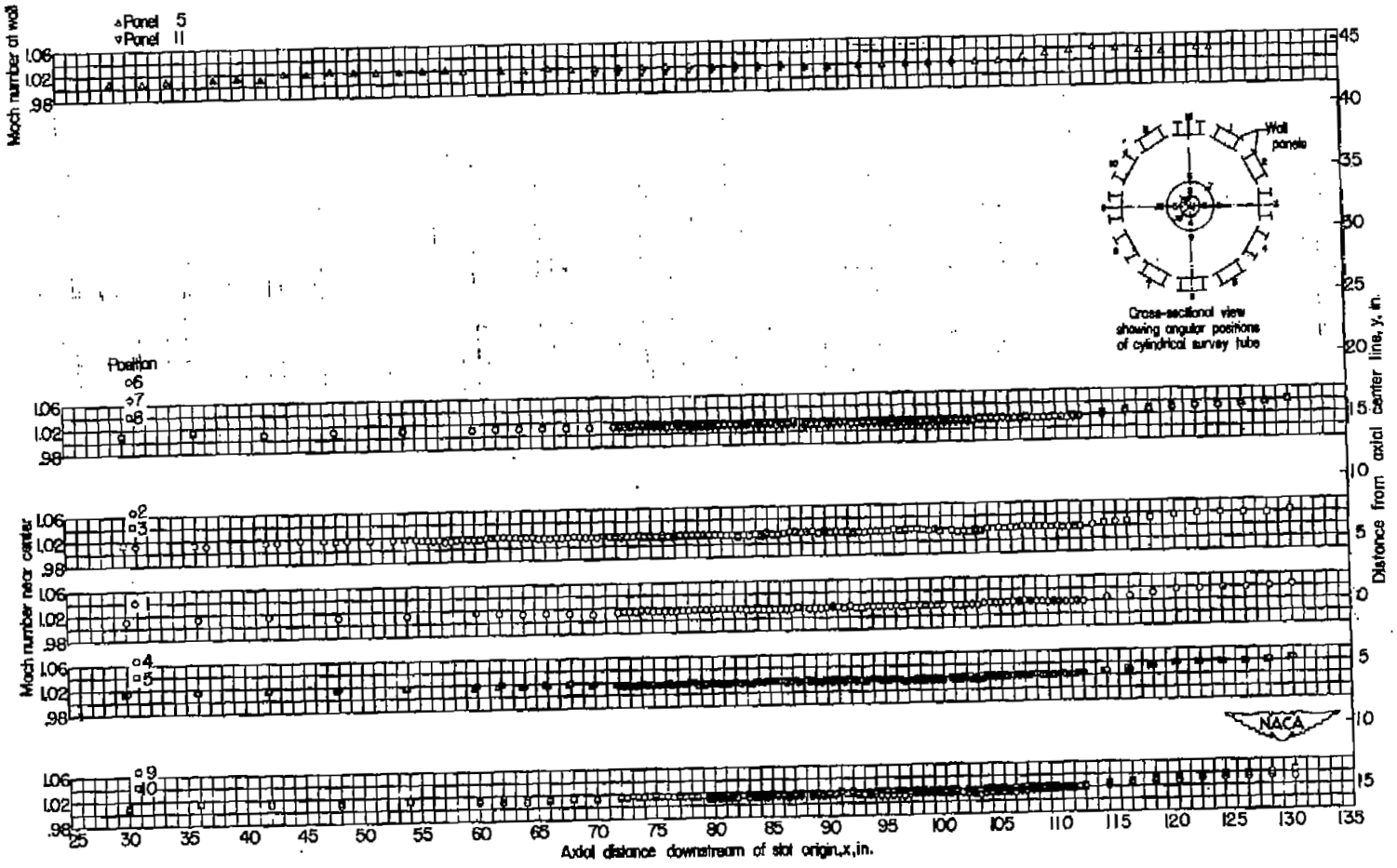

(f) $M_{TC} = 1.02$.

Figure 8.- Continued.

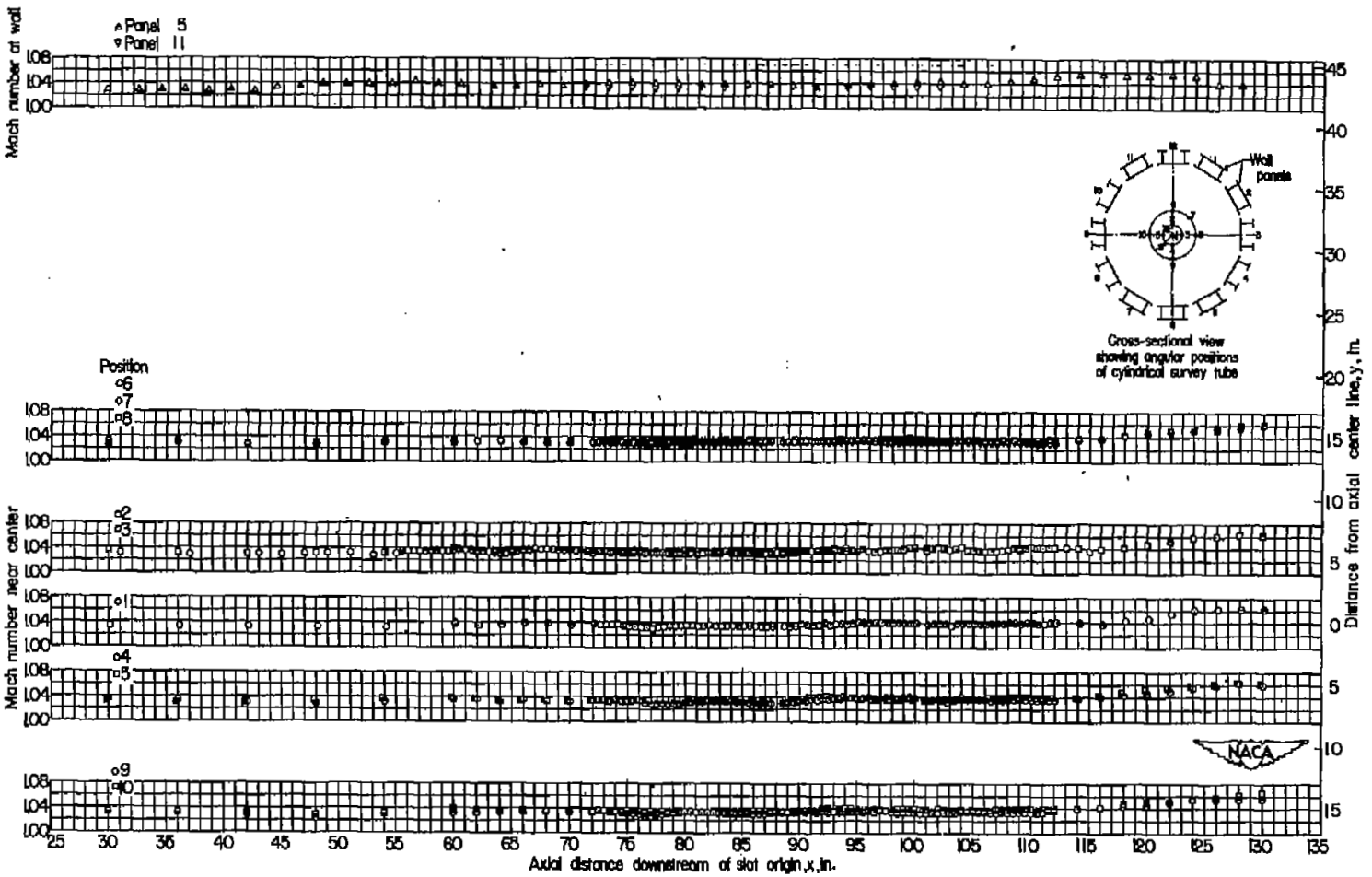

(g) $M_{TC} = 1.04$.

Figure 8.- Continued.

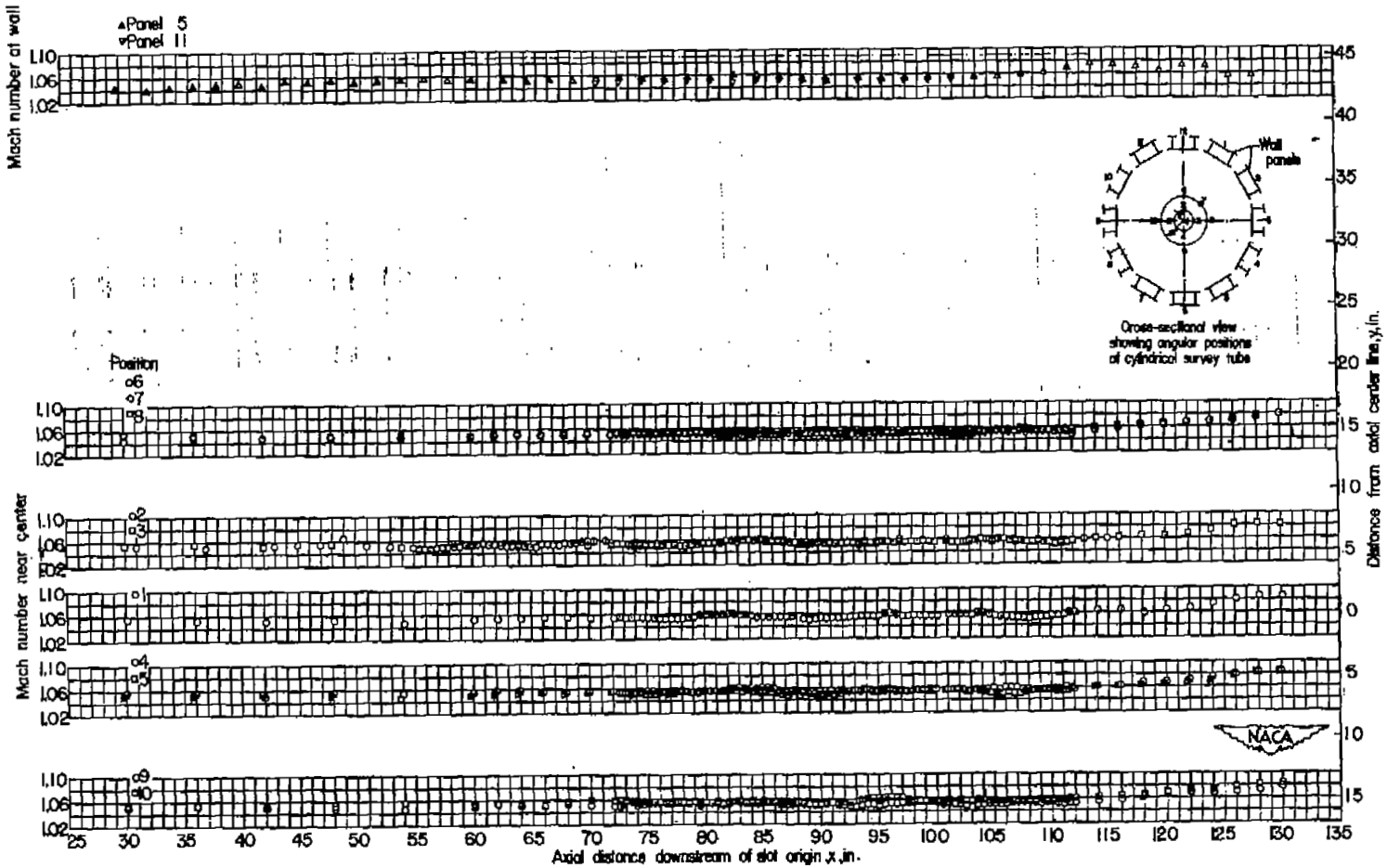

(h) $M_{TC} = 1.06$.

Figure 8.- Continued.

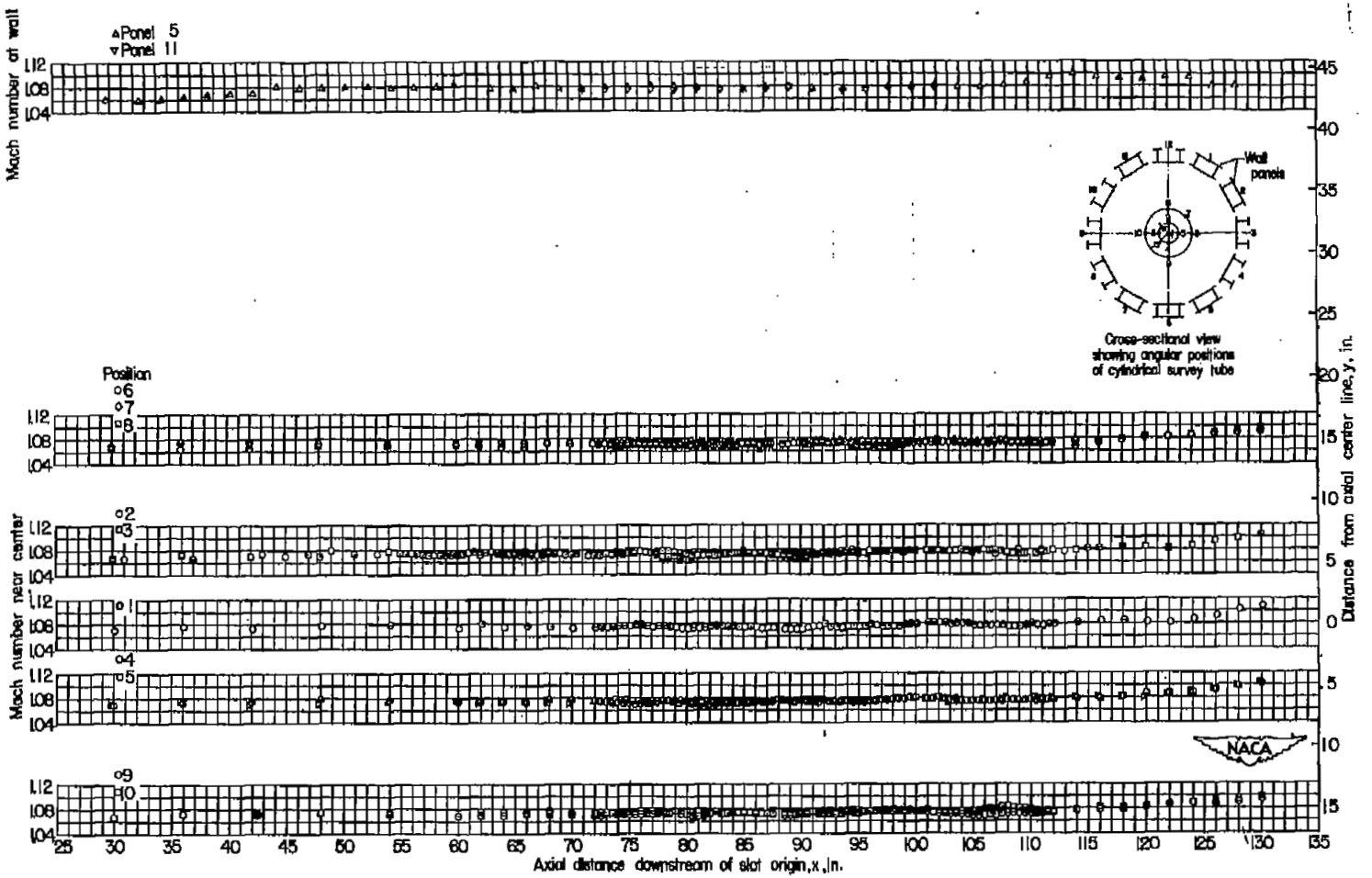

(i) $M_{TC} = 1.08$.

Figure 8.- Continued.

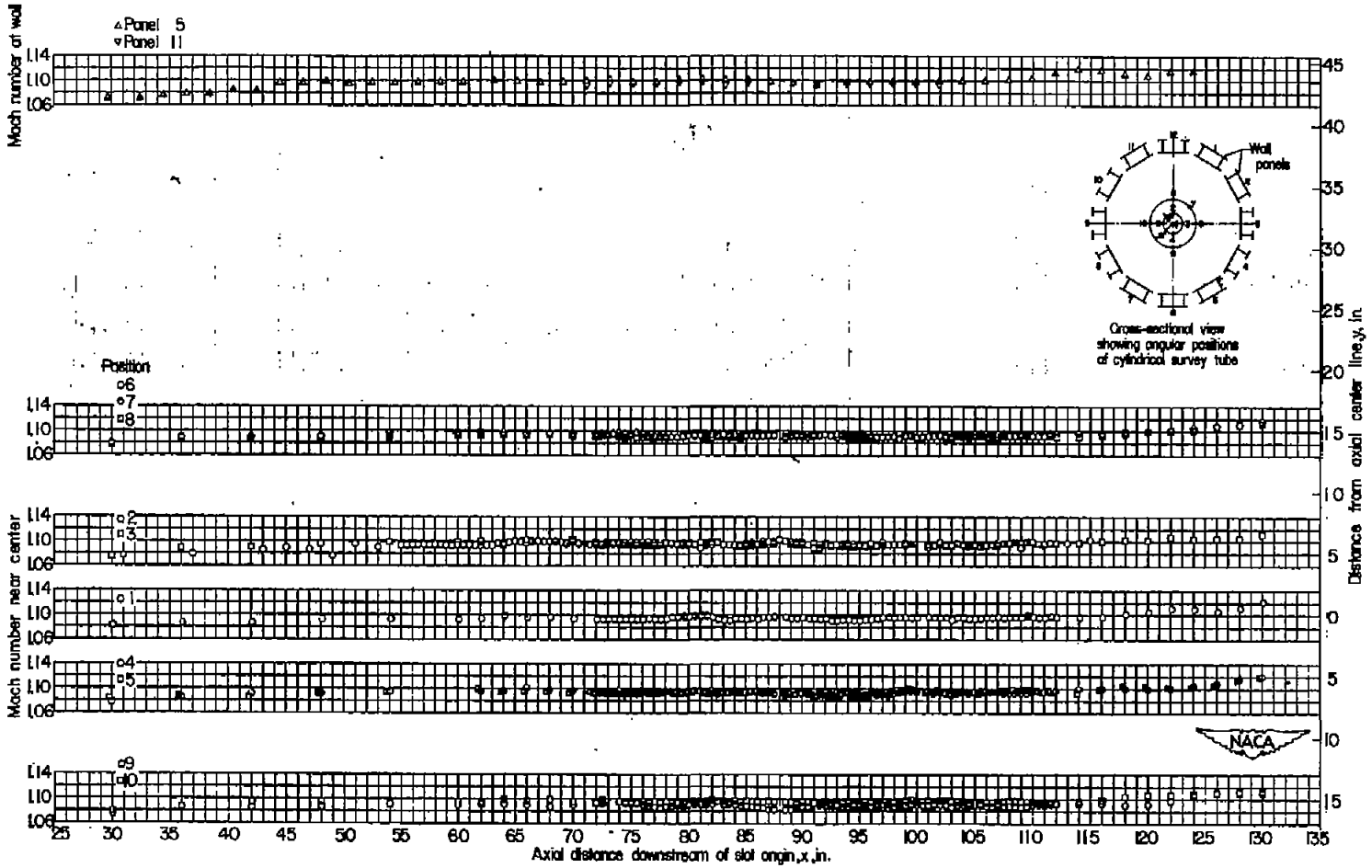

(j) $M_{TC} = 1.10$.

Figure 8.- Continued.

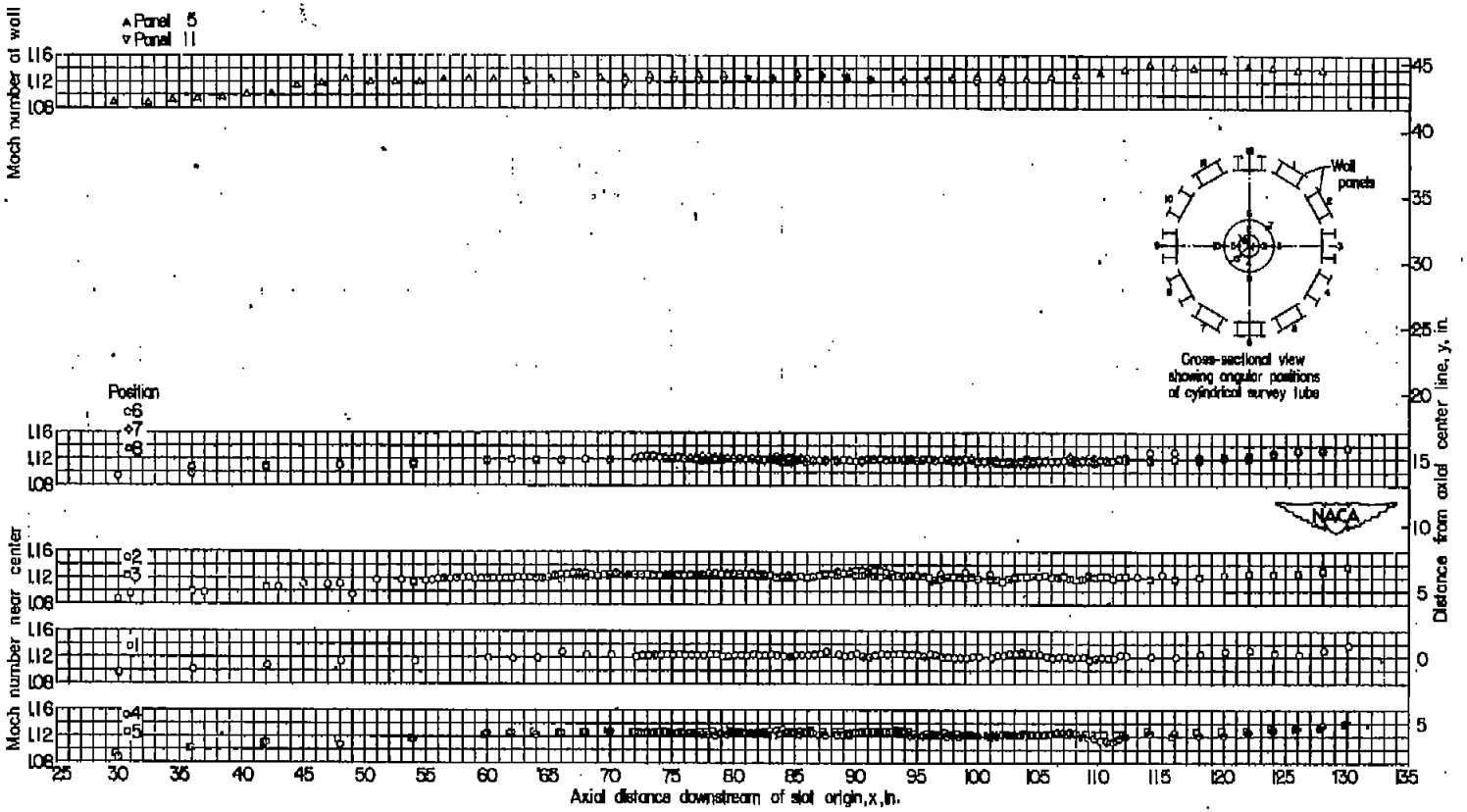

(k) $M_{TC} = 1.13$.

Figure 8.- Concluded.

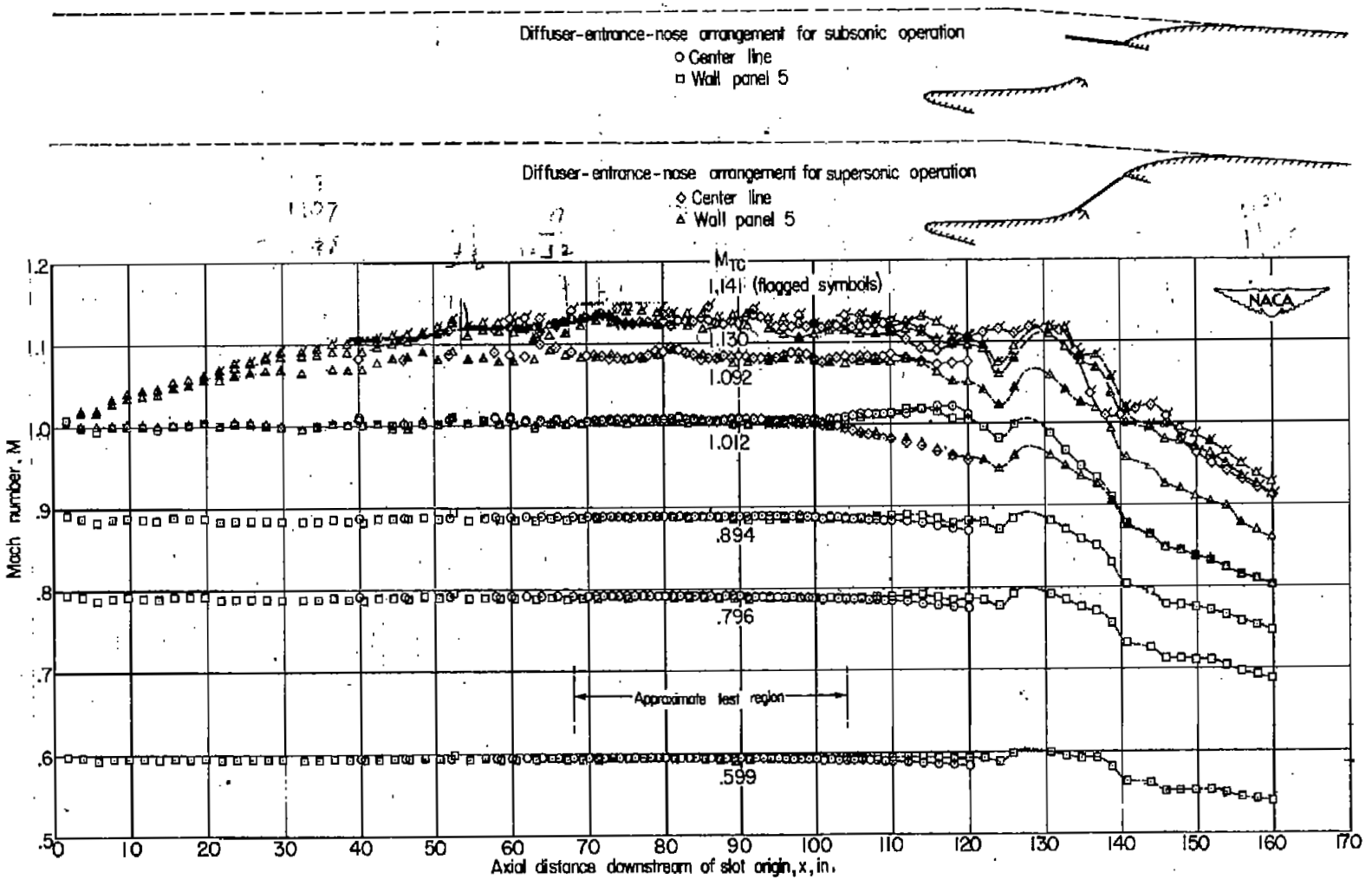

Figure 9.- Model-removed Mach number distribution measured axially along center line and wall of slotted test section with a diffuser-entrance nose arrangement for reduction of tunnel power requirements and attainment of higher Mach number. Diffuser-entrance nose B.

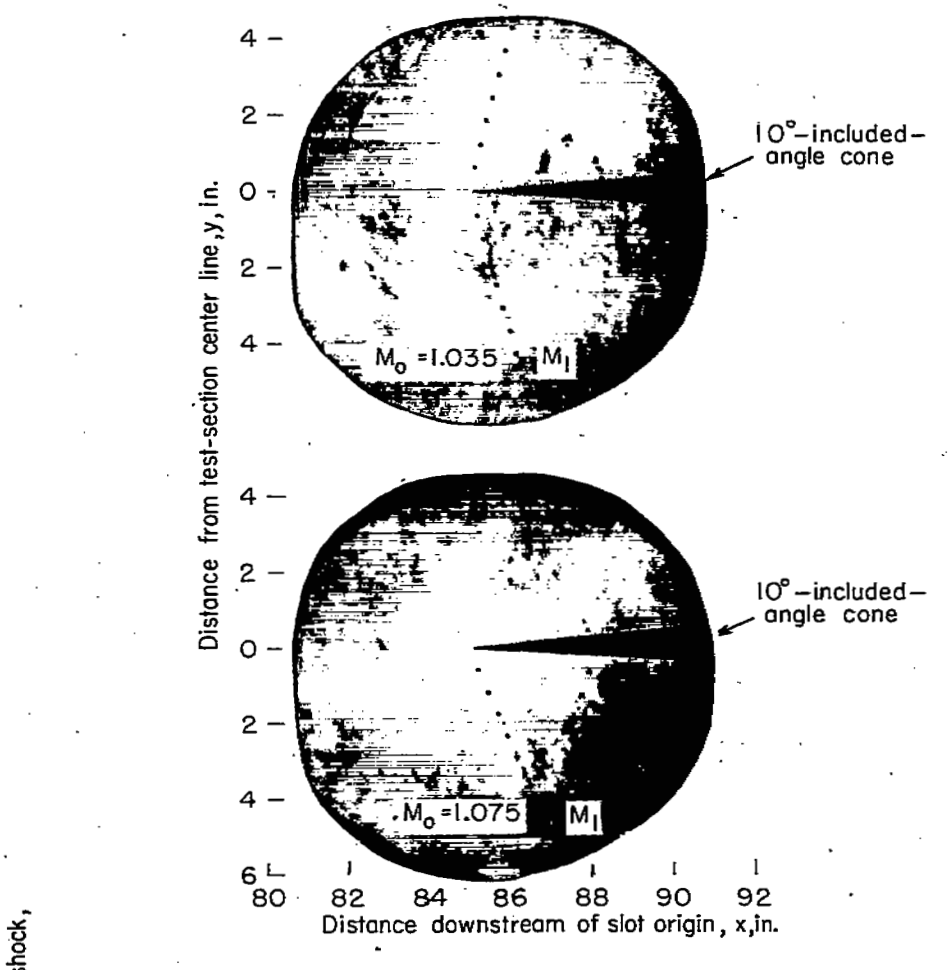

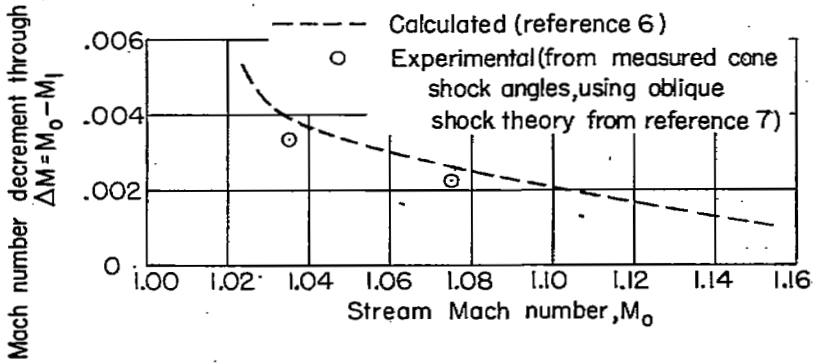

NACA L-72678

Figure 10.- An illustration of the degree of flow uniformity in a region of the slotted test section, using shock waves (produced by a 10° included-angle cone at zero angle) of known strength as the flow-uniformity criterion. Diffuser-entrance nose A.

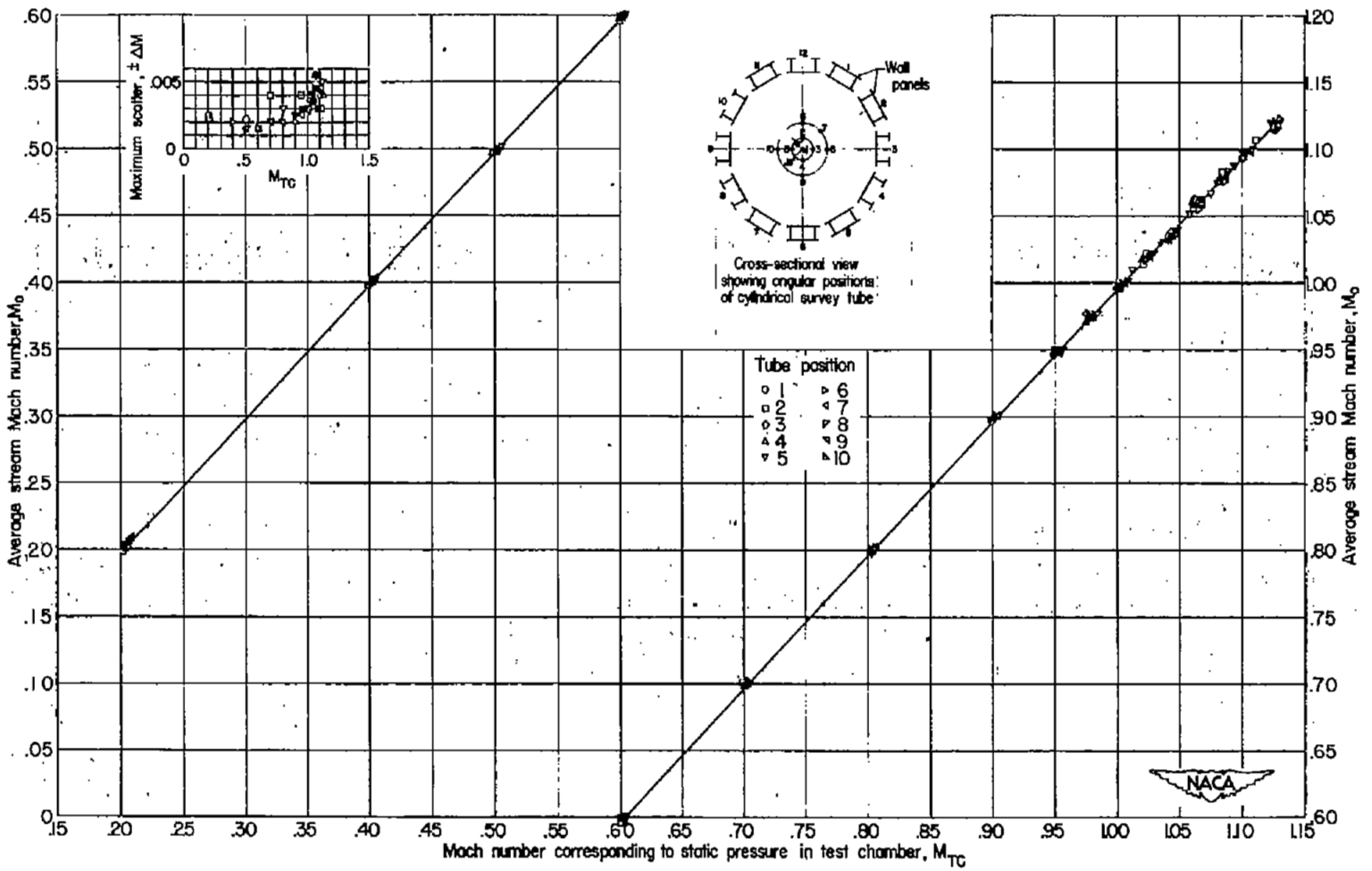

Figure 11.- Typical model-removed calibration curve showing the variation with test-chamber Mach number of the average Mach number over a test region 36 inches long and 30 inches in diameter near the center line of the slotted test section with diffuser-entrance nose A.

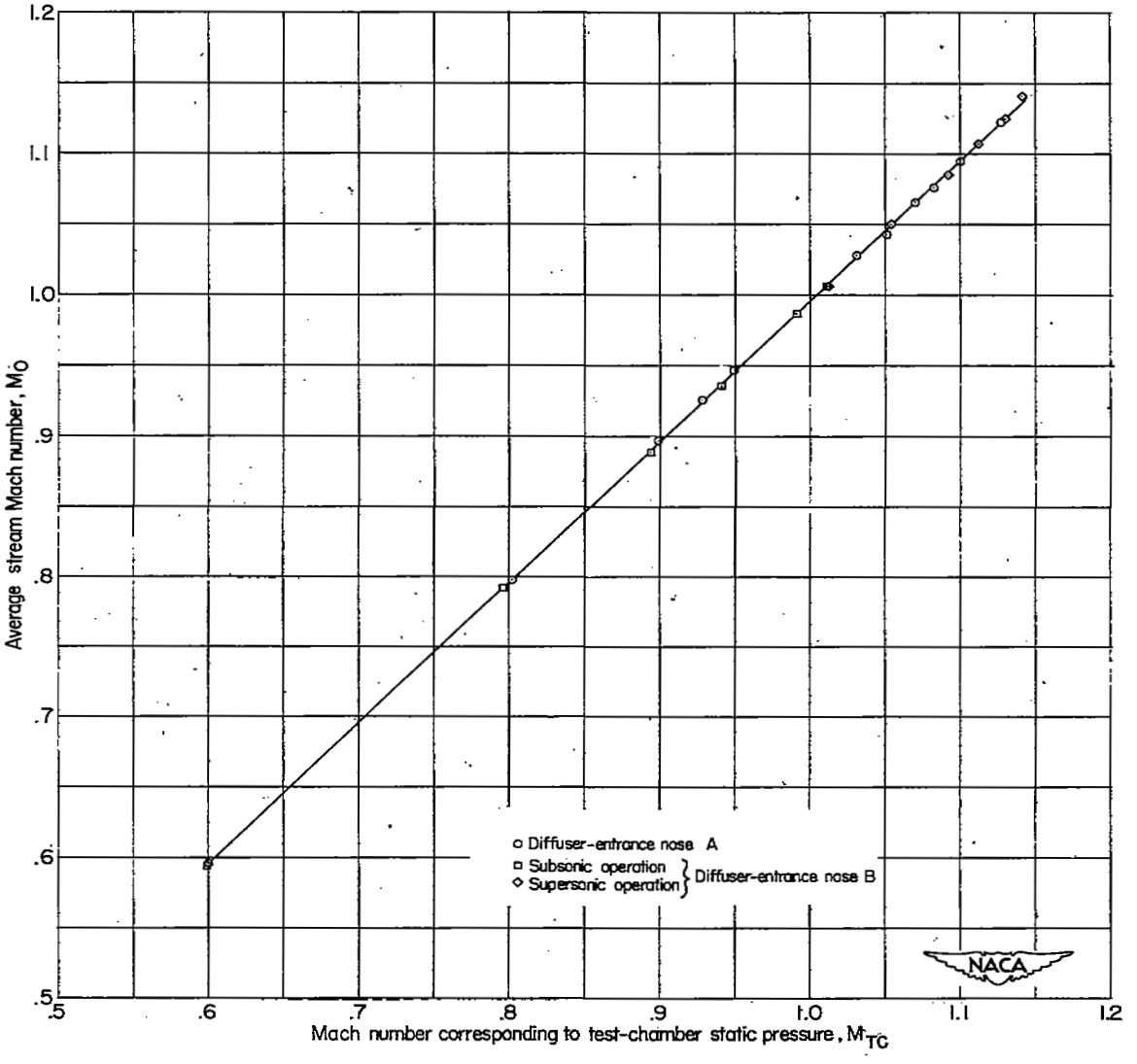

Figure 12.- Agreement of model-removed calibrations of the average Mach number over a 36-inch-long region at the center line of the slotted test section with diffuser-entrance noses A and B. Maximum deviations in Mach number for nose-A and nose-B surveys within 0.006 and 0.010, respectively.

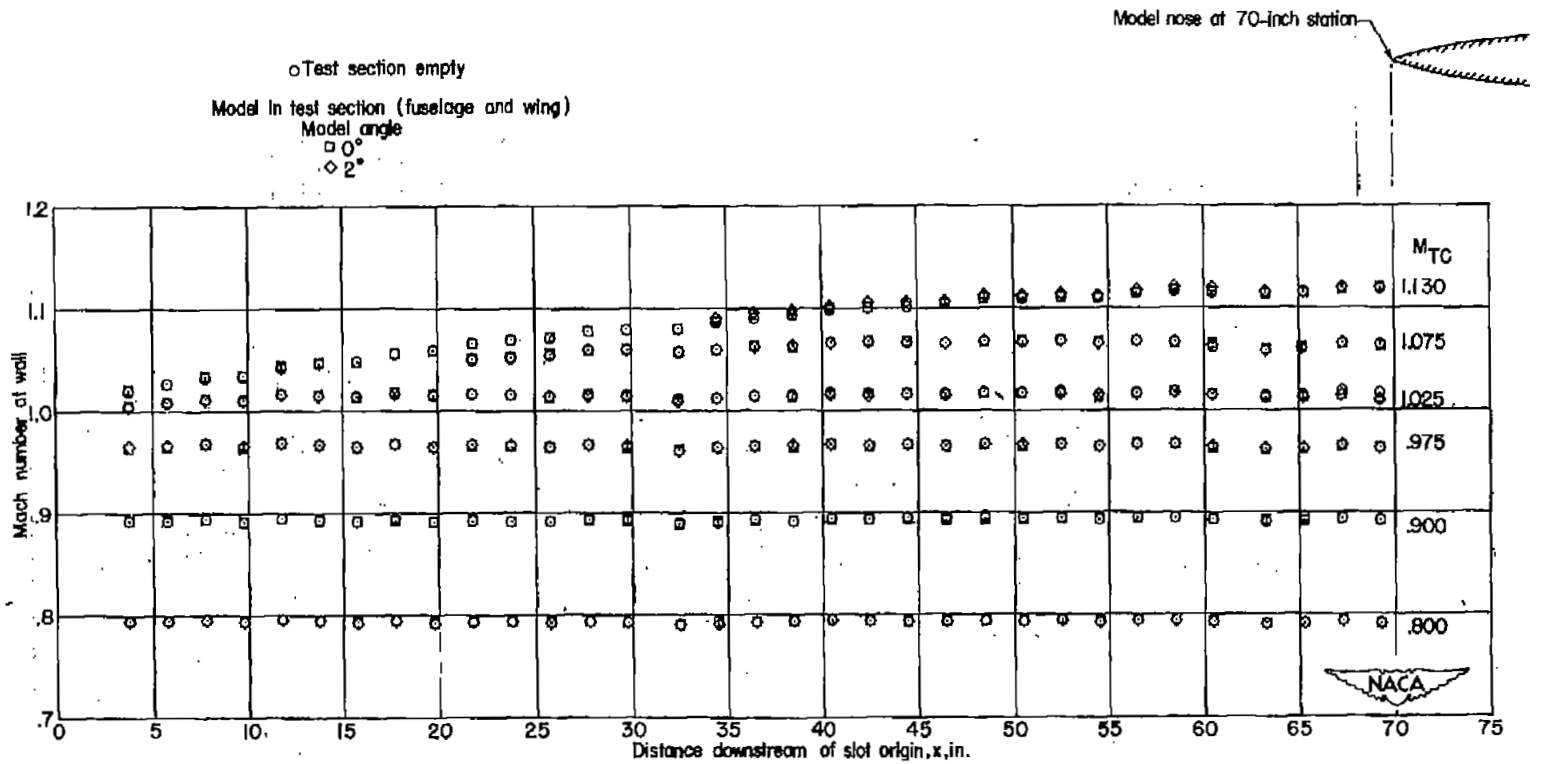

Figure 13.- Agreement of model-in and model-removed Mach number distributions axially along wall of slotted test section upstream of model location. Diffuser-entrance nose A.

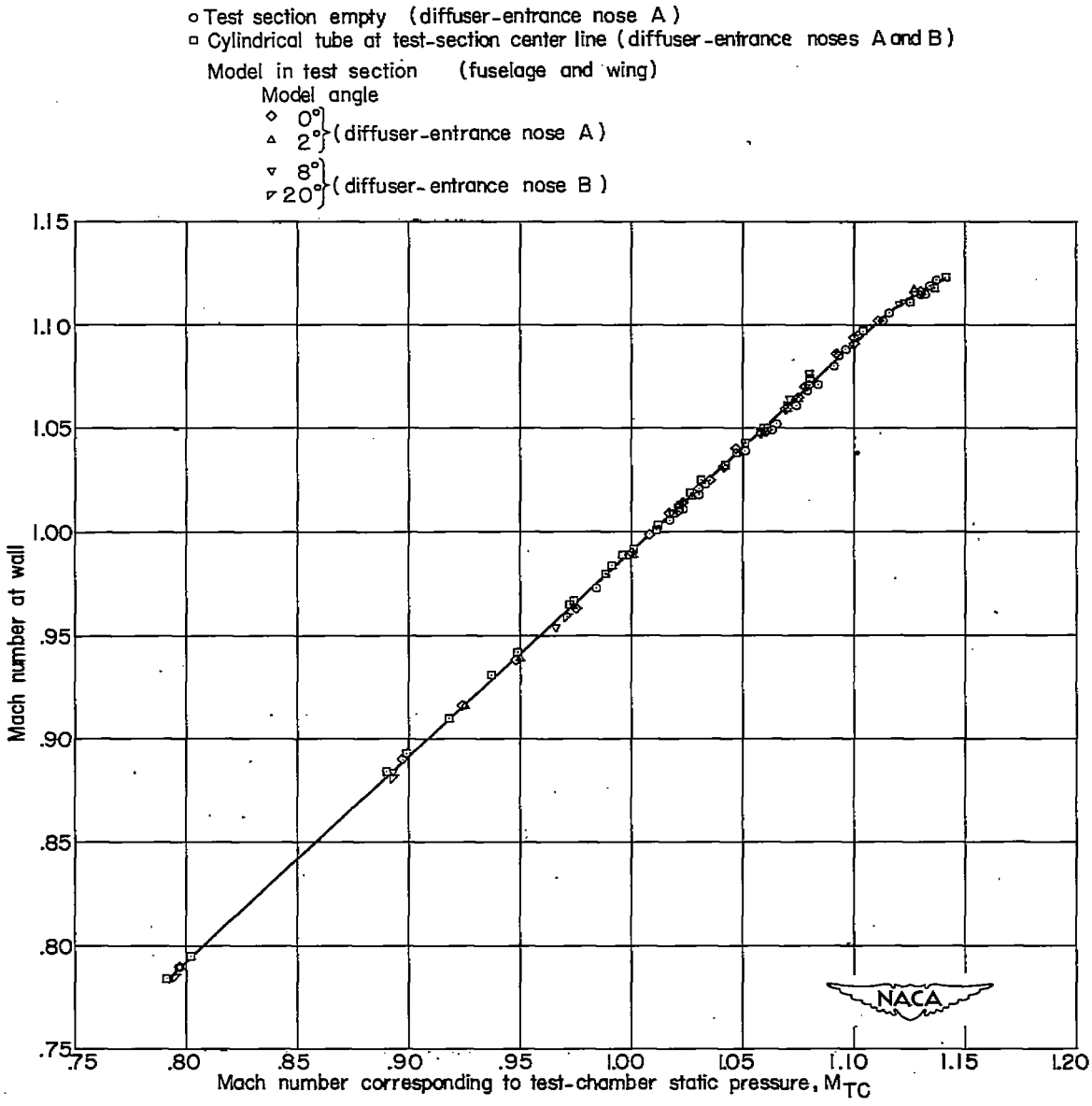

Figure 14.- Variation with test-chamber Mach number of model-in Mach numbers measured on tunnel wall approximately 10 inches upstream of model nose (model at different angles of attack) and model-removed Mach numbers measured at the same axial station.

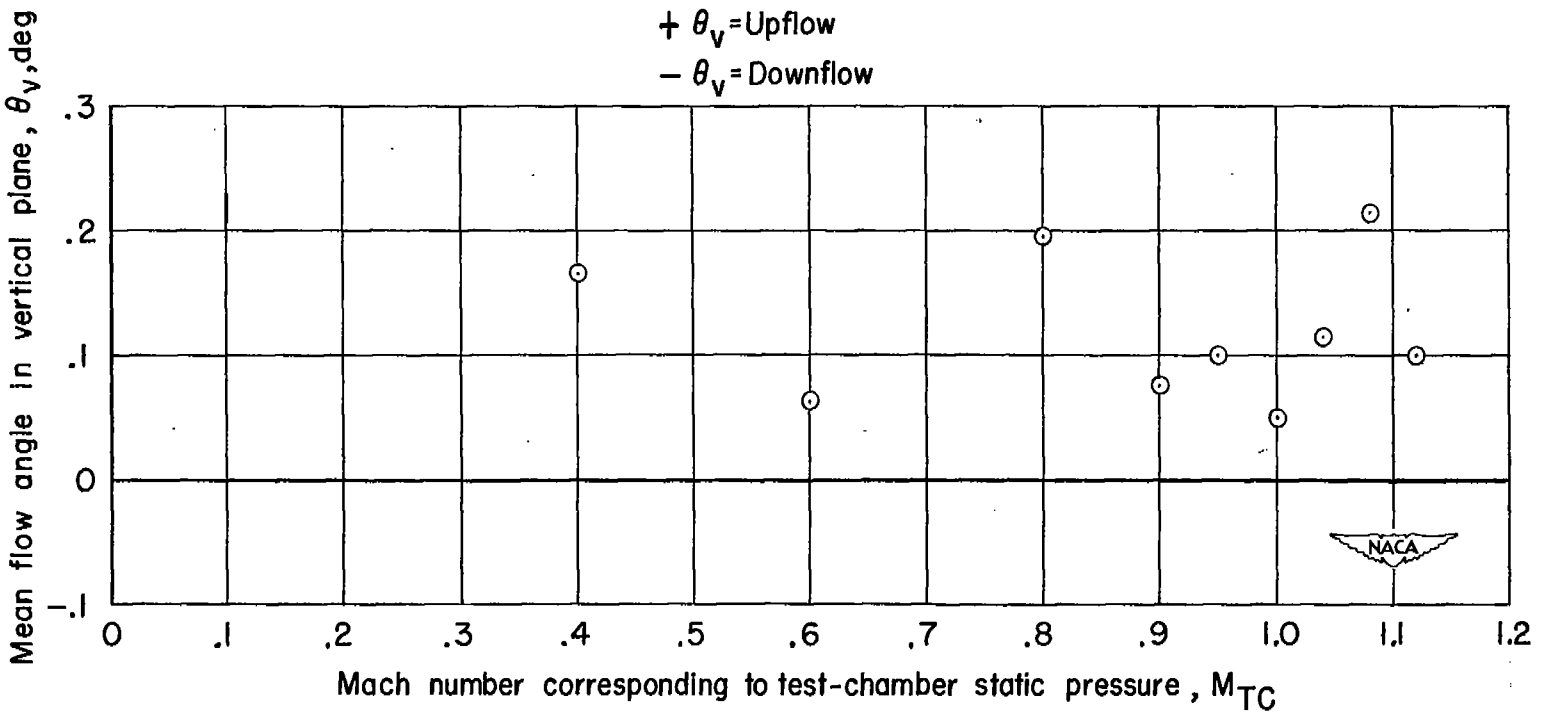

Figure 15.- Flow angularity in vertical plane, indicated by null-pressure cone-surface measurements, at test-section center line 85 inches downstream of slot origin.

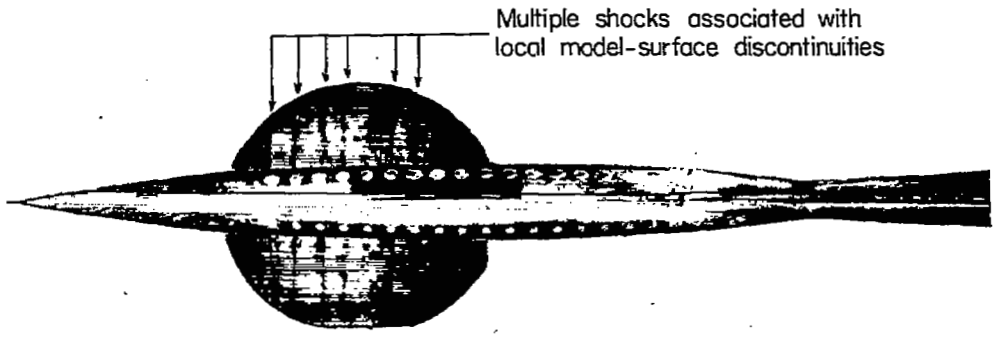

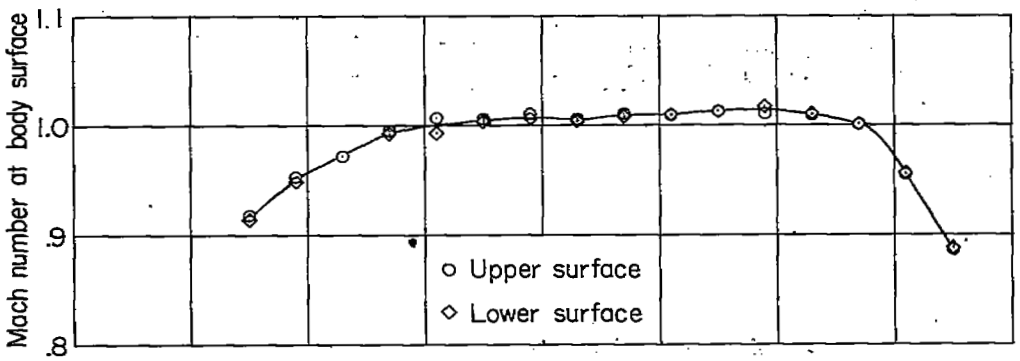

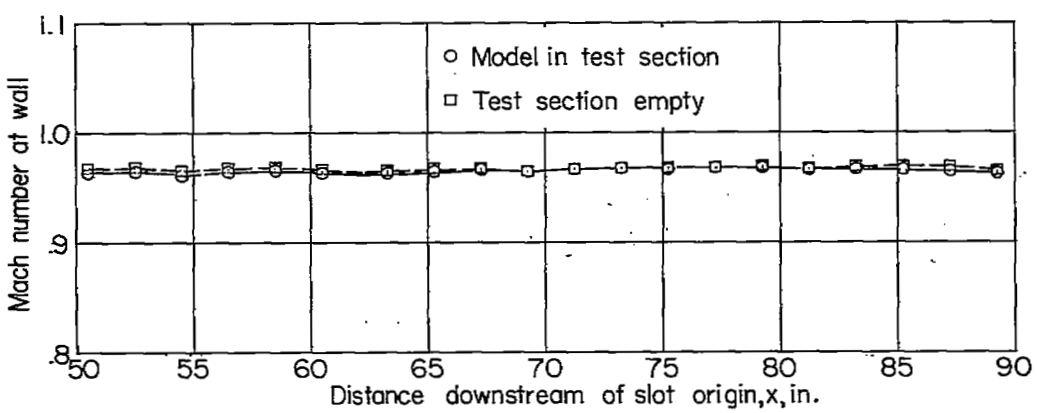

(a) $M_o = 0.970$.

NACA
L-72679

Figure 16.- Shock formations and reflections at transonic speeds with body-of-revolution model at center line of slotted test section. $\alpha = 0^\circ$. Diffuser-entrance nose A.

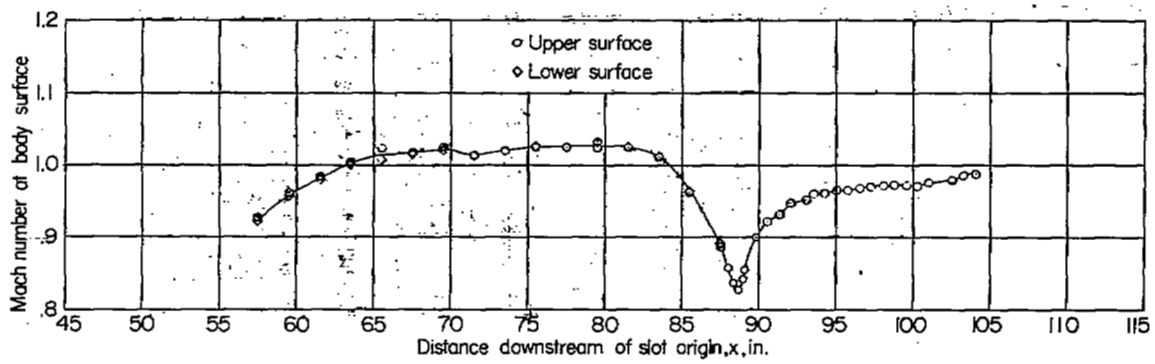

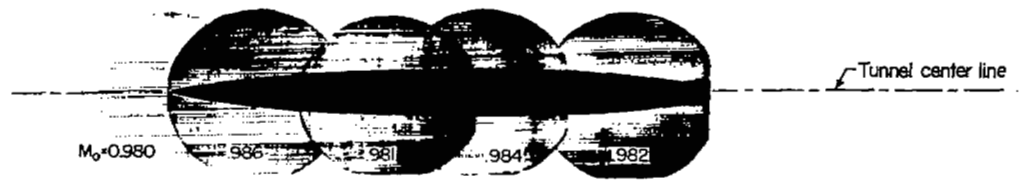

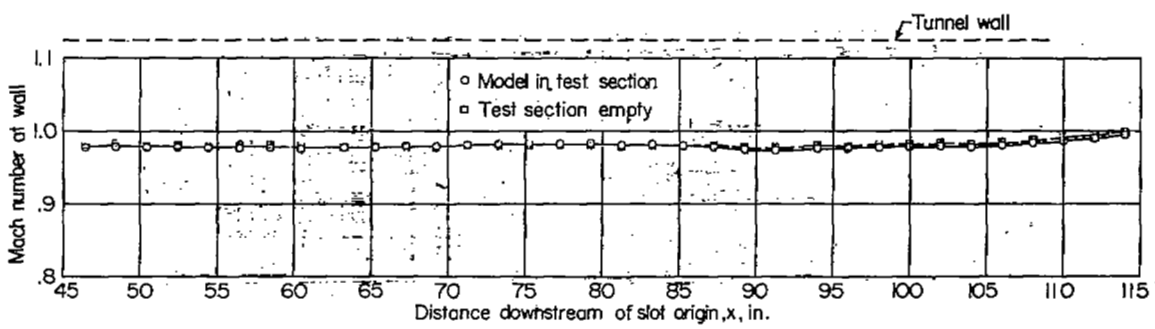

(b) M_o = 0.980.

Figure 16.- Continued.

NACA L-72680

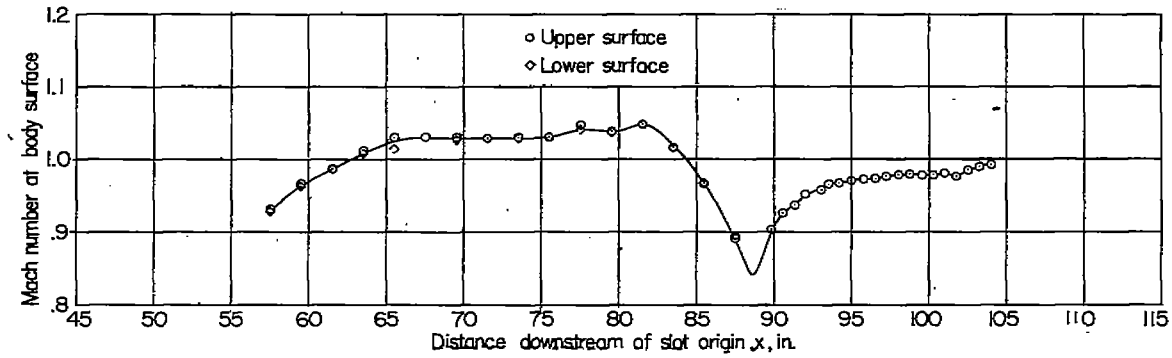

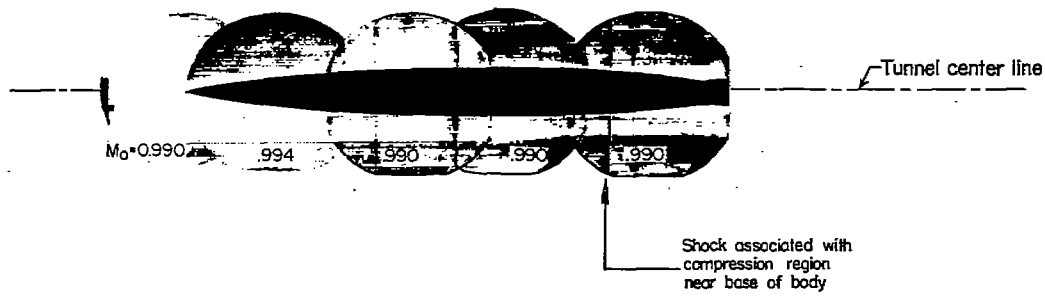

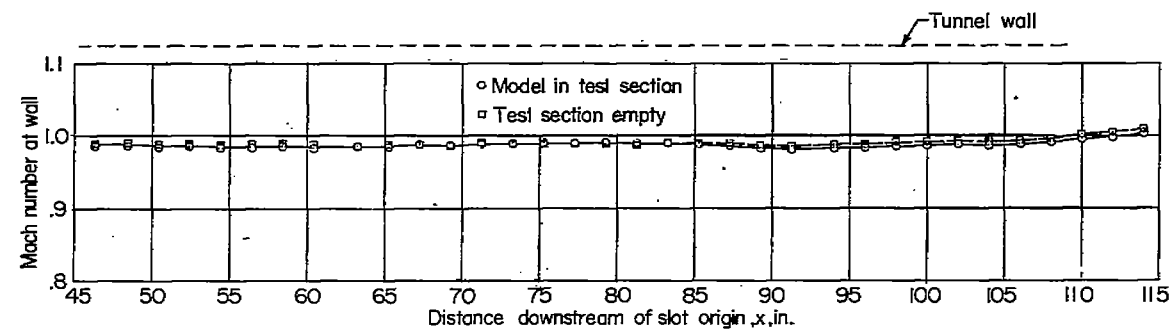

(c) M_o = 0.990.

NACA L-72681

Figure 16.- Continued.

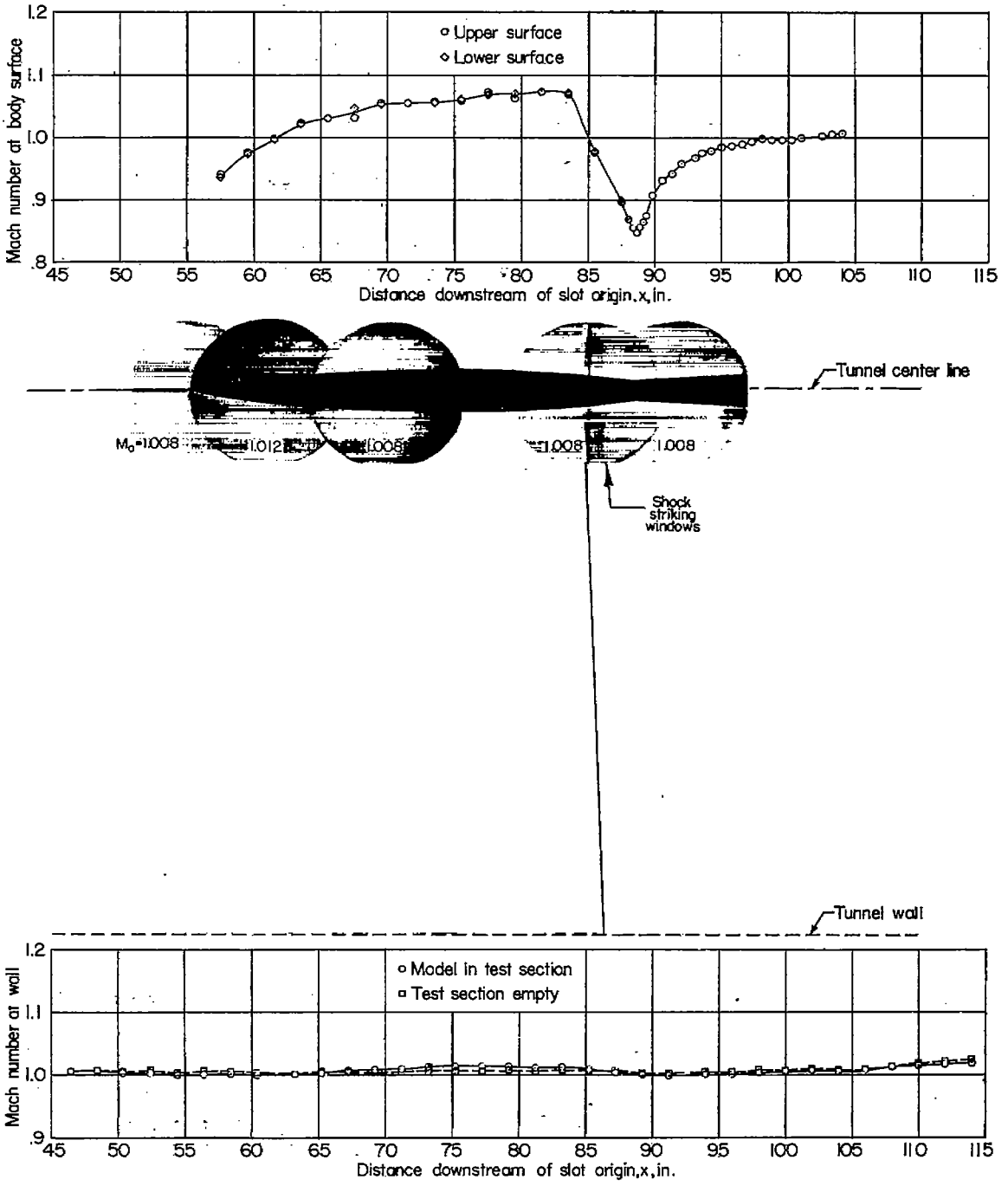

(d) M_o = 1.008.

NACA L-72682

Figure 16.- Continued.

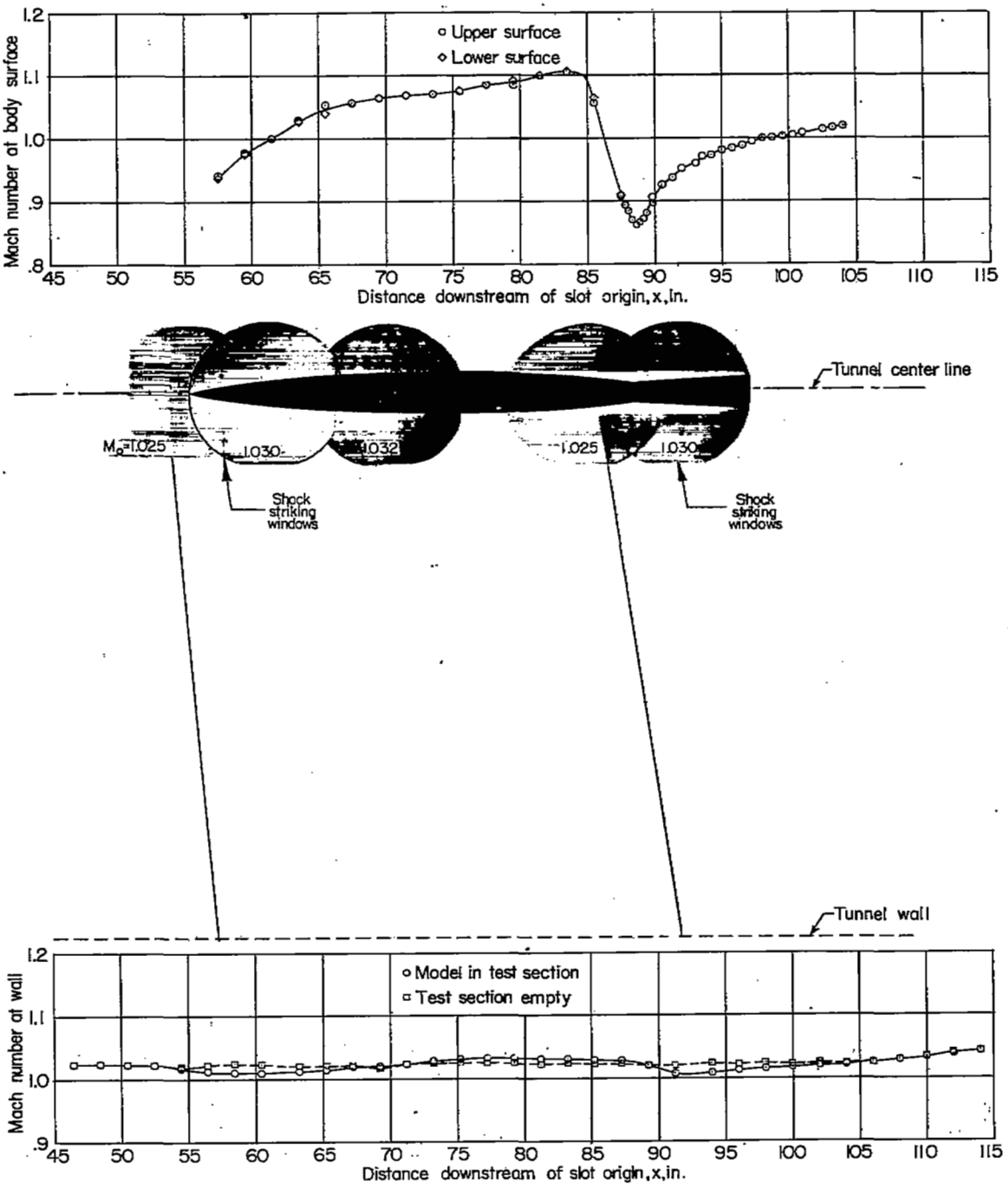

(e) M_o = 1.025.

NACA L-72683

Figure 16.- Continued.

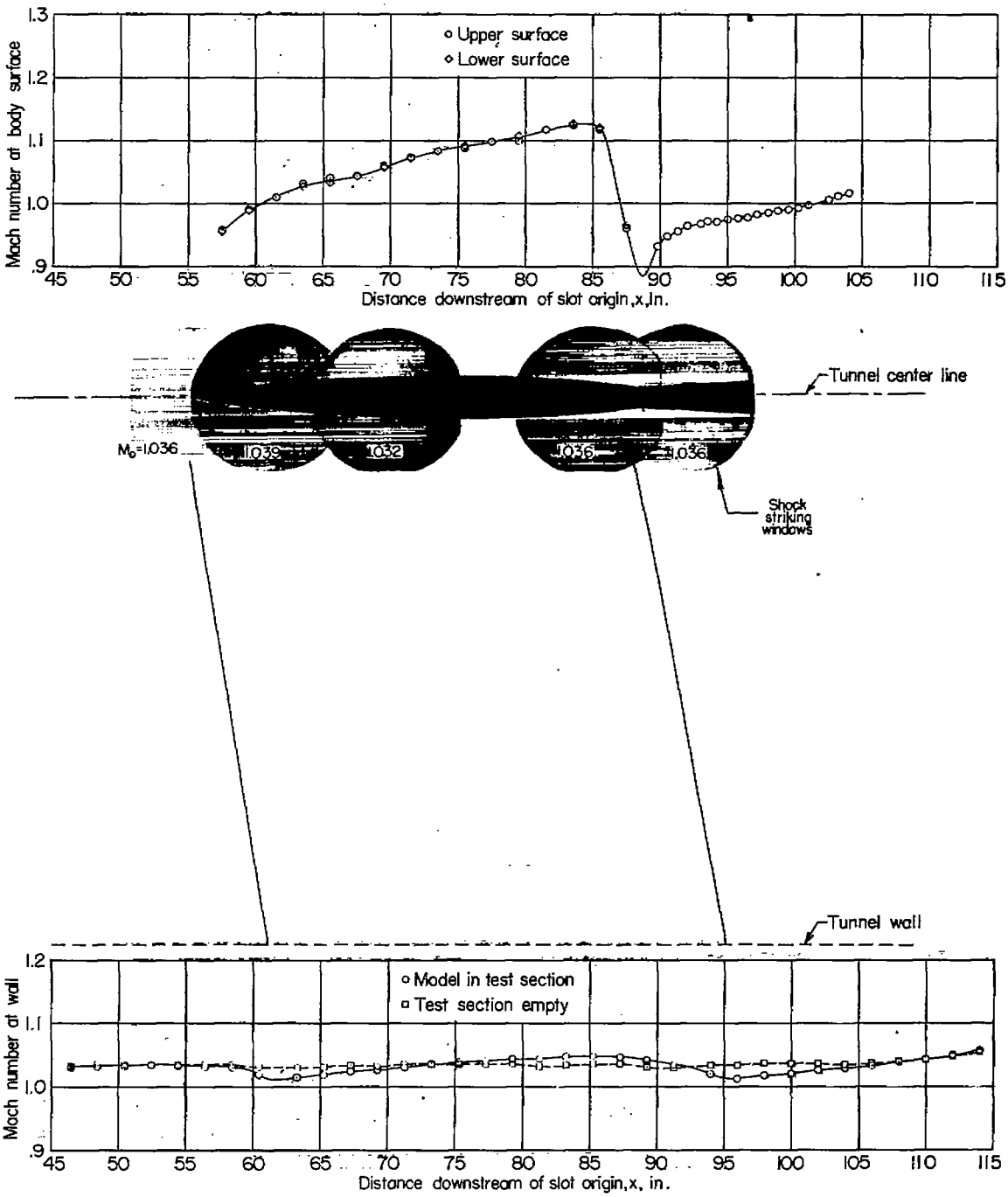

(f) M_o = 1.036.

NACA L-72684

Figure 16.- Continued.

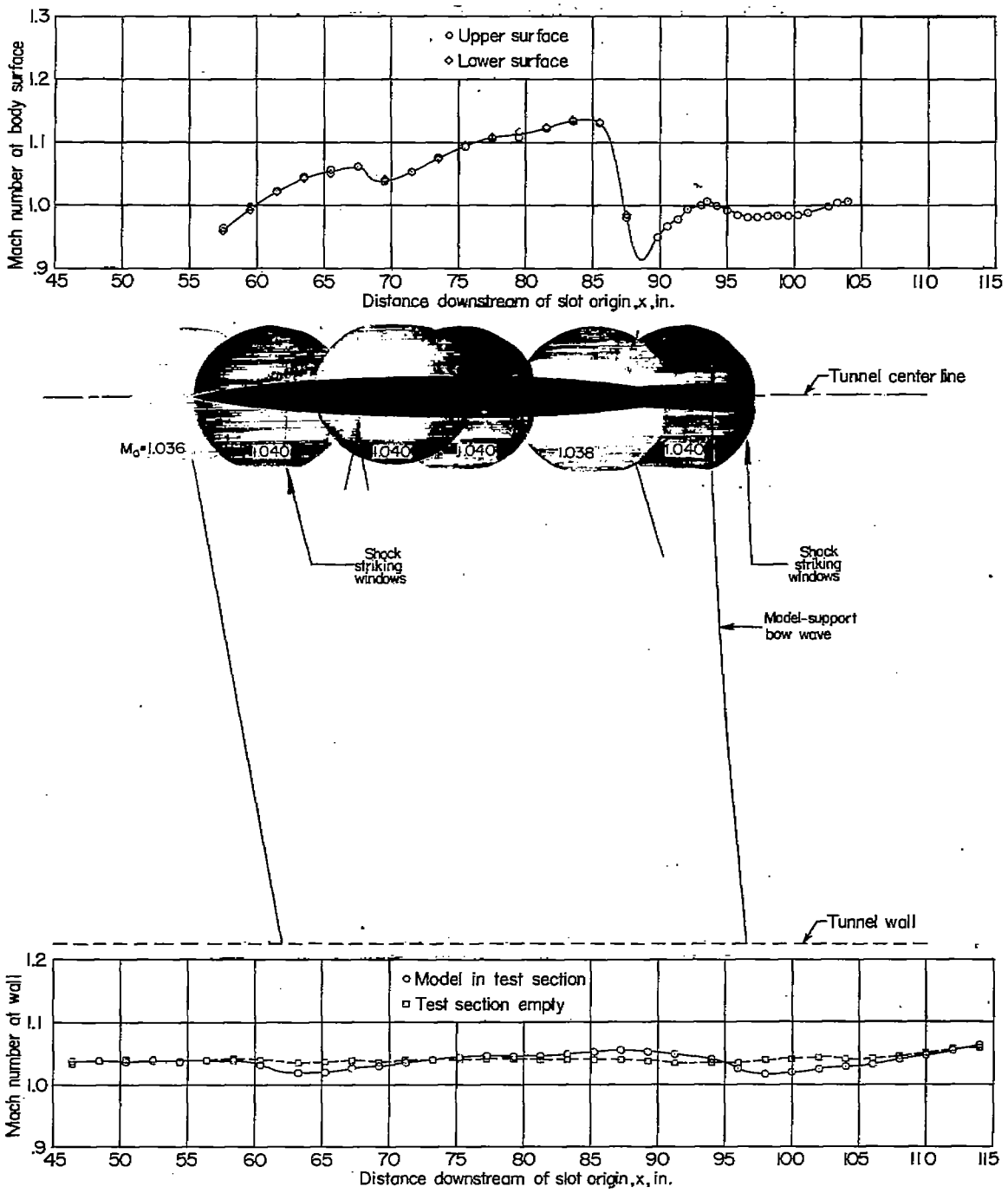

(g) M_o = 1.042.

NACA L-72685

Figure 16.- Continued.

[redacted]

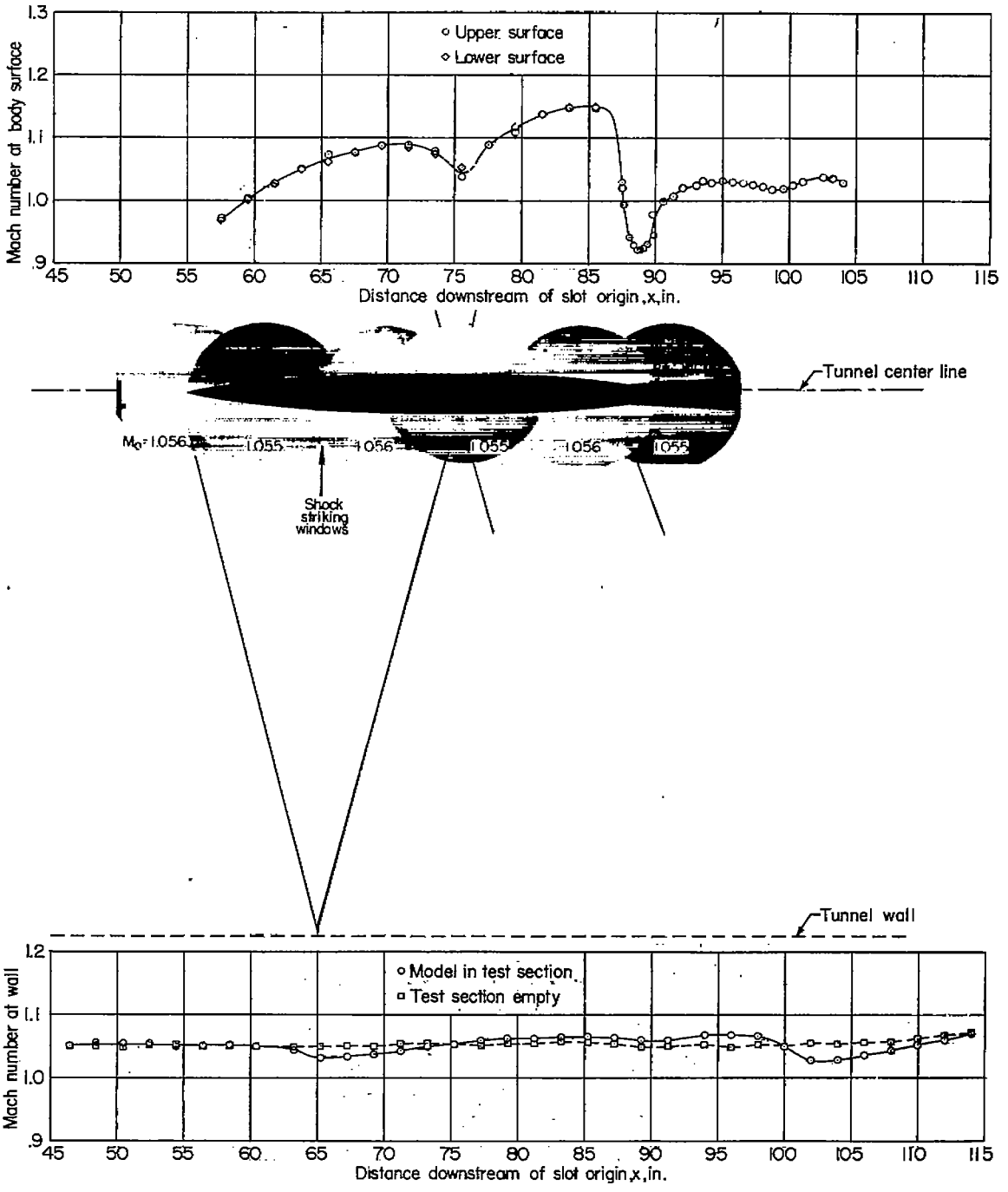

(h) M_o = 1.056.

NACA L-72686

Figure 16.- Continued.

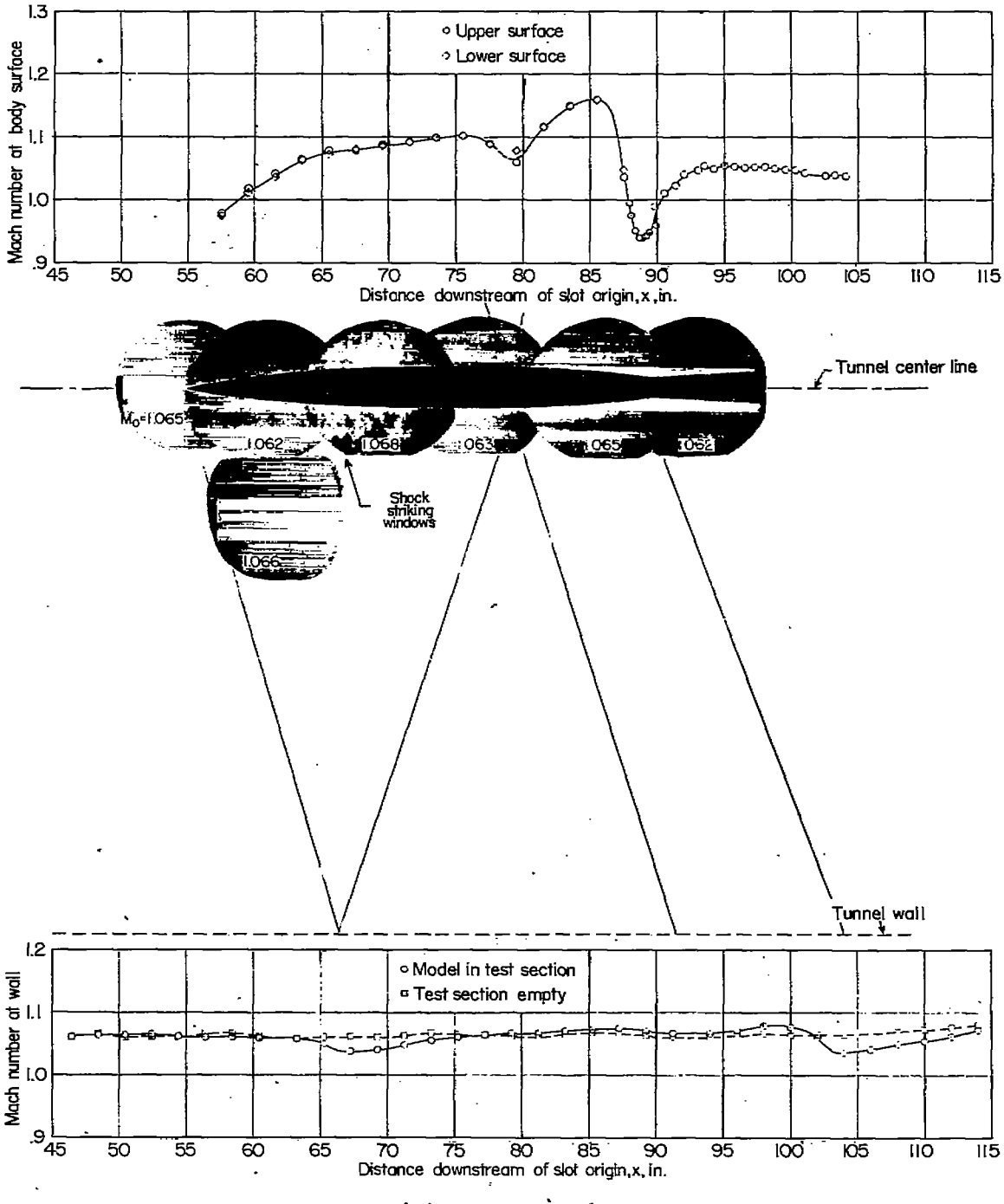

(i) M_o = 1.065.

NACA L-72687

Figure 16.- Continued.

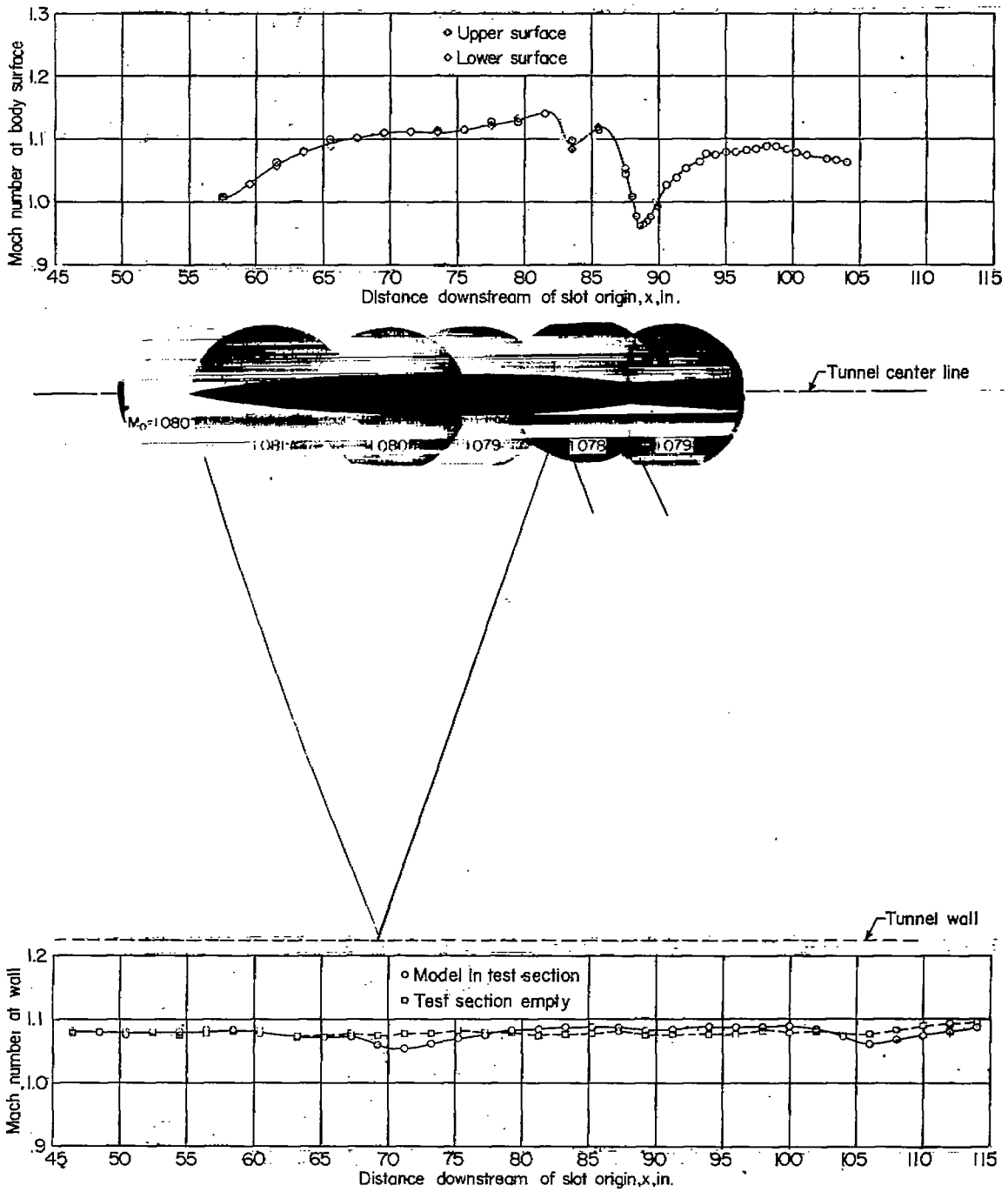

(j) M_o = 1.080.

NACA L-72688

Figure 16.- Continued.

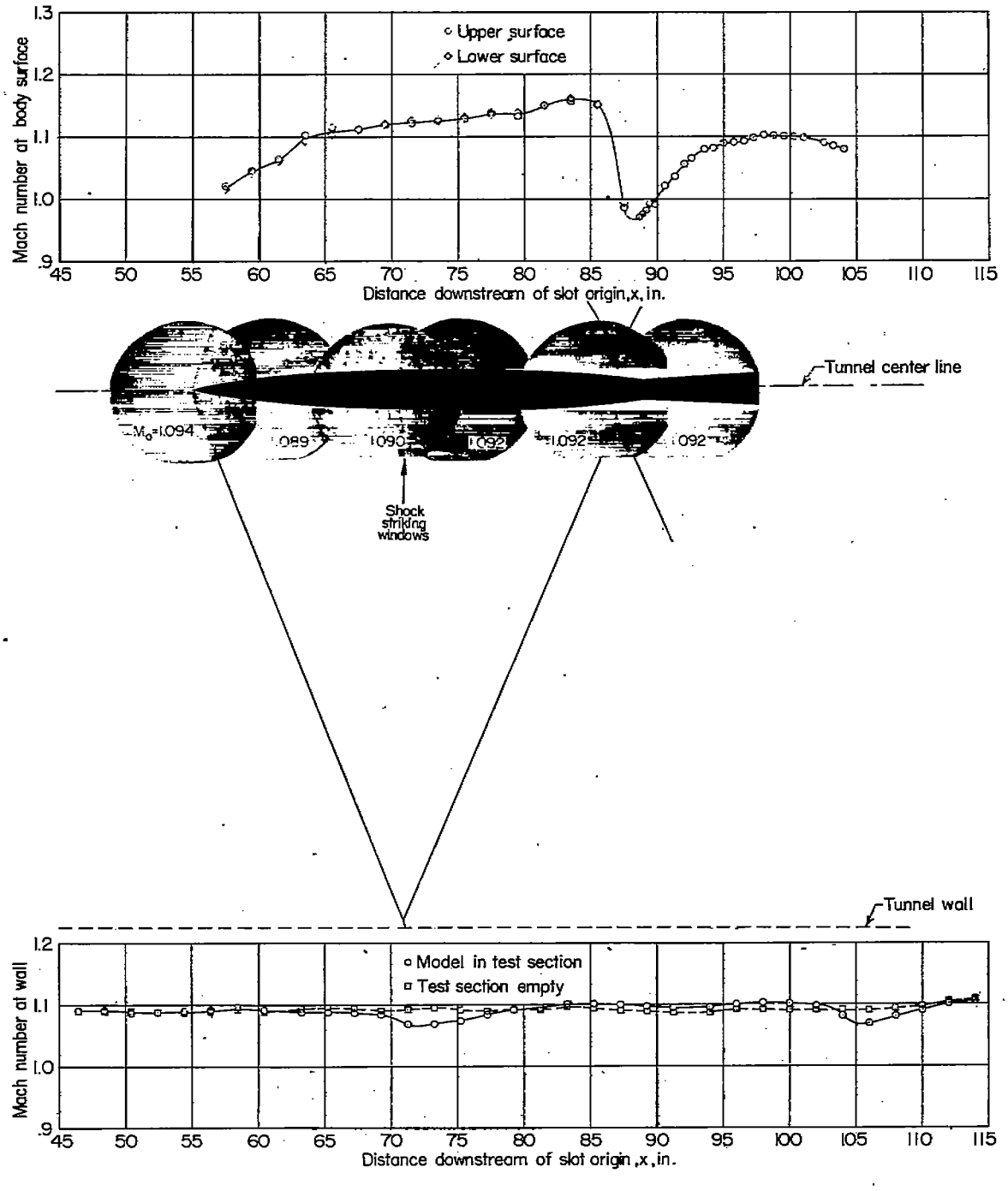

(k) M_o = 1.092.

NACA L-72689

Figure 16.- Continued.

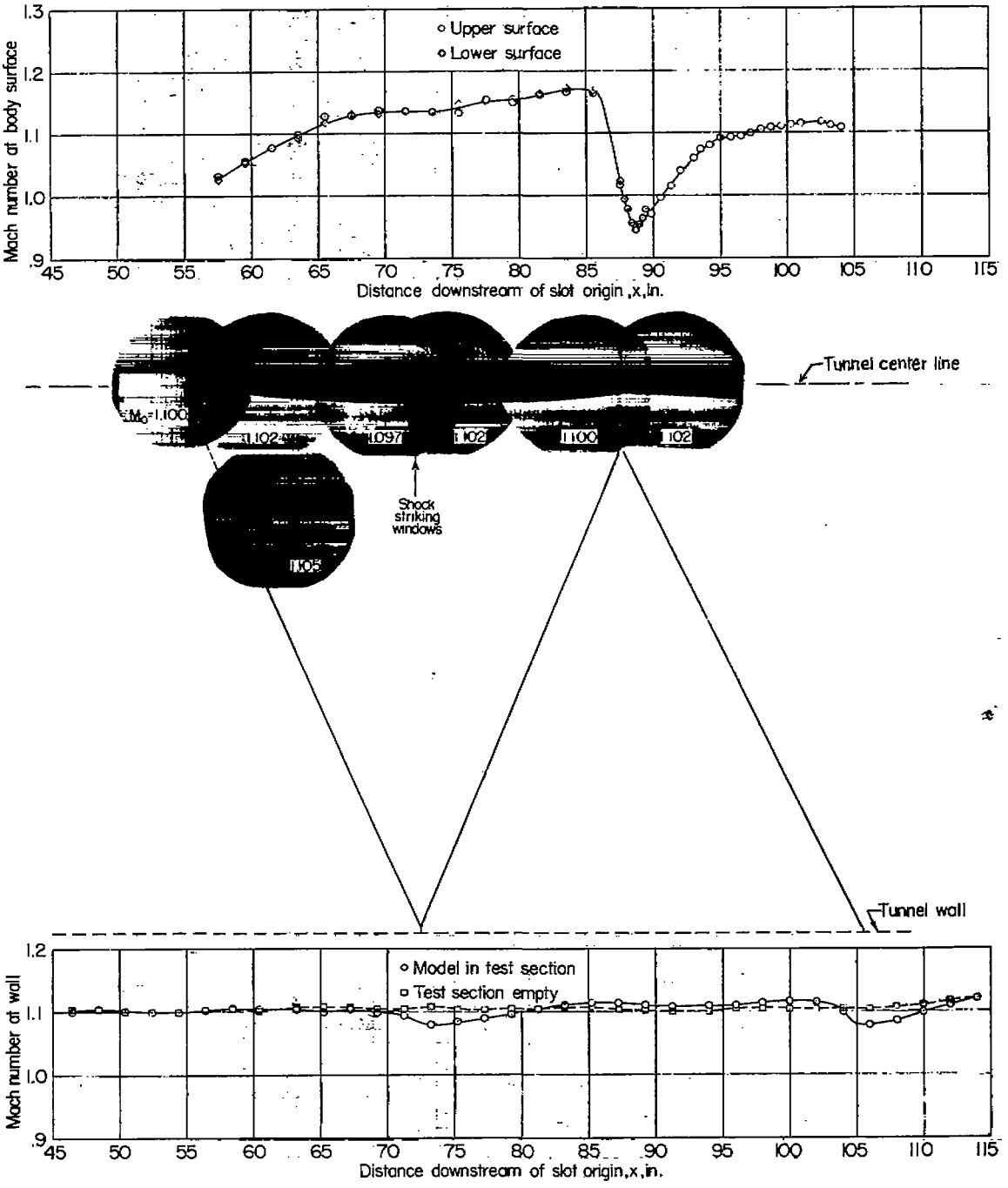

(l) M_o = 1.105.

NACA L-72690

Figure 16.- Continued.

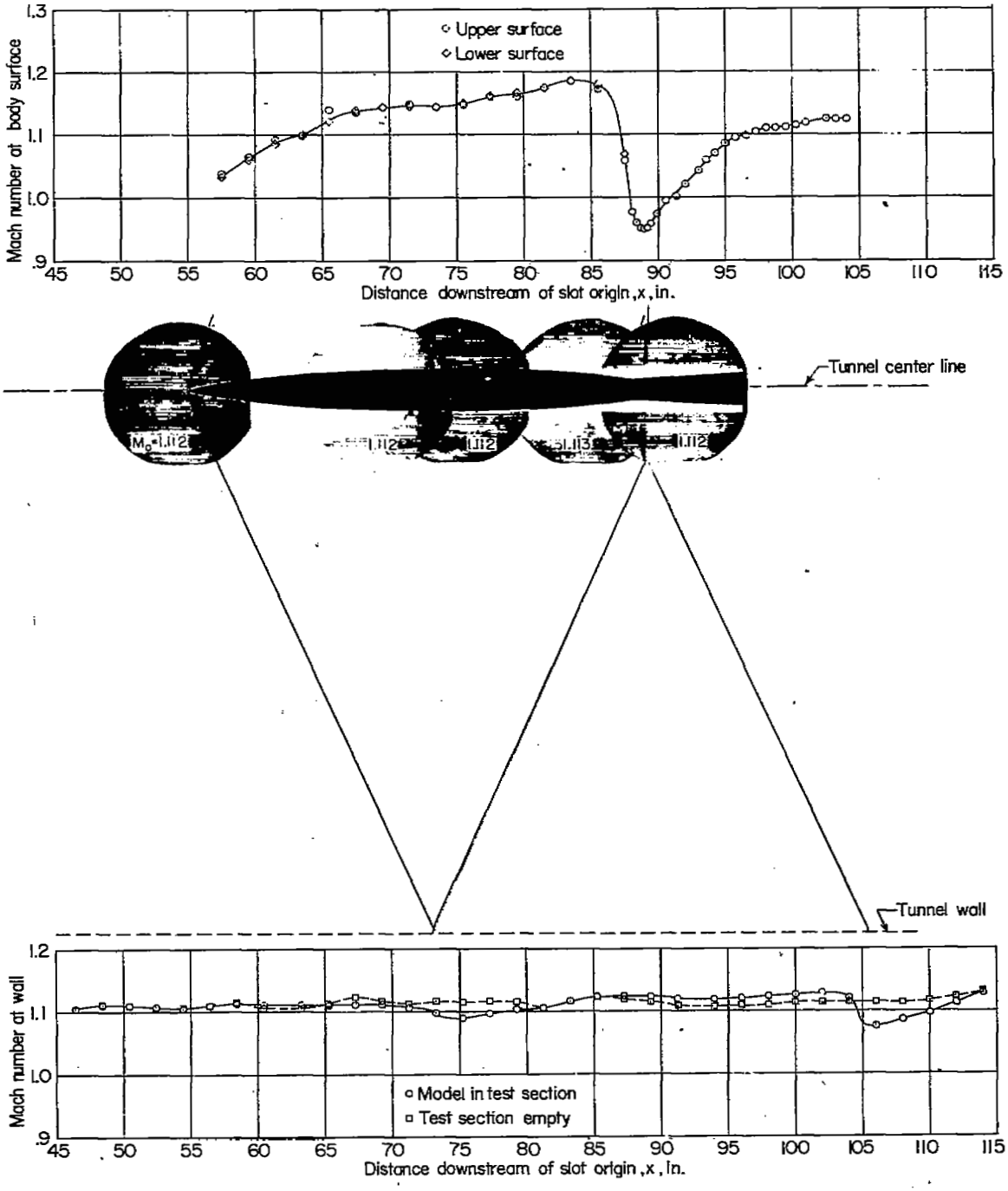

(m) M_o = 1.113.

NACA L-72691

Figure 16.- Continued.

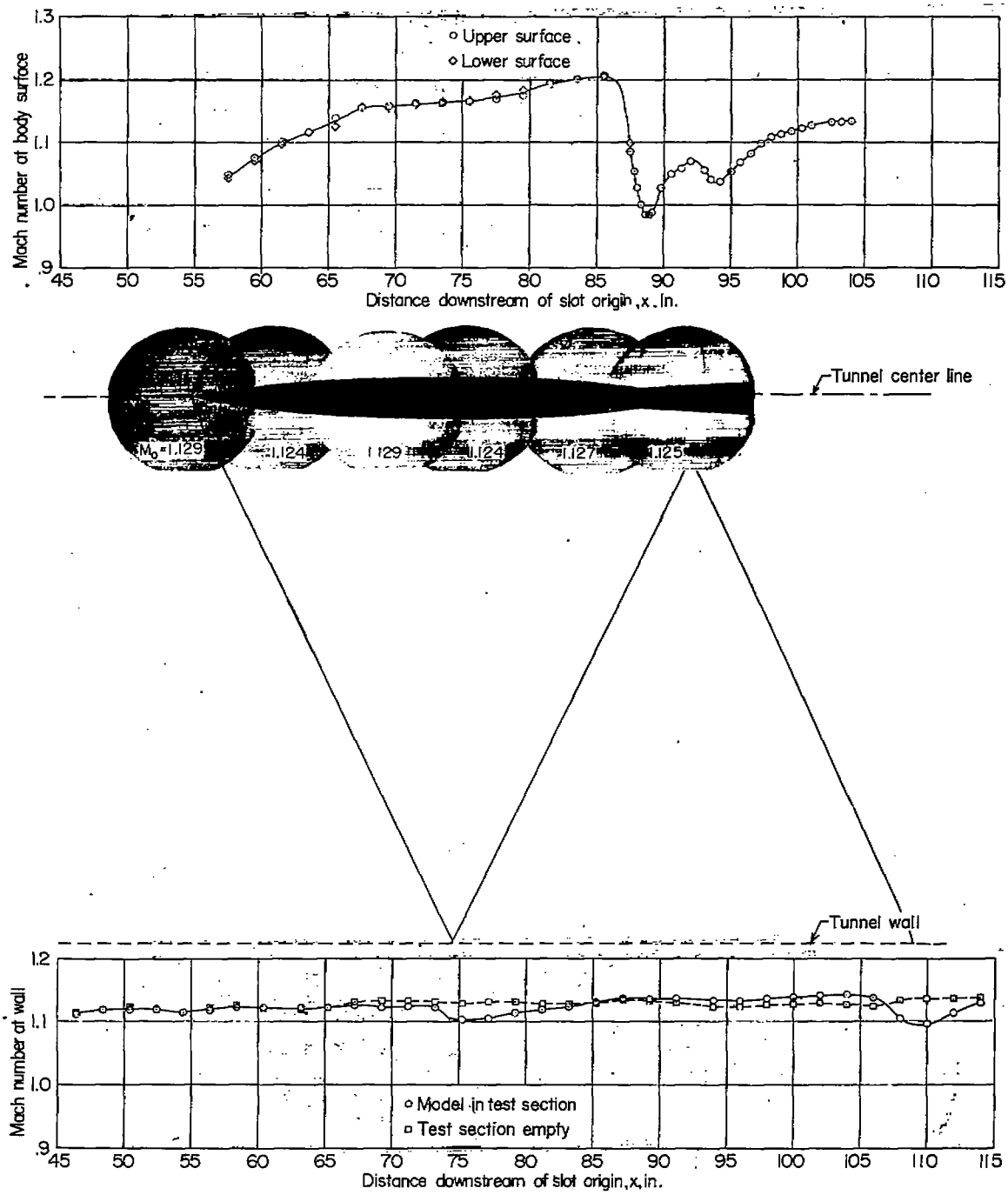

(n) M_o = 1.129.

NACA L-72692

Figure 16.- Concluded.

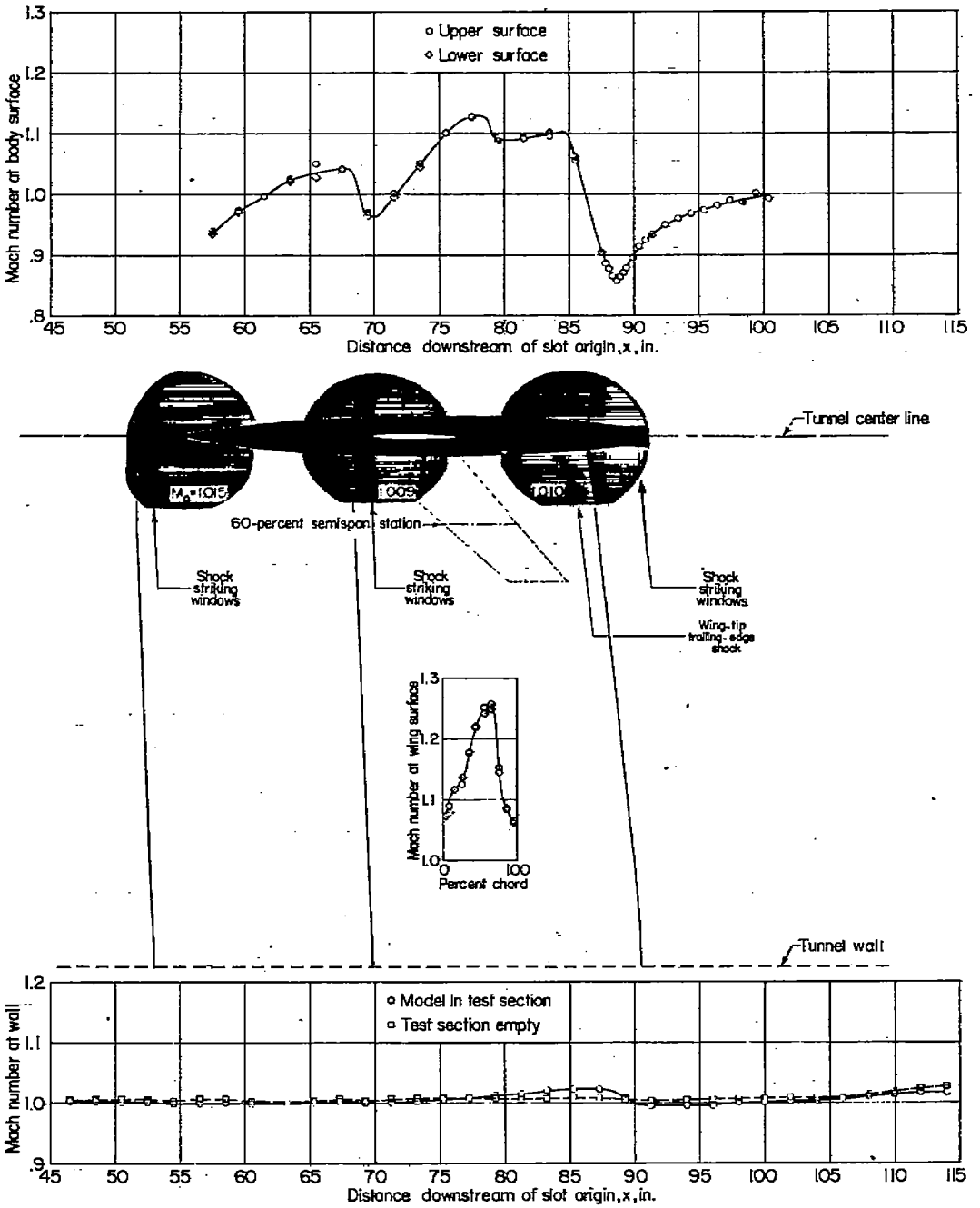

(a) M_o = 1.009.

NACA L-72693

Figure 17.- Shock formations and reflections at low-supersonic speeds with wing-body model at center line of slotted test section. $\alpha = 0^\circ$. Diffuser-entrance nose A.

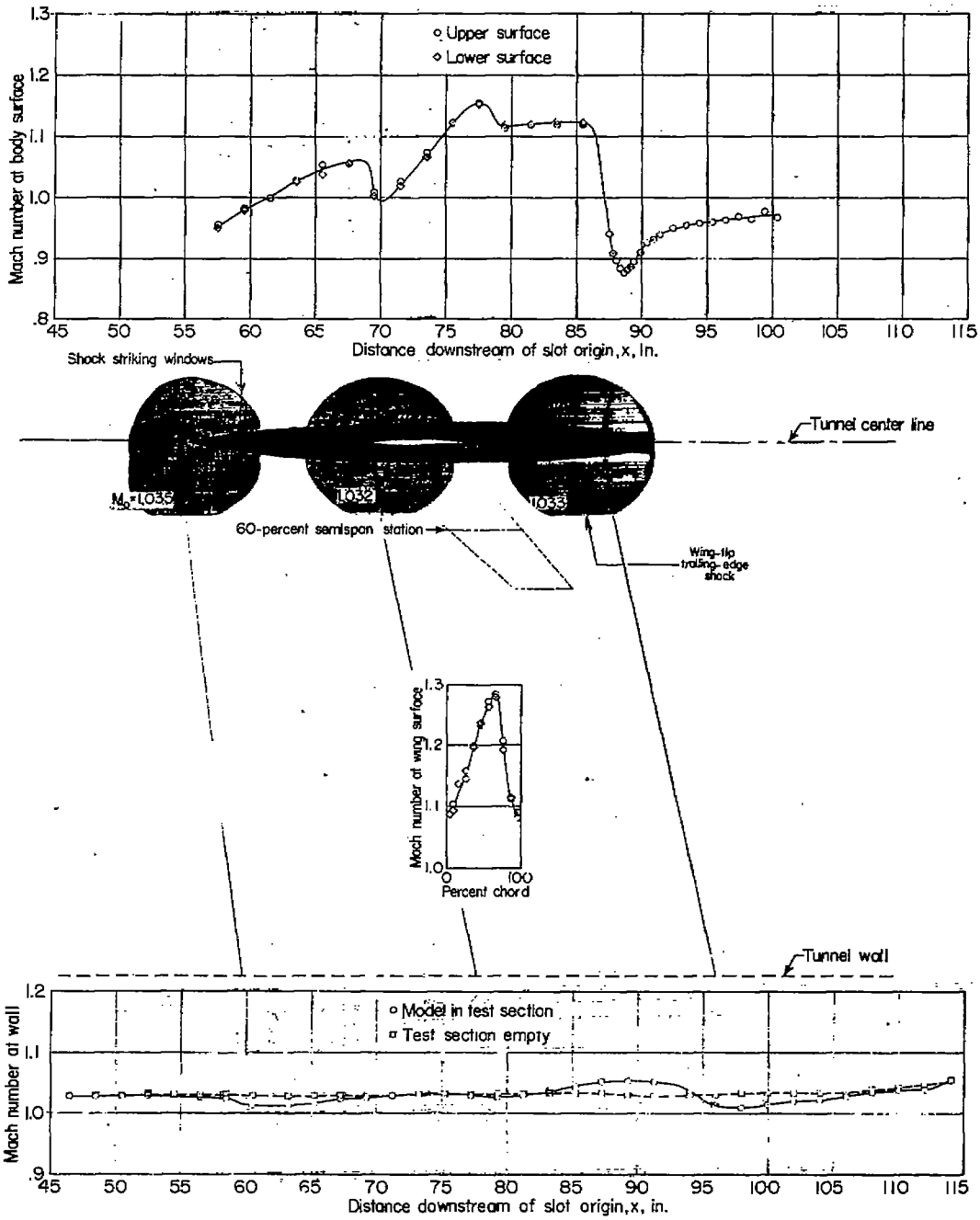

(b) M_o = 1.034.

NACA L-72694

Figure 17.- Continued.

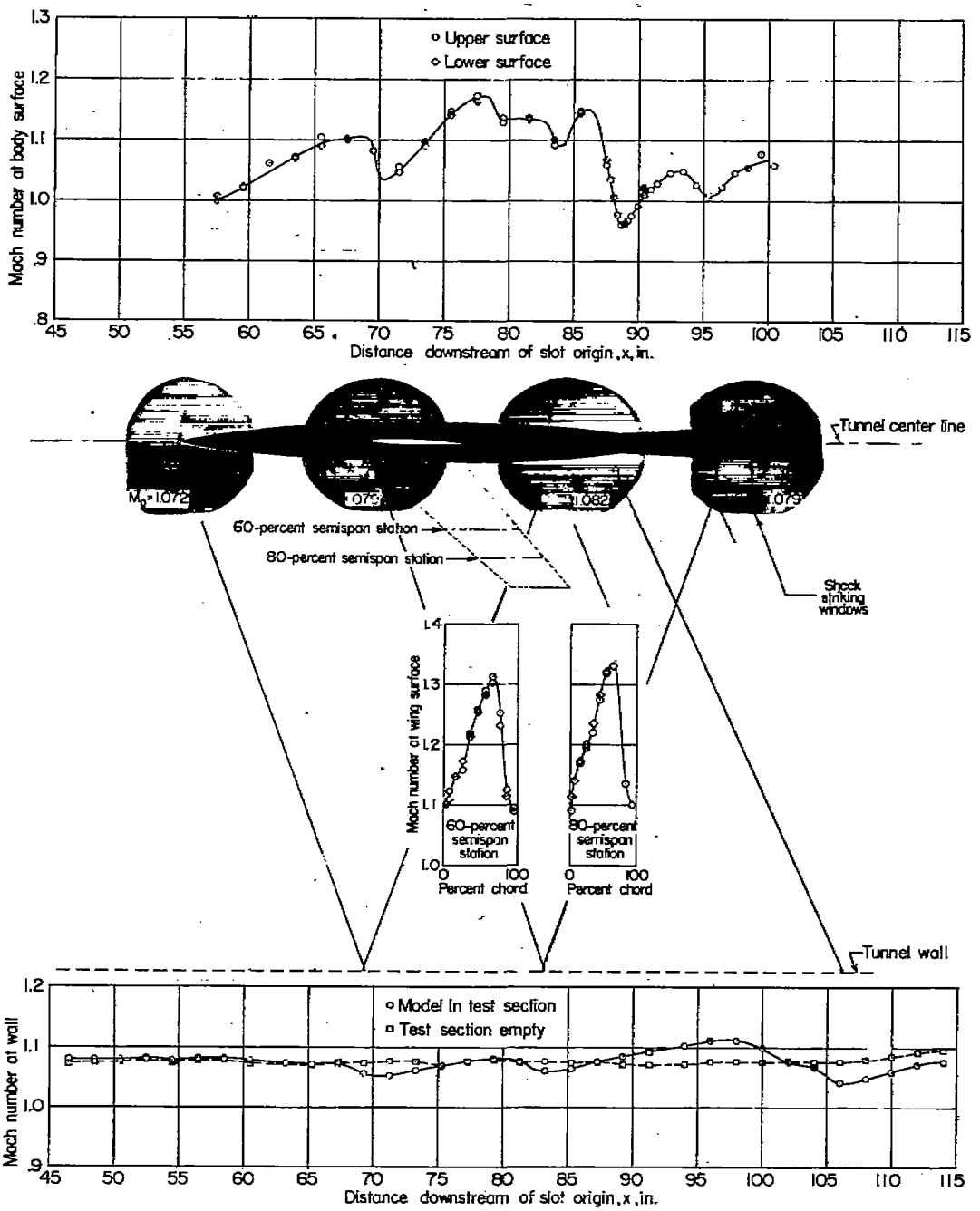

(c) M_o = 1.079.

NACA L72695

Figure 17.- Continued.

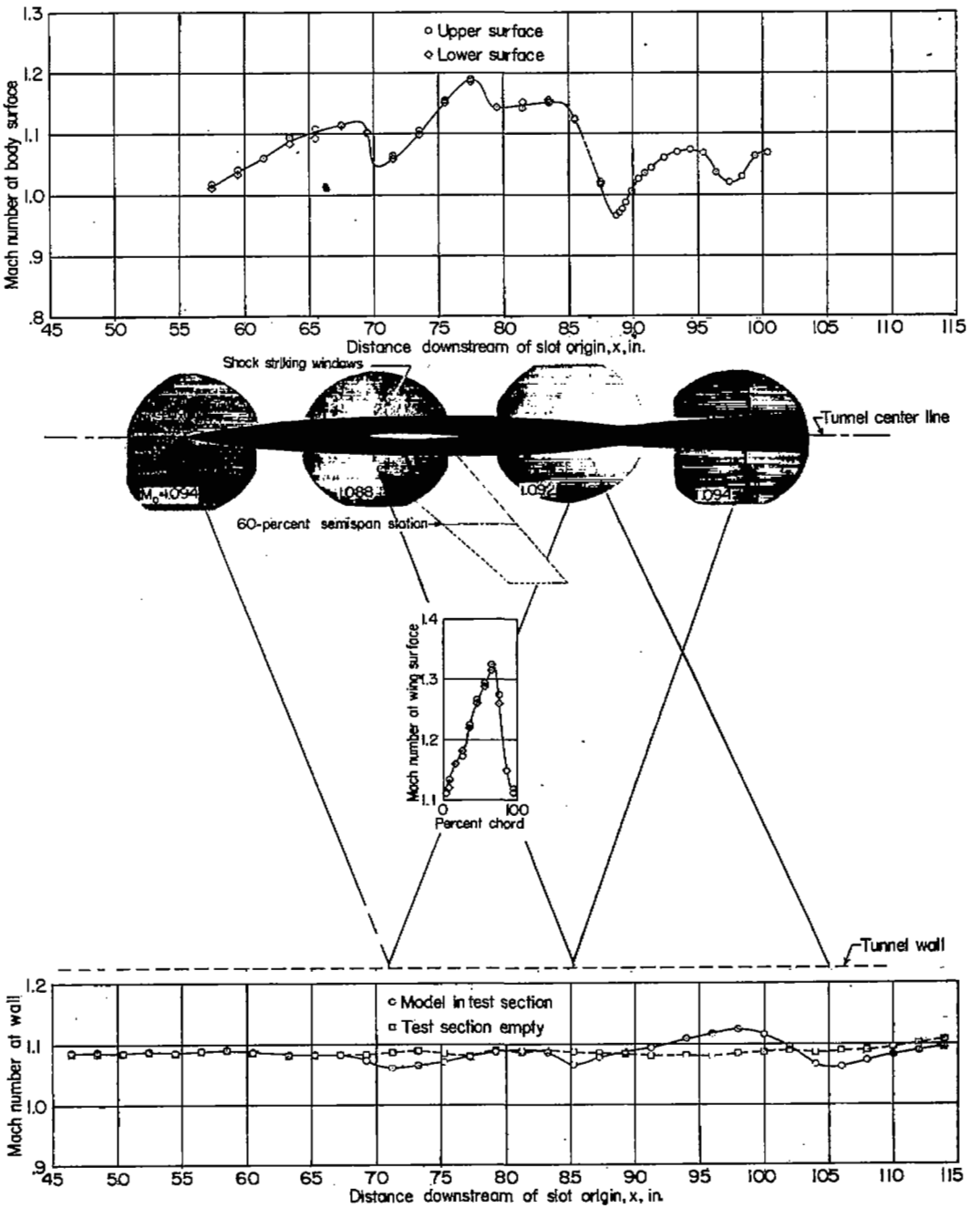

(d) M_o = 1.088.

NACA L-72696

Figure 17.- Continued.

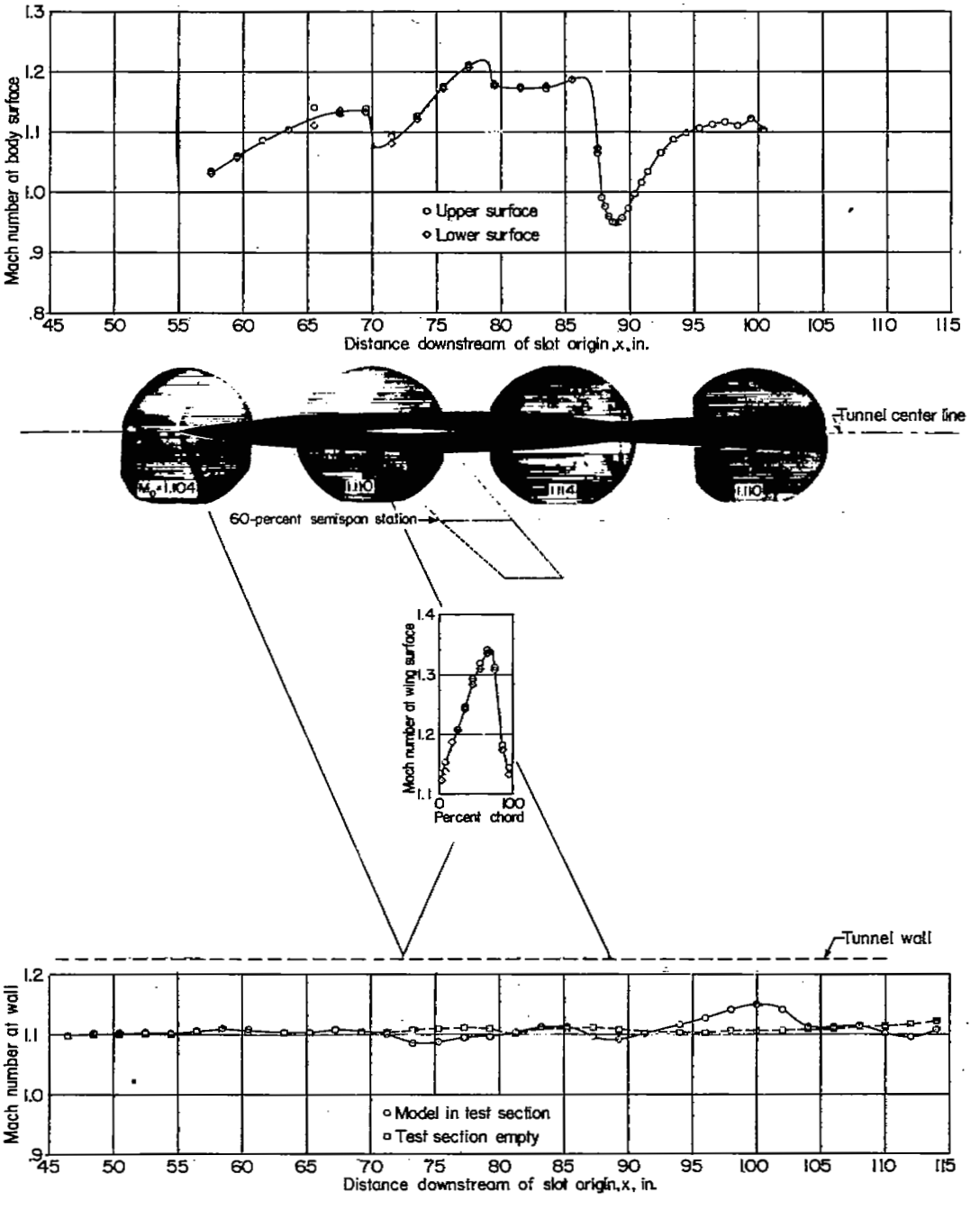

(e) $M_o = 1.110$.

NACA L-72697

Figure 17.- Continued.

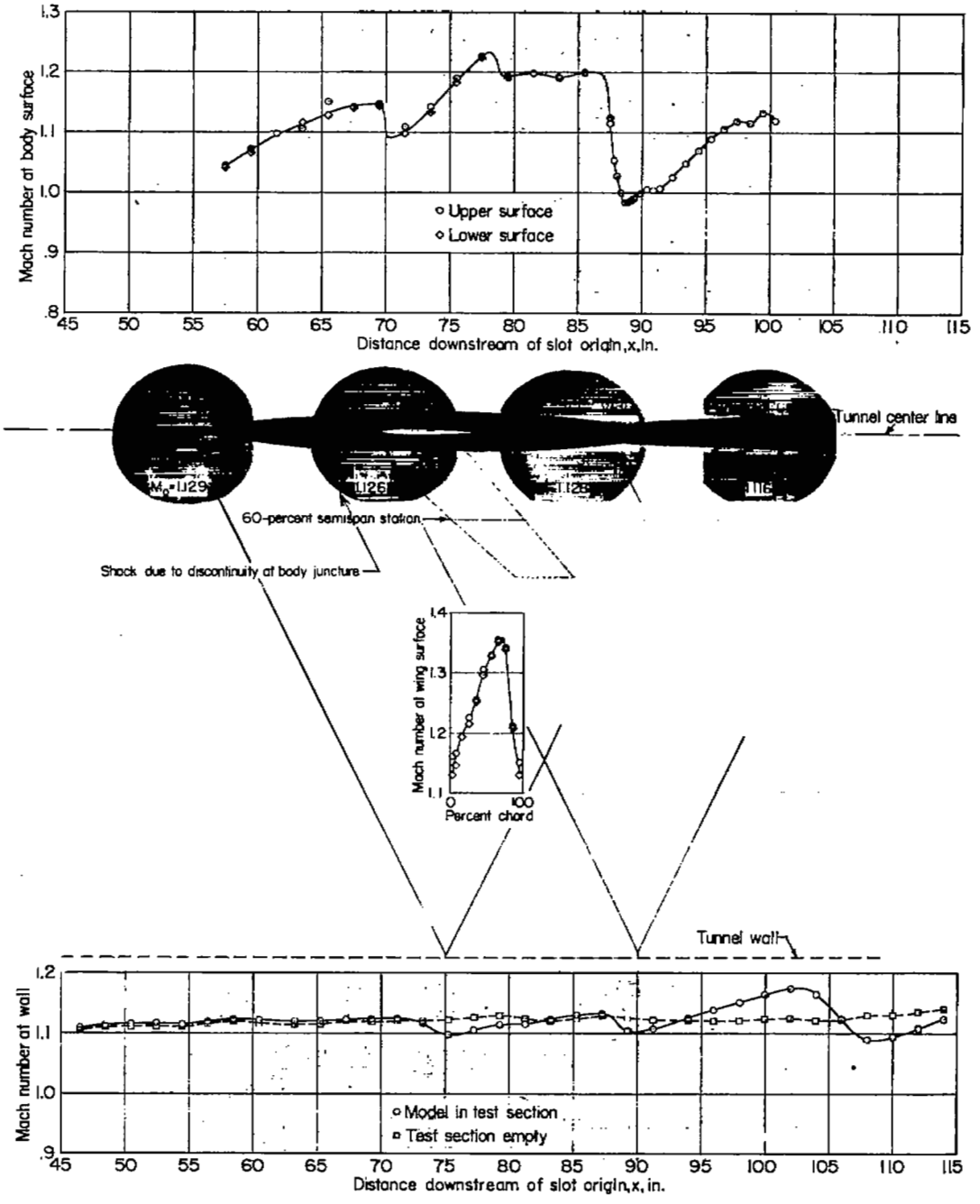

(f) M_o = 1.126.

Figure 17.- Concluded.

NACA L-72698

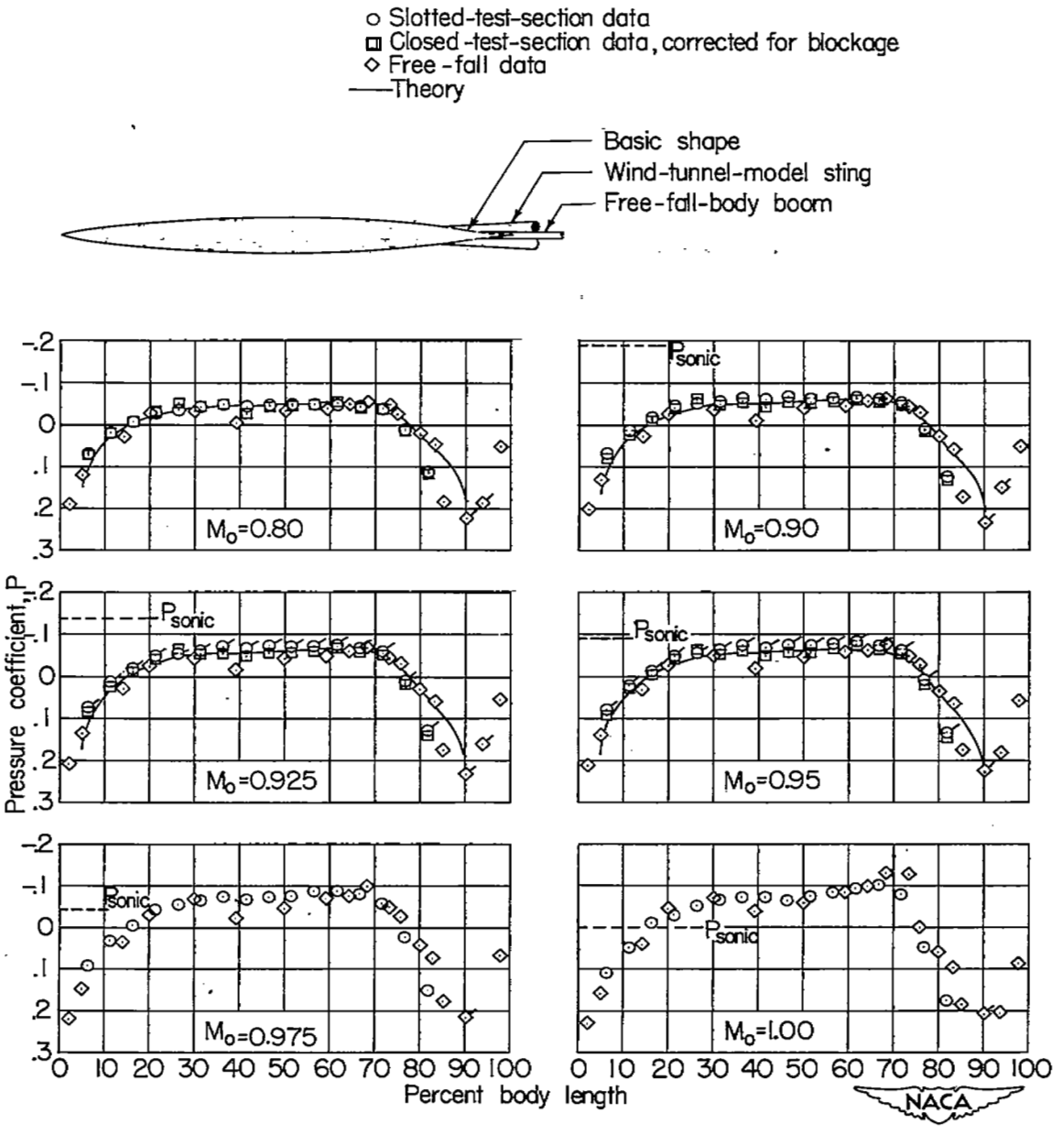

(a) Subsonic and sonic speeds.

Figure 18.- Comparison of body-surface pressure distributions obtained from tests of a body of revolution in the slotted test section with those from closed-test-section tests, free-fall tests, and theory. Flagged symbols (○ and ◇) indicate faired data.

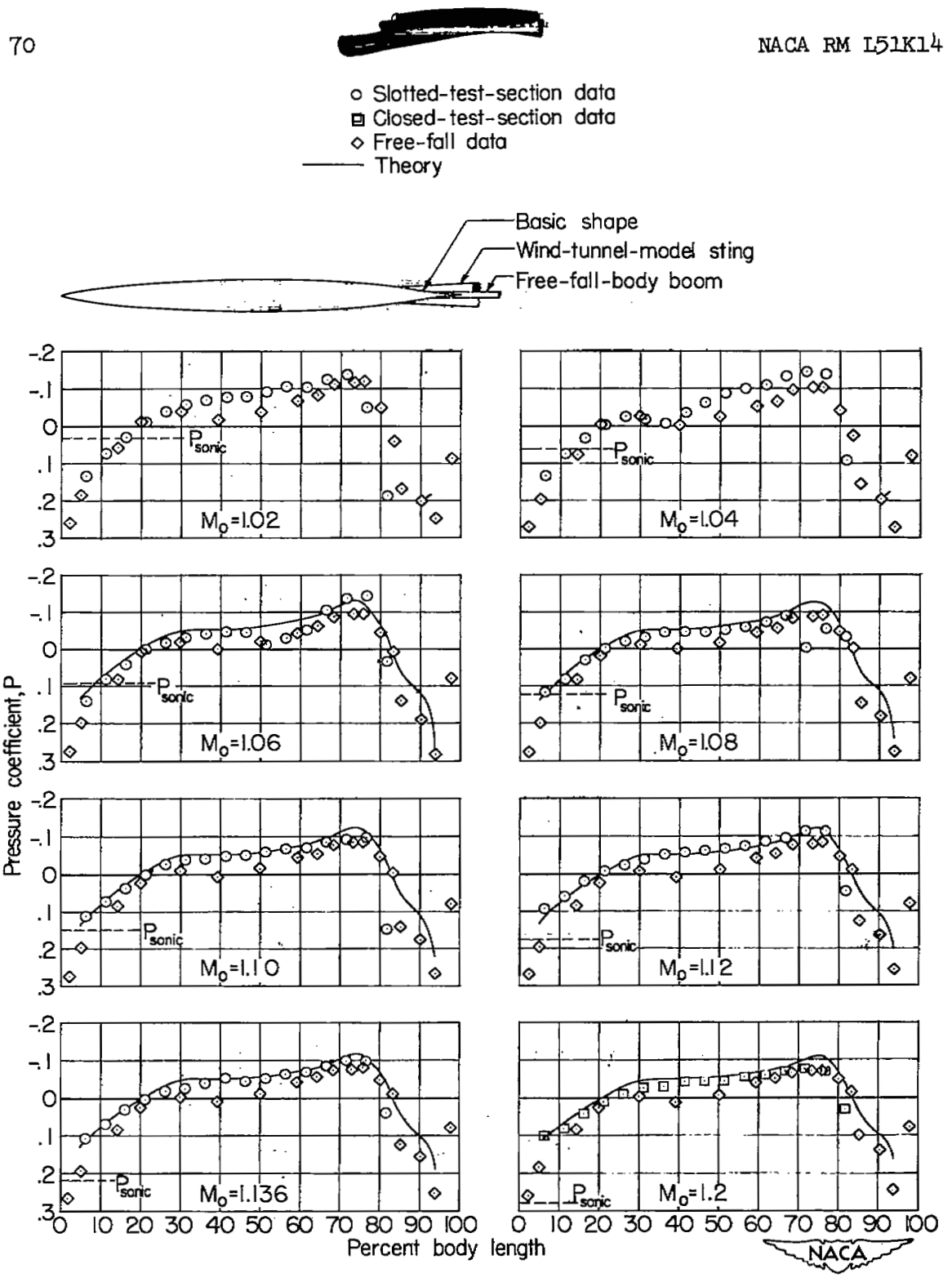

(b) Supersonic speeds.

Figure 18.- Concluded.

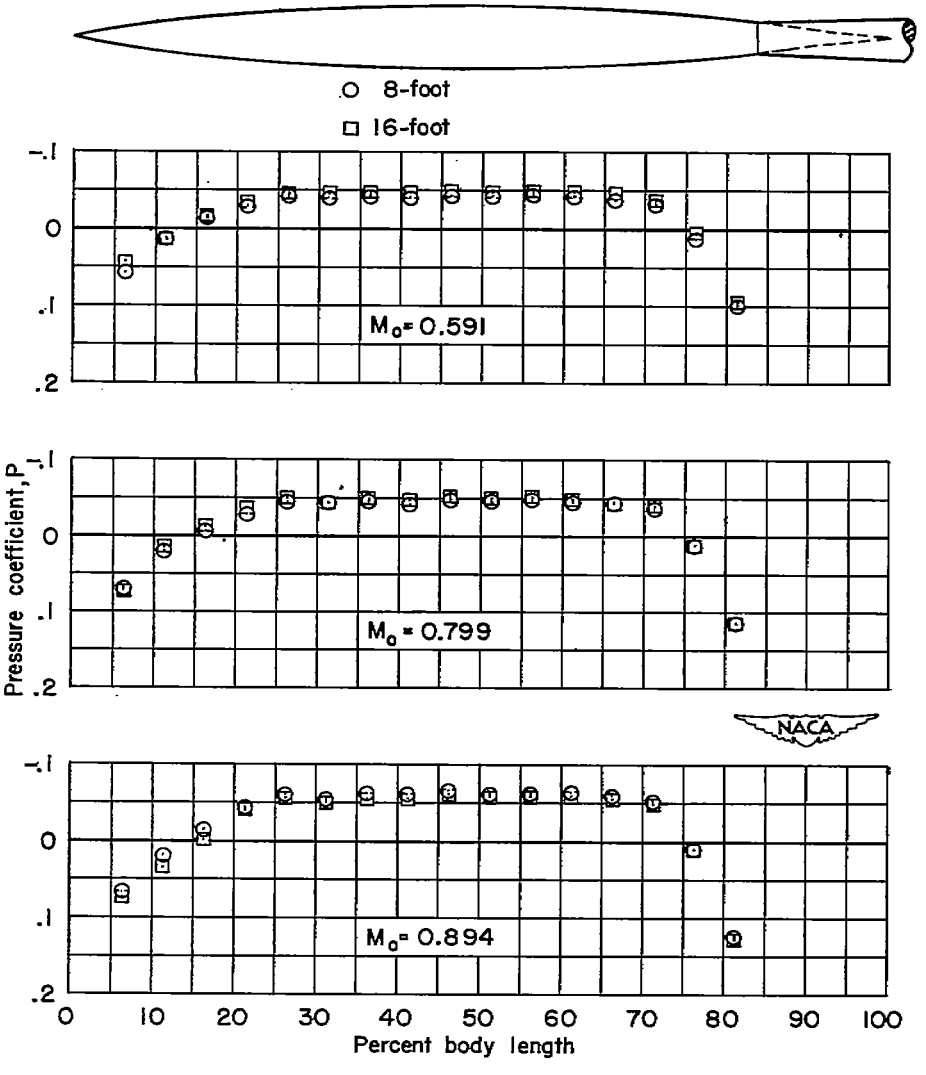

(a) Subsonic speeds (M_o from 0.591 to 0.894).

Figure 19.- Comparison of body-surface pressure distributions obtained from tests of a body of revolution at zero angle of attack in the slotted test sections of the Langley 8-foot and 16-foot transonic tunnels.

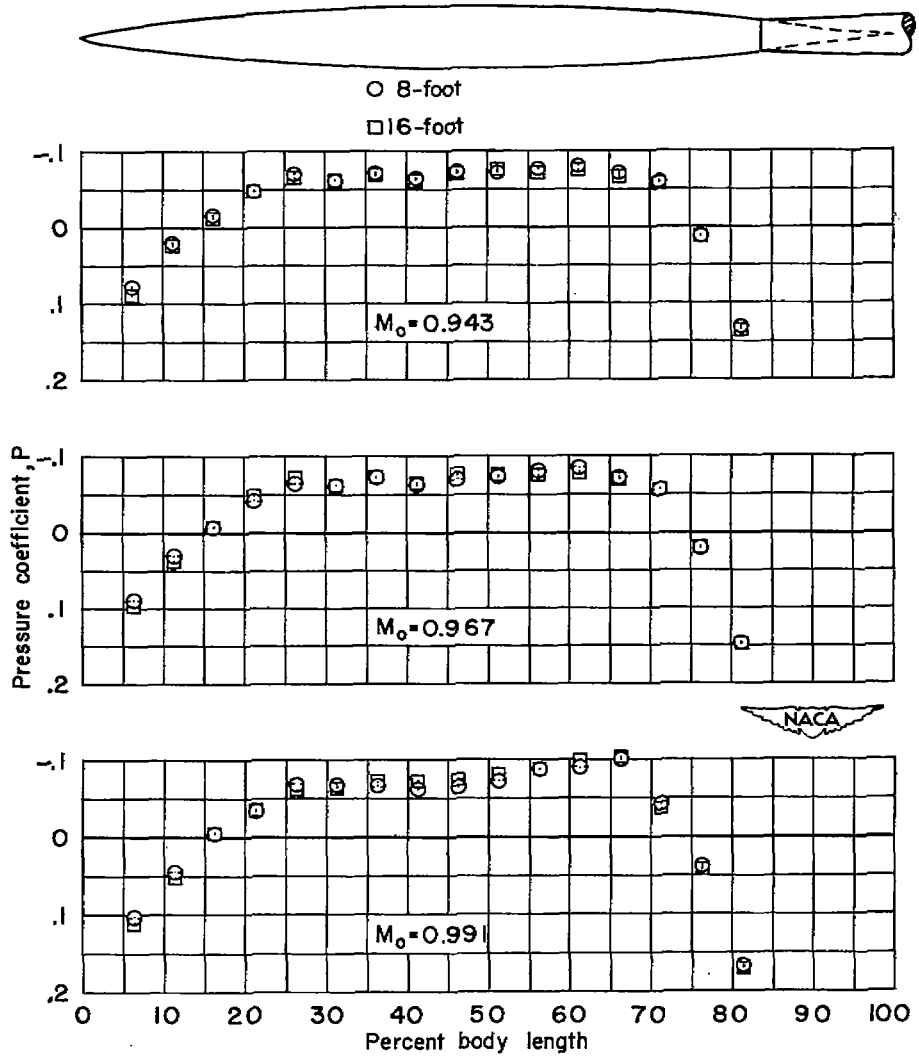

(b) Subsonic speeds (M_o from 0.943 to 0.991).

Figure 19.- Continued.

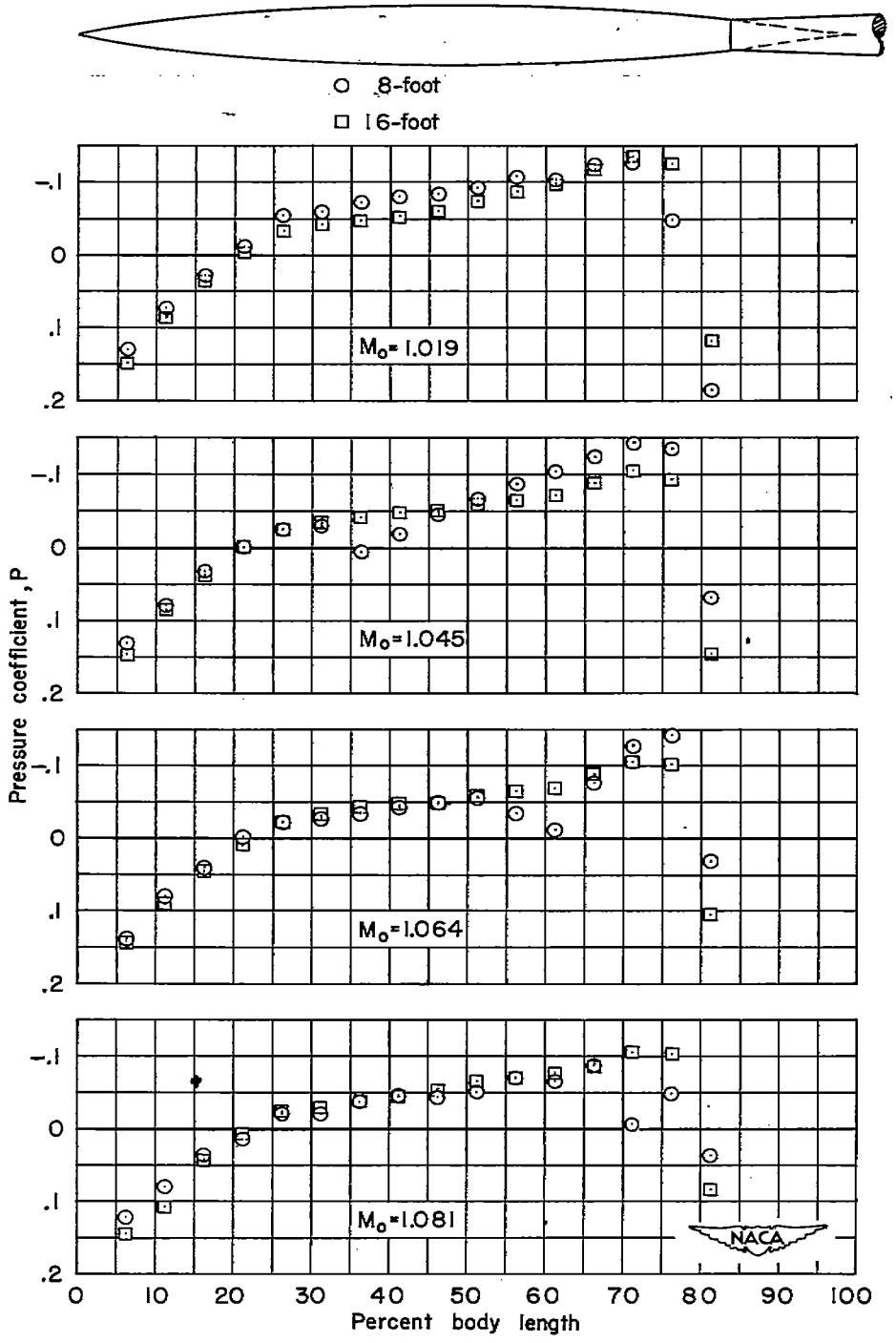

(c) Supersonic speeds (M_o from 1.019 to 1.081)

Figure 19.- Concluded.

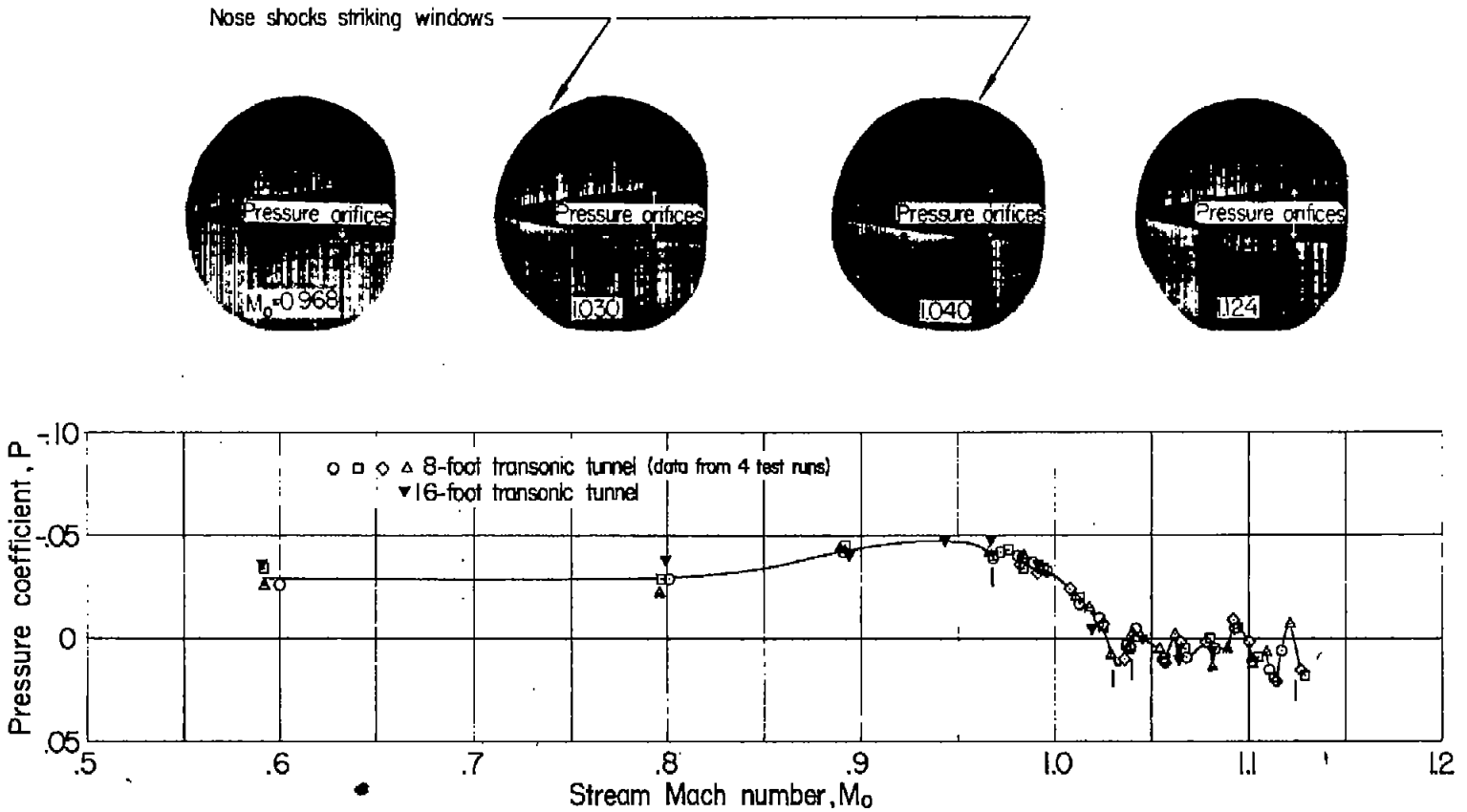

(a) $\frac{x}{l} = 0.2125$.

NACA
L-72699

Figure 20.- The variation with stream Mach number of the pressure coefficient at six axial stations on the body of revolution and comparison of coefficients measured in the slotted test sections of the Langley 8-foot and 16-foot transonic tunnels.

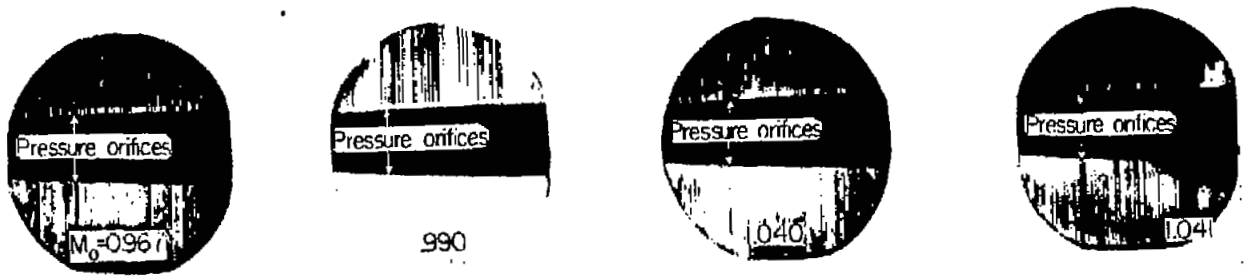

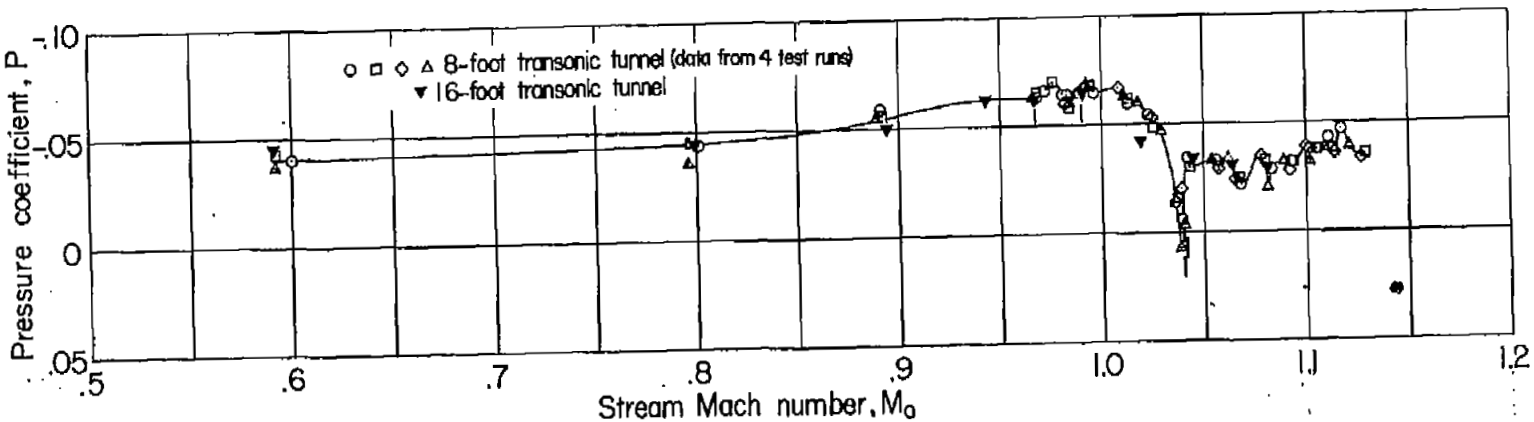

(b) $\frac{x}{l} = 0.3125$.

NACA
L-72700

Figure 20.- Continued.

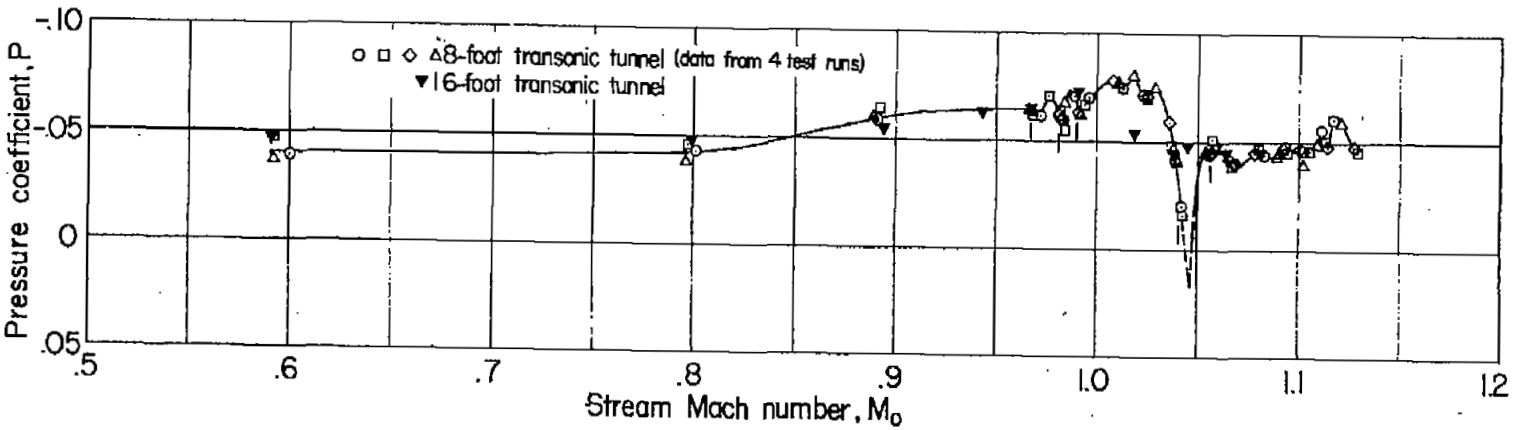

(c) $\frac{x}{l} = 0.4125$

NACA
L-72701

Figure 20.- Continued.

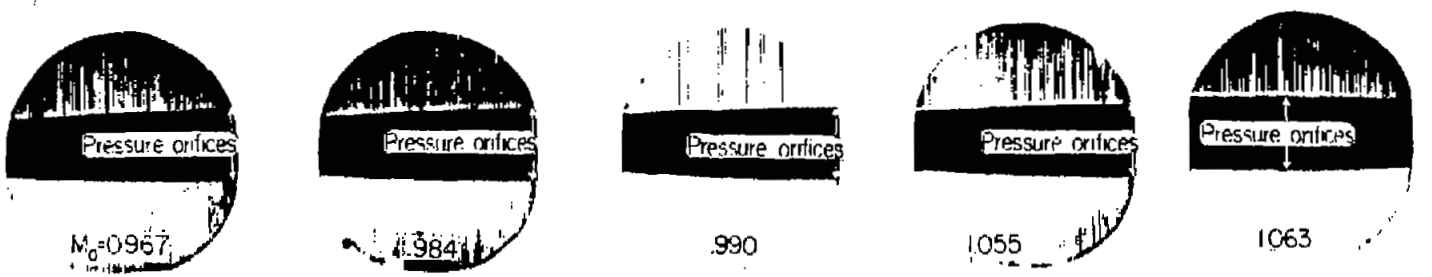

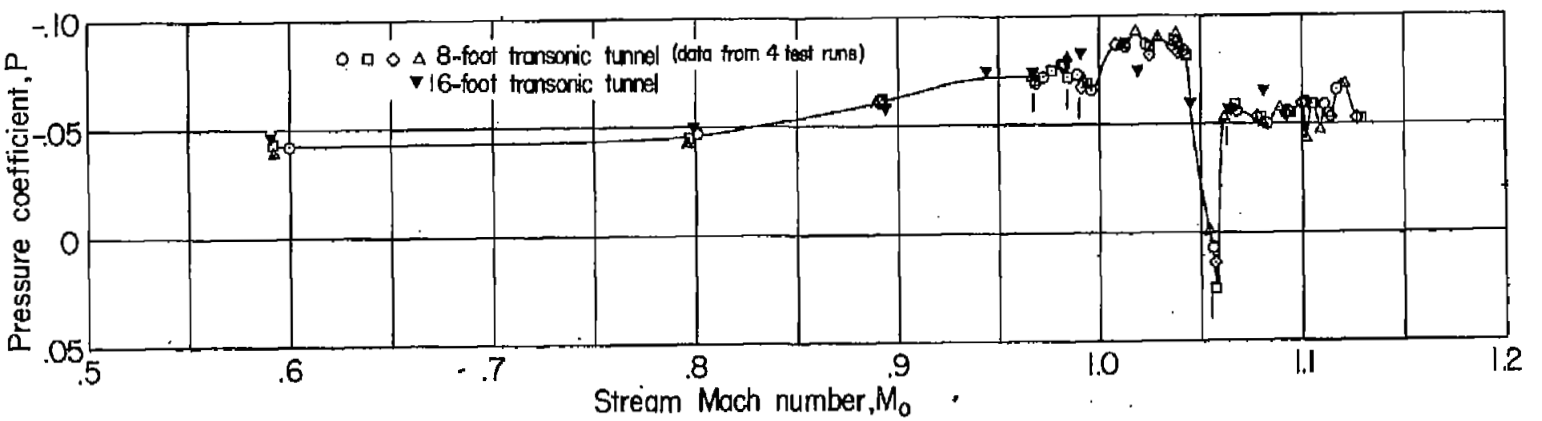

(d) $\frac{x}{l} = 0.5125$.

NACA

L-72702

Figure 20.- Continued.

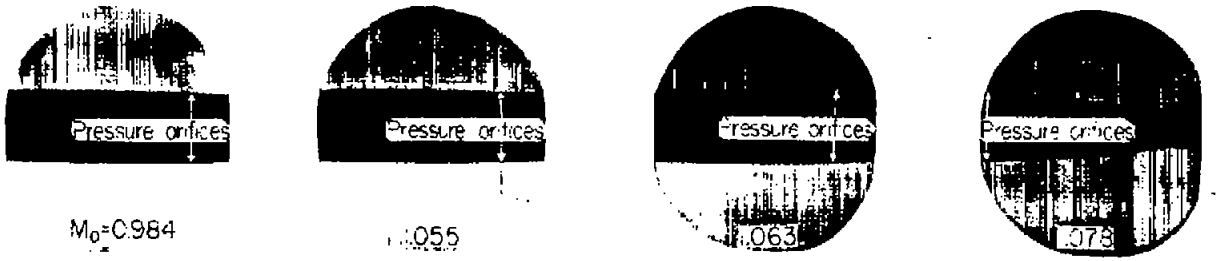

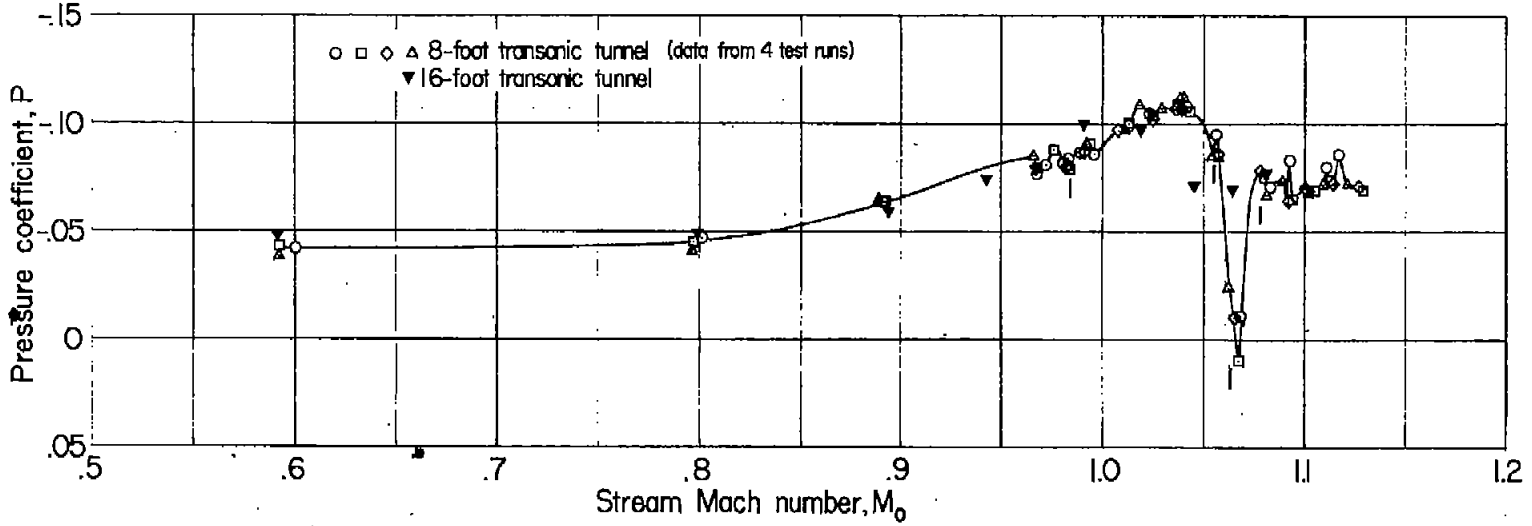

(e) $\frac{x}{l} = 0.6125$

NACA
L-72703

Figure 20.- Continued.

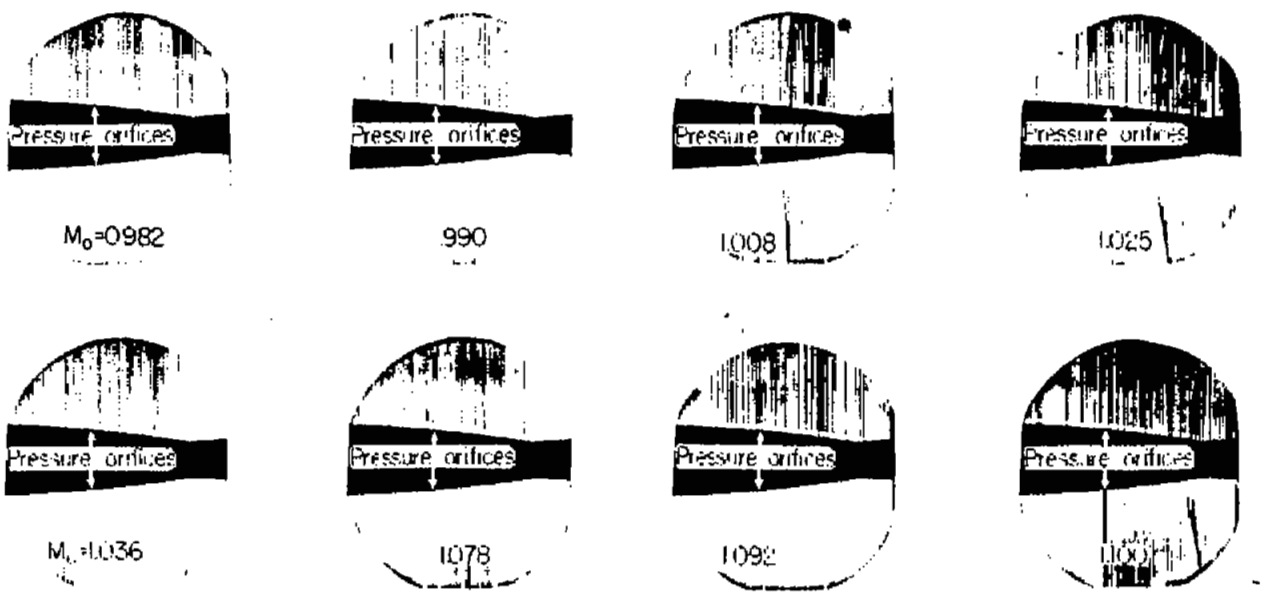

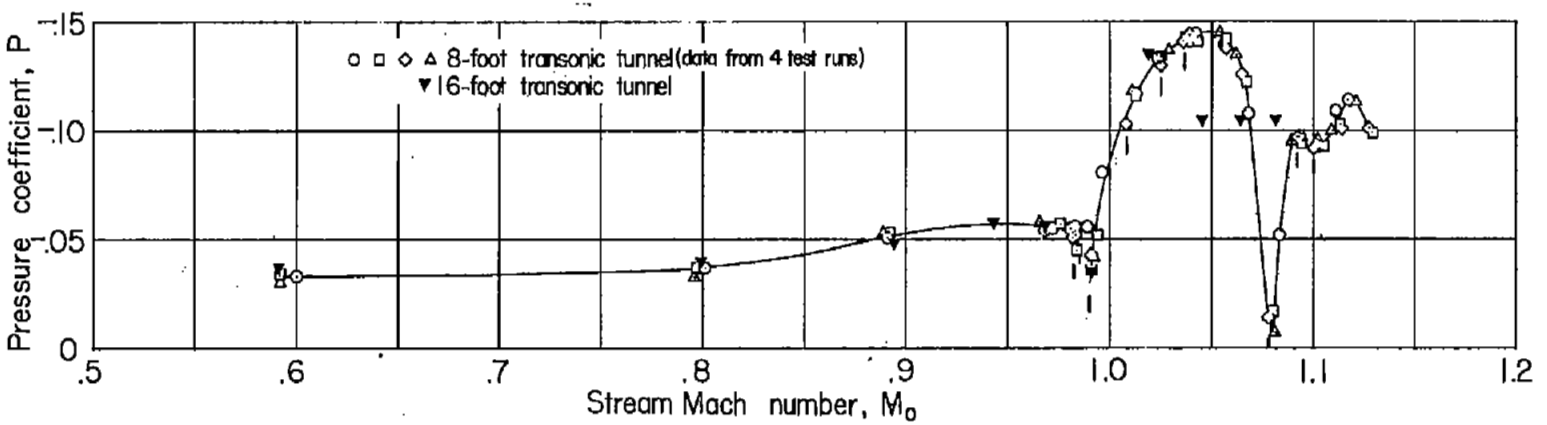

(f) $\frac{x}{l}$ = 0.7125.

NACA
L-72704

Figure 20.- Concluded.

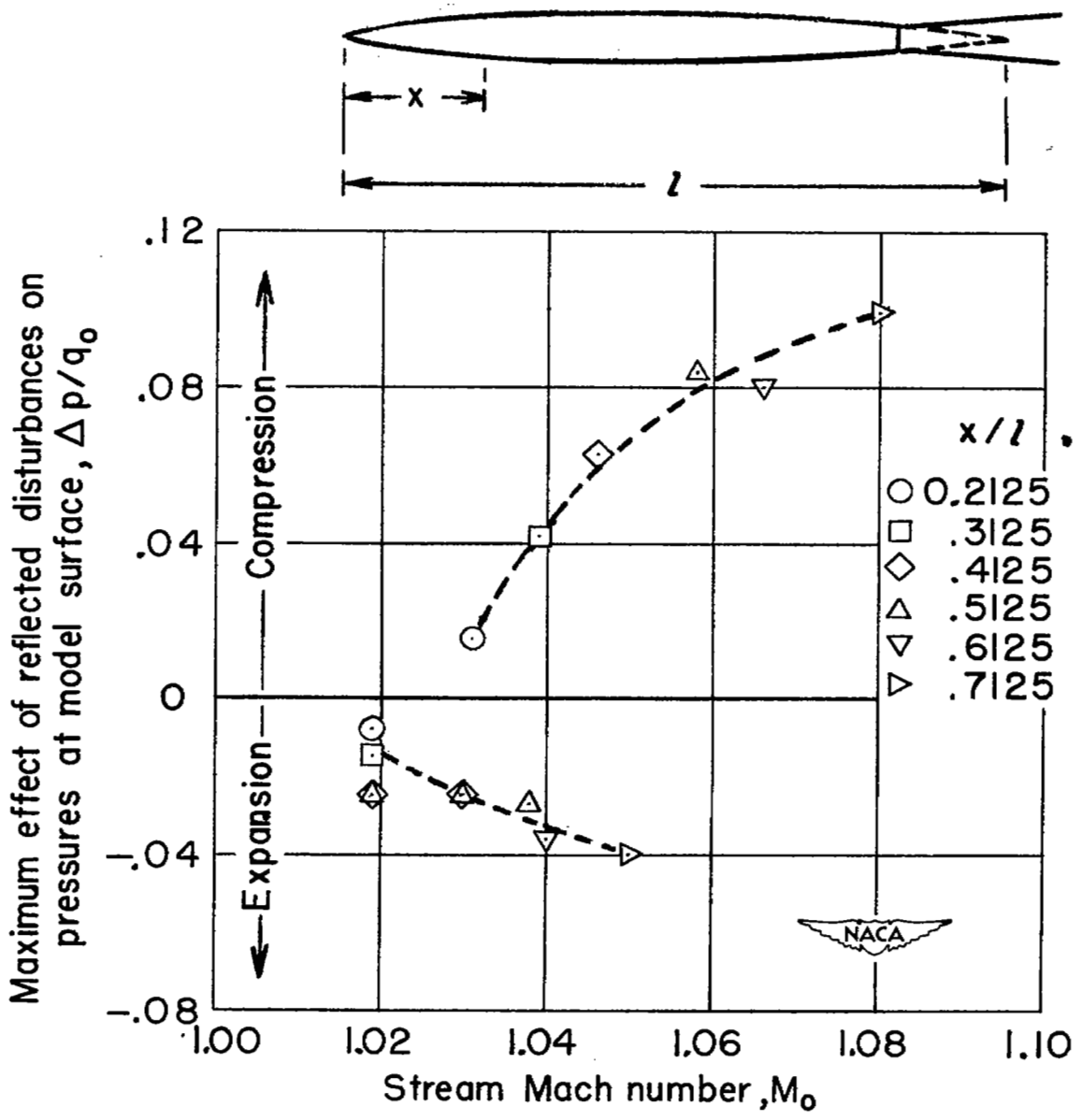

Figure 21.- Maximum effect of reflected compressions and expansions on pressure coefficients at model surface, as indicated by differences between measurements in the Langley 8-foot and 16-foot transonic tunnels.

Langley 8-foot transonic tunnel (boundary interference present)

○ Body at center line; Force-test data (corrected for tares)

□ Body at center line

◇ Body 10.3 inches off center line } Pressure-distribution data (includes skin friction estimated from reference 11)

Langley 16-foot transonic tunnel (no boundary interference)

△ Pressure-distribution data (includes skin friction estimated from reference 11)

– – – – Free-fall data (reference 4)

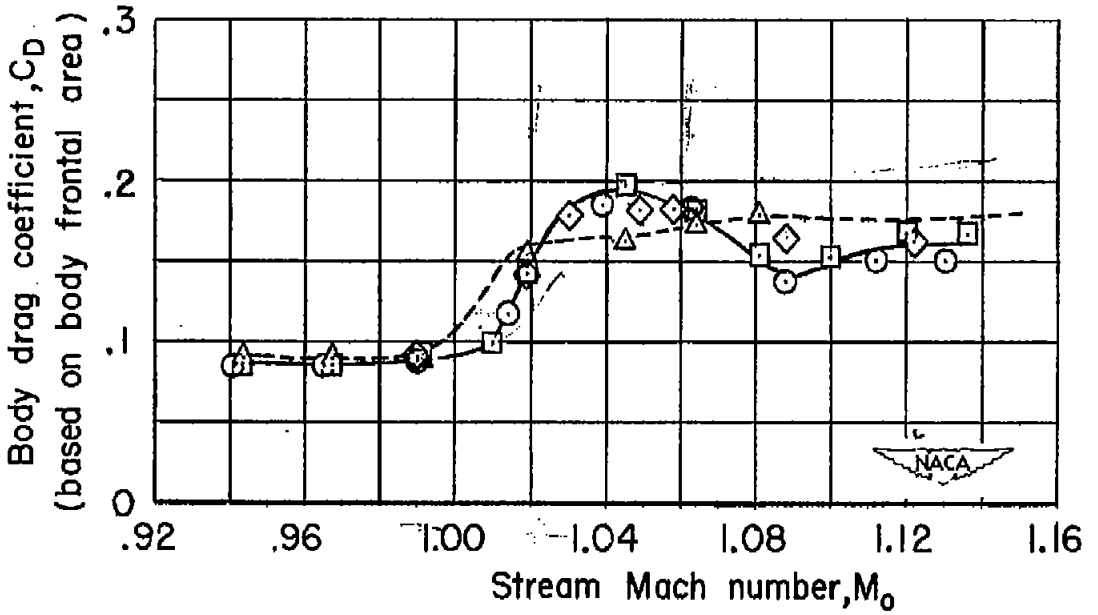

Figure 22.- Effect of boundary-reflected disturbances on body drag coefficients for a 33.5-inch-long nonlifting body of revolution in the slotted test section.

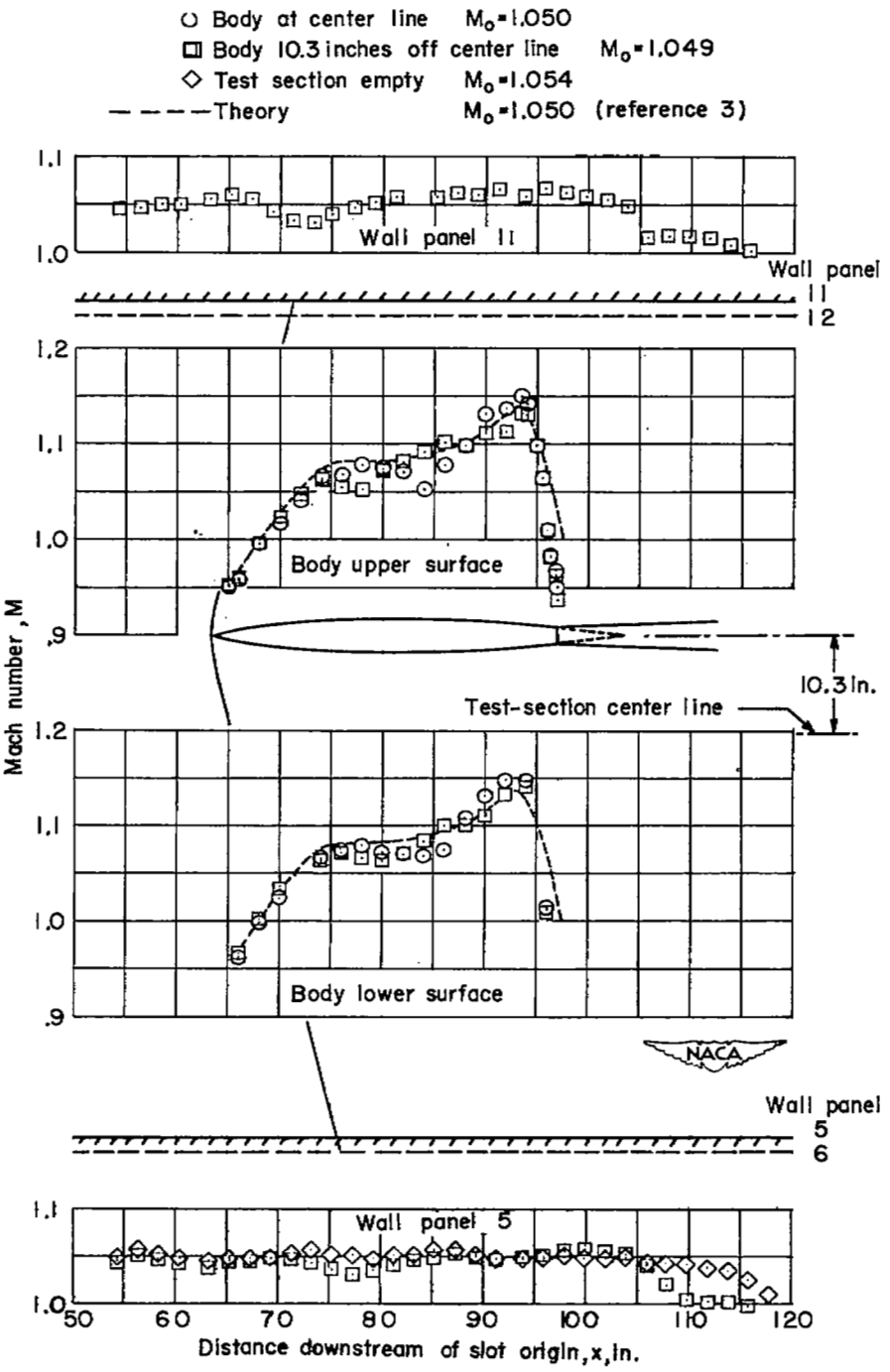

Figure 23.- Comparison of body-surface Mach number distributions obtained from tests of a body of revolution at the center line and approximately 10.3 inches off the center line of the slotted test section. $\alpha = 0^{\circ}$; $M_o = 1.050$ (approximately).

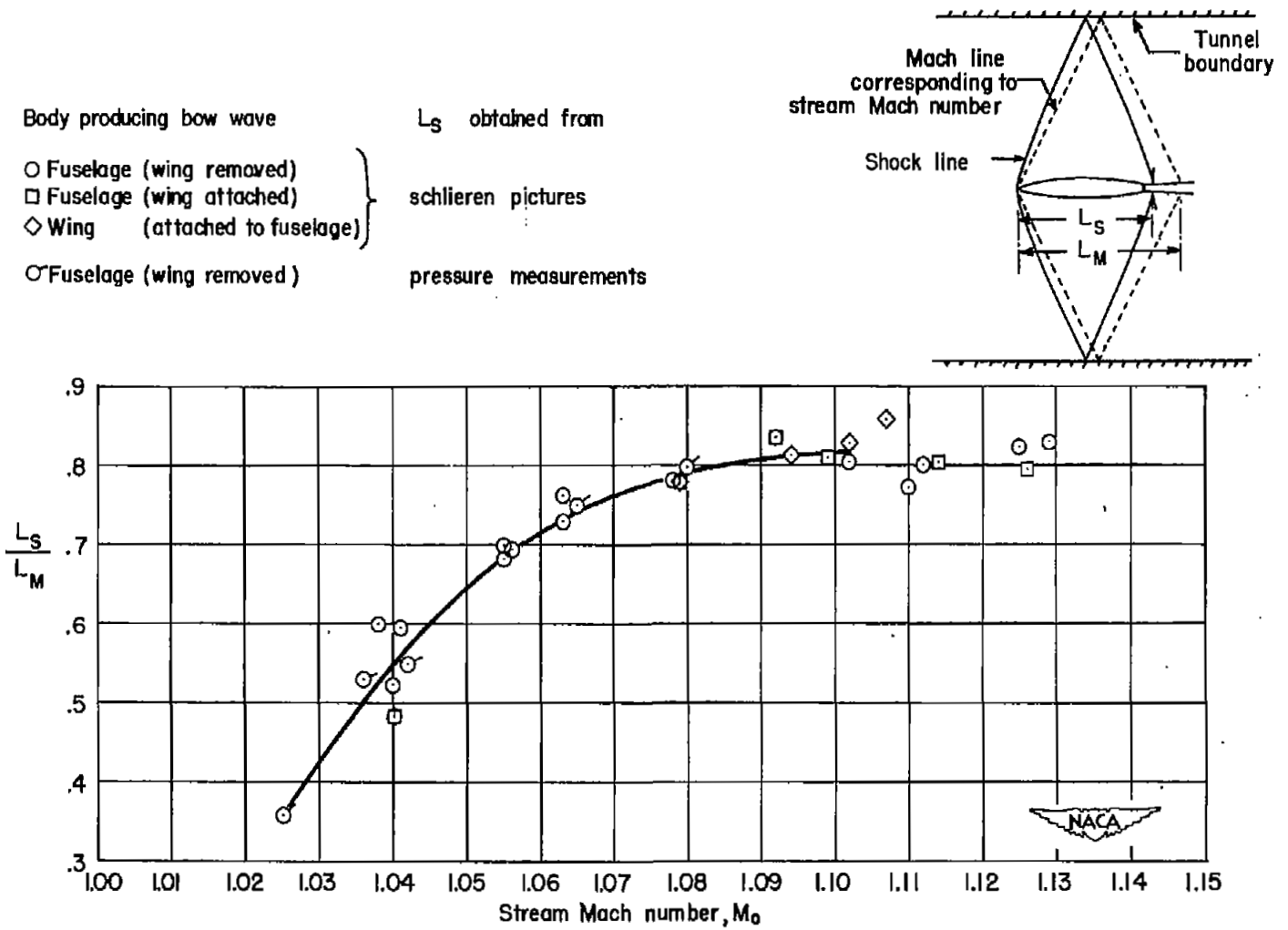

Figure 24.- Axial distance required for model bow wave to reflect from test-section wall and strike surface of model near center line. $\alpha = 0^\circ$.

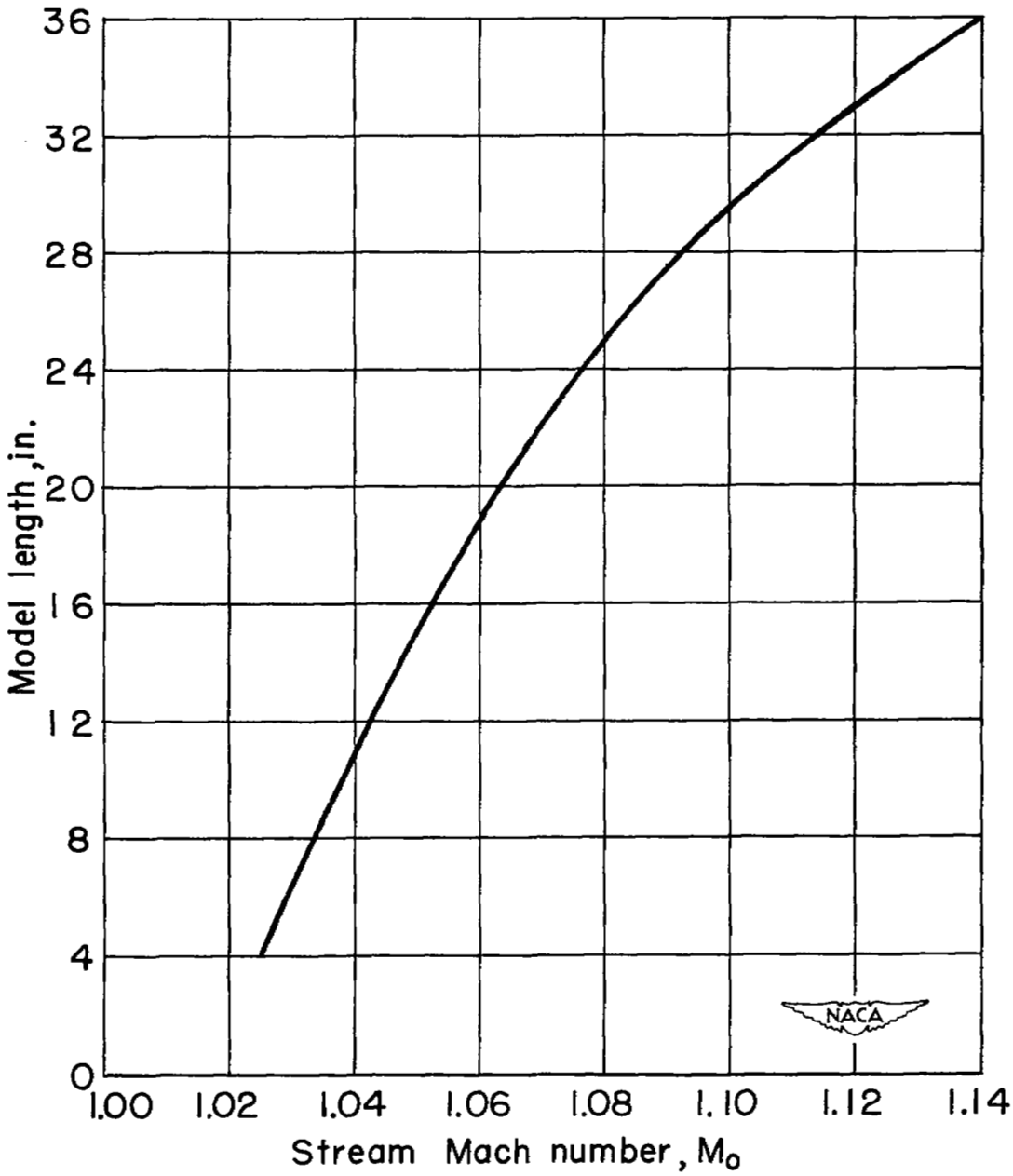

Figure 25.- Approximate model lengths for interference-free supersonic testing at center line of slotted test section measuring approximately 43.8 inches from center line to wall.

Figure 26.- Shock formations at transonic speeds with total-pressure rake (0.050-inch-diameter tubes projecting 3 inches ahead of 1° included-angle wedge) near center line of slotted test section.

NACA L-72705

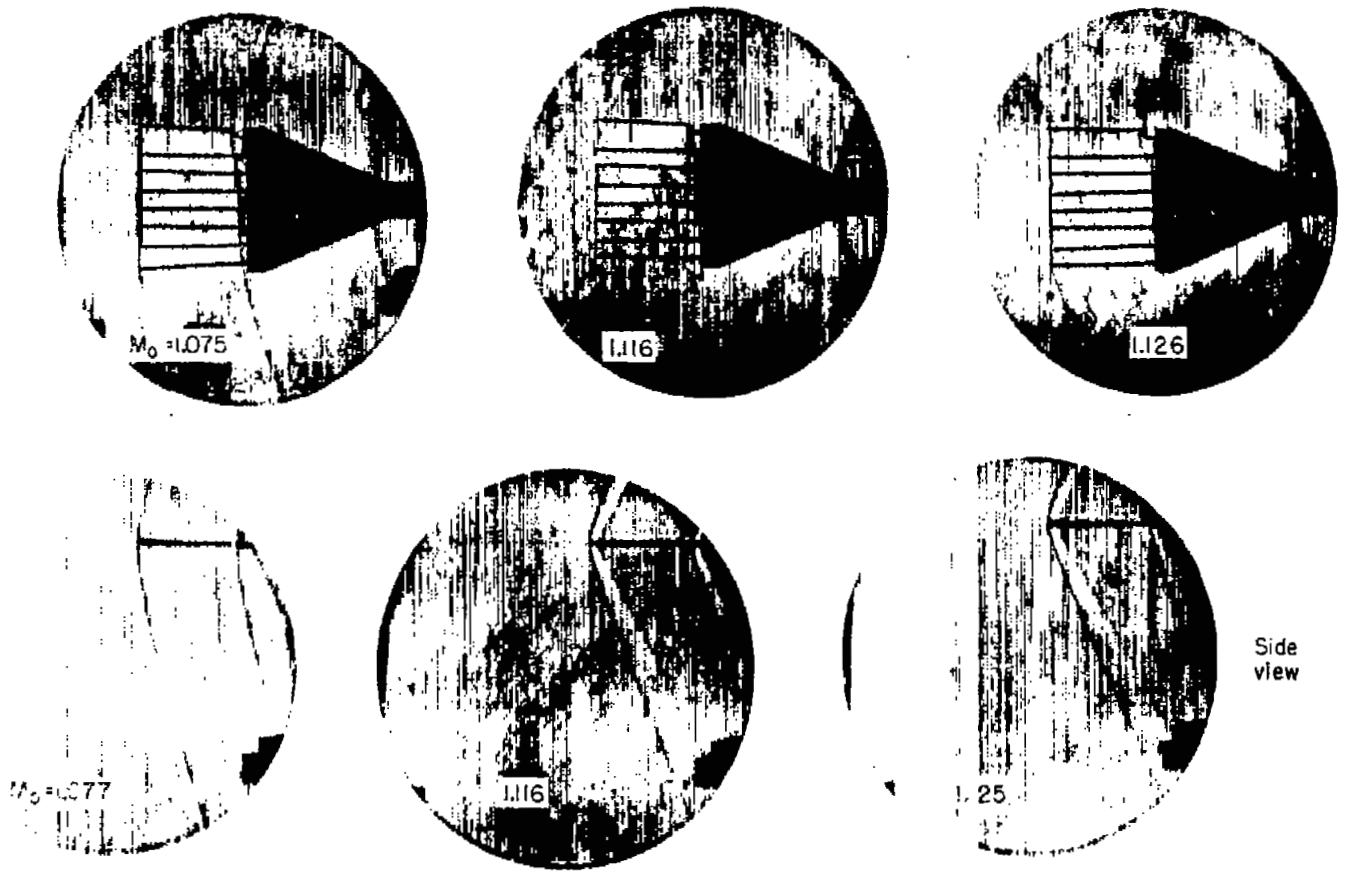

Figure 26.- Concluded.

NACA
L-72706

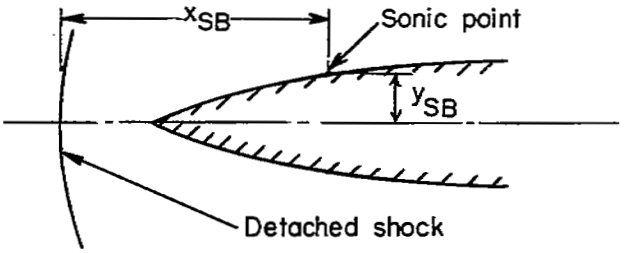

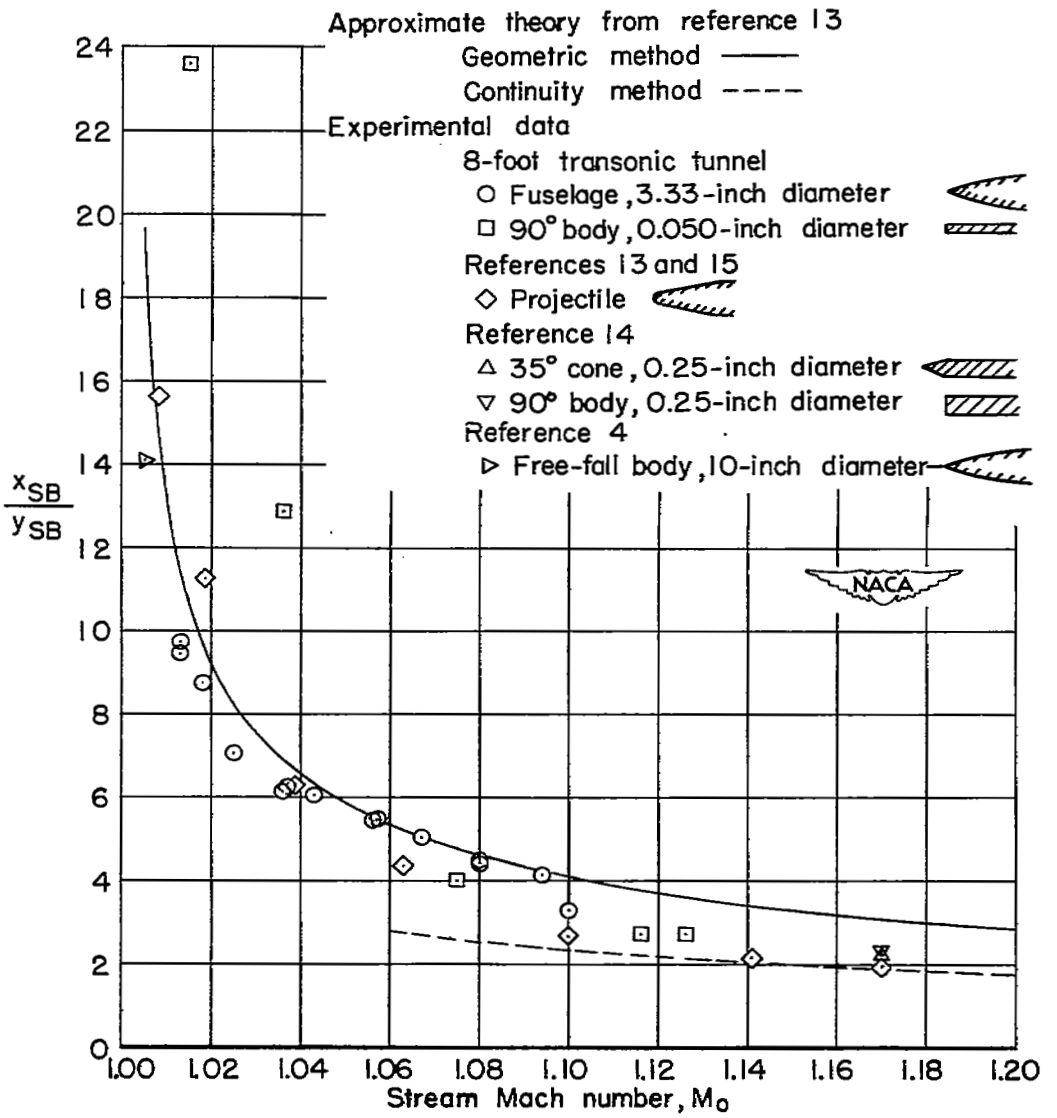

Figure 27.- Location of detached shock waves ahead of various axially symmetric bodies at low-supersonic speeds. $\alpha = 0^\circ$.

NACA-Langley - 7-7-52 - 400